# EXPERIMENTAL INVESTIGATION OF NEUROPROTECTIVE DRUGS IN MODELS OF RETINAL CELL DEATH

by

**Darryl Cassius Baptiste**

**Submitted in partial fulfillment of the requirements for the degree of Doctor of Philosophy**

**at**

**Dalhousie University**
**Halifax, Nova Scotia**
**May 2004**

*Your file Votre référence*
*ISBN: 0-612-94040-3*
*Our file Notre référence*
*ISBN: 0-612-94040-3*

DALHOUSIE UNIVERSITY

To comply with the Canadian Privacy Act the National Library of Canada has requested that the following pages be removed from this copy of the thesis:

Preliminary Pages

Examiners Signature Page (pii)

Dalhousie Library Copyright Agreement (piii)

Appendices

Copyright Releases (if applicable)

# DEDICATION

For my grandmother, Mary Baptiste, the most influential person in my life: I am forever grateful for having you as my guardian in life. I wish you were still here to share in my accomplishments.

# TABLE OF CONTENTS

# LIST OF FIGURES

# LIST OF TABLES

# ABSTRACT

Glaucomatous optic neuropathy (GON) results in retinal ganglion cell (RGC) death and vision loss. The underlying mechanism(s) for RGC death in GON may include glutamate-induced excitotoxicity, trophic factor deprivation (TFD), inflammatory reactions or axonal injury. Drugs that intervene at various points in the apoptotic pathways leading to neuronal death may provide neuroprotection. Recent studies have demonstrated that the intraocular pressure-reducing drugs betaxolol, a β1-adrenergic receptor (AR) antagonist, and brimonidine, an α2-AR agonist, as well as the tetracycline derivative, minocycline, are neuroprotective in models of the degenerating retina and central nervous system. The main objectives of this thesis research were to determine the efficacy and mechanism(s) of action of the AR drugs and tetracycline derivatives in inhibiting retinal neuron death in experimental models.

Betaxolol, brimonidine, and minocycline were all neuroprotective in retinal cell culture, with increased viability occurring at concentrations ranging from 0.02-200 μM. In comparison to other β-AR antagonists, betaxolol was the only drug with neuroprotective capabilities, suggesting that the neuroprotective actions by betaxolol occur independent of interactions with β-ARs. In contrast, the increased neuronal survival mediated by brimonidine could be blocked by the α2-AR antagonist, yohimbine, suggesting that the neuroprotective actions of brimonidine occur via an α2-AR pathway. Minocycline, but not tetracycline, increased neuron survival following excitotoxicity or TFD. The anti-apoptotic actions of minocycline in retinal cell cultures appeared independent of interactions with N-methyl-D-aspartate receptors and were associated with a reduction in caspase-3 mRNA and protein activation. Minocycline was also able to inhibit TFD-induced apoptosis in pure differentiated pheochromocytoma cell cultures, implying that the neuroprotective actions mediated by minocycline may arise, in part, via direct actions on neurons.

The neuroprotective actions of the tetracycline drugs on RGC survival and MG activation were also assessed in a rat model of ON axotomy. Treatment of axotomized animals with minocycline, but not tetracycline, significantly increased the viability of RGCs. Minocycline also decreased MG activation suggesting that minocycline can provide neuroprotection for RGCs following ON injury, and that this property is not shared by all tetracycline drugs.

# LIST OF ABBREVIATIONS & SYMBOLS USED

| | |
|---|---|
| AD | Alzheimer's disease |
| AH | aqueous humor |
| AIDS | autoimmune deficiency syndrome |
| AIF | apoptosis-inducing factor |
| Akt | protein kinase B |
| ALS | amyotrophic lateral sclerosis |
| ALT | argon laser trabeculoplasty |
| AMPA | 2-amino-3-(3-hydroxy-5-methylisoxazol-4-yl) proprionate |
| AO/EB | acridine orange-ethidium bromide |
| Apaf-1 | apoptosis protease activating factor-1 |
| ARs | adrenergic receptors |
| Bad | Bcl-2 associated death protein |
| Bax | Bcl-2-associated X protein |
| BBB | blood-brain-barrier |
| Bcl-2 | B-cell lymphoma (leukaemia)-2 |
| BDNF | brain derived tropic factor |
| bFGF | basic fibroblastic growth factor |
| BH | Bcl-2 homology |
| Bid | BH3-interacting homology death domain agonist |
| Bim | Bcl-2 interacting mediator of cell death |
| BRB | blood retinal barrier |

| | |
|---|---|
| Brn-3C | Pit, Onc, Unc (POU) domain transcription factor |
| CAIs | carbonic anhydrase inhibitors |
| $Ca^{2+}$ | calcium |
| $CaCl_2$ | calcium chloride |
| $[Ca^{2+}]_i$ | intracellular calcium concentration |
| $Cl^-$ | chloride |
| CMF | calcium magnesium free |
| cNOS | constitutive NOS |
| CNS | central nervous system |
| CNTF | ciliary neurotrophic factor |
| $CO_2$ | carbon dioxide |
| COX-2 | cyclooxygenase-2 |
| CREB | cAMP-response element binding protein |
| cyt c | cytochrome c |
| D-MEM | Dulbecco's modified Eagle's medium |
| DMSO | dimethyl sulfoxide |
| EDTA | ethylenediaminetetraacetic acid |
| eNOS | endothelial NOS |
| ERKs | extracellular signal-regulated kinases |
| ET-1 | endothelin-1 |
| FGF | fibroblast growth factor |
| GABA | gamma-aminobutyric acid |

| | |
|---|---|
| GCL | ganglion cell layer |
| GLC | glaucoma genes |
| GluR | glutamate receptor |
| GGA | geranylgeranylacetone |
| GM | growth media |
| GON | glaucomatous optic neuropathy |
| HD | Huntington's disease |
| Hg | mercury |
| Hrk | harakiri |
| Hsps | heat shock proteins |
| IL | interleukin |
| INL | inner nuclear layer |
| iNOS | inducible nitric oxide synthase |
| IOP | intraocular pressure |
| IPL | inner plexiform layer |
| JNK | c-Jun N-terminal kinase |
| KA | kainate |
| $K^+$ | potassium |
| LGN | lateral geniculate nucleus |
| MAPK | mitogen-activated protein kinase |
| MG | microglia |
| MHC | major histocompatibility complex |

| | |
|---|---|
| MK-801 | dizocilpine |
| mm | millimetre |
| MMPs | matrix metalloproteinases |
| mRNA | messenger ribonucleic acid |
| MS | multiple sclerosis |
| MYOC | myocilin |
| $Na^+$ | sodium |
| NGF | nerve growth factor |
| NF-κB | nuclear factor kappa-B |
| NMDA | N-methyl-D-aspartate |
| NMDAR | N-methyl-D-aspartate receptor |
| nNOS | neuronal NOS |
| NO | nitric oxide |
| NOS | nitric oxide synthase |
| NRP | nuclear factor kappa-B essential modulator related protein |
| NT | neurotrophin |
| NTG | normal tension glaucoma |
| ON | optic nerve |
| ONH | optic nerve head |
| ONL | outer nuclear layer |
| OPL | outer plexiform layer |
| OPTN | optineurin |

| | |
|---|---|
| $O_2$ | oxygen |
| PCNA | proliferating cell nuclear antigen |
| PD | Parkinson's disease |
| PI-3K | phosphatidylinositol 3-kinase |
| POAG | primary open angle glaucoma |
| RGC | retinal ganglion cell |
| ROS | reactive oxygen species |
| RPE | retinal pigment epithelium |
| SC | superior colliculus |
| SD | standard deviation |
| TFD | trophic factor deprivation |
| TGF | transforming growth factor |
| TIGR | trabecular meshwork-induced glucocorticoid response protein |
| TM | treatment media |
| TNF-α | tumor necrosis factor-alpha |
| TNFR | tumor necrosis factor receptor |
| UTR | 5'-untranslated region |
| VDCCs | voltage-dependent calcium channels |

# ACKNOWLEDGEMENTS

This thesis represents five years of work, for which I must thank a number of people whom have contributed to my understanding of skills required to succeed in scientific research.

Firstly, I would like to thank my supervisor, Dr. Melanie Kelly, for taking me into her laboratory and allowing me the freedom to choose this research topic on retinal neuroprotection. I am truly grateful for all of the opportunities that you have presented to me over the years. The experiences I have gained in your laboratory have helped to shape me into the scientist that I am today.

I would like to acknowledge the mentorship I have received from Drs. Steven Barnes, Bill Baldridge, Francois Tremblay and Balwantray Chauhan whose insightful ideas and constructive criticism throughout the years has been greatly appreciated. Thank you Christine Jollimore, Terry LeVatte and Michelle Archibald for taking the time to teach me the skills necessary to get my thesis research underway. Also my graduate student experience would not be as enjoyable had it not been for the friendships I have made over the years with everyone in the Retina & Optic Nerve Research Laboratory and the Department of Pharmacology.

Lastly, I would like to thank my Aunt Sue whom always treated me as one of her own children. Thank you for always being there for me whenever life got challenging and helping me to always remain focused on the task at hand.

# CHAPTER 1

# INTRODUCTION

## *1.1. General Overview*

The retina is a semi-transparent, multi-layered sheet of neural tissue that lines the inner two-thirds of the posterior eye globe (Riordan-Eva, 1999). The outer surface of the retina is in juxtaposition to the retinal pigment epithelium (RPE), whereas the inner surface is apposed to the vitreous. The retina is connected to the RPE at the ora serrata and at the optic disc (Figure 1.1). The retina is considered to be part of the central nervous system (CNS) and due to its relative easy accessibility; the retina serves as a valuable model for studying CNS function (He et al., 2003).

Anatomically the vertebrate retina is composed of two synaptic or plexiform, layers intercalated between three nuclear layers housing neuronal cell bodies (Dowling, 1987). Within these layers are 5 main types of retinal neurons: (1) the photoreceptors, light sensing neurons located within the outer nuclear layer (ONL); (2) horizontal cells which line the distal margin of the inner nuclear layer (INL); (3) bipolar cells are found within the INL and which in association with horizontal cells, receive inputs from photoreceptors via synaptic connections made within the outer plexiform layer (OPL) (Morgan & Morrison, 2003); (4) amacrine cells, located at the proximal INL margin; (5) the retinal ganglion cells (RGCs), which are found within the most proximal retinal region, the ganglion cell layer (GCL) (Dowling, 1987). The inner plexiform layer (IPL) is the area in which ganglion cells synapse with amacrine and bipolar cells. Non-

**Figure 1.1 Schematic of the eye.**

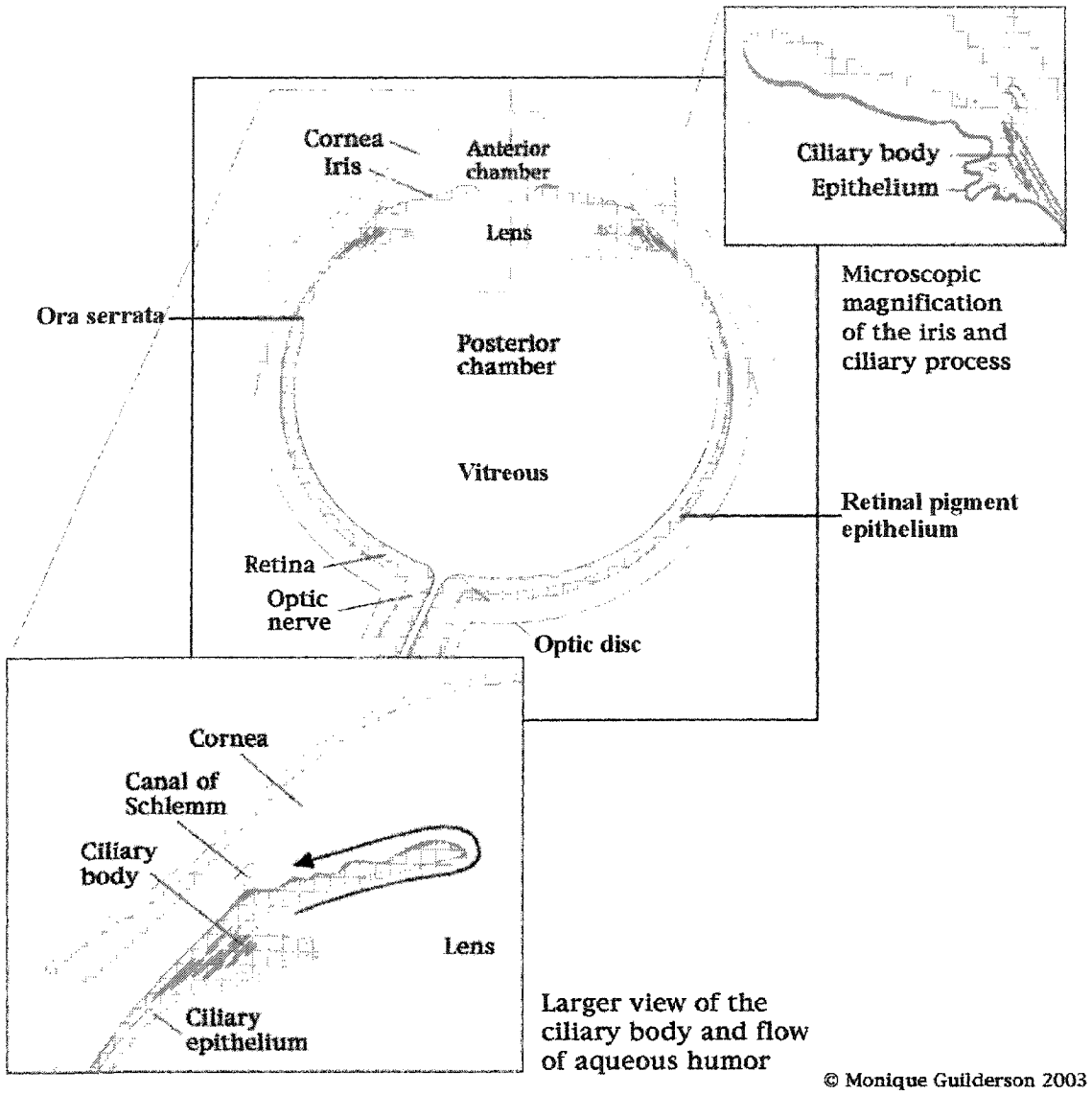
Cornea
Iris
Anterior chamber
Lens
Ora serrata
Posterior chamber
Vitreous
Retina
Optic nerve
Optic disc
Ciliary body
Epithelium
Microscopic magnification of the iris and ciliary process
Retinal pigment epithelium
Cornea
Canal of Schlemm
Ciliary body
Lens
Ciliary epithelium
Larger view of the ciliary body and flow of aqueous humor
© Monique Guilderson 2003

**Figure 1.1**

neuronal cells also inhabit the retina. Although the chief glial cell type in the retina is the Müller glia (Dowling, 1987), astrocytes and microglia (MG) also populate the retina. Müller glial cells extend vertically from the distal limits of the ONL to the proximal confines of the GCL, whereas astrocytes and MG tend to reside within the inner regions of the retina (Figure 1.2.).

Visual perception of objects within our external environment is a concerted effort between the retina and the brain. The model for phototransduction and visual signal processing within the vertical retinal pathway begins with light entering the eye and passing through the retinal layers to be absorbed by the photoreceptor visual pigments (Thompson & Gal, 2003). Once photoreceptor-mediated transduction of light energy has occurred, the signal is then passed from the photoreceptors to the bipolar cells and eventually to the RGCs (Neves & Lagnado, 1999). Horizontal and amacrine cells modify signals traveling in the vertical pathway at synapses within the OPL and IPL, respectively. The importance of RGCs for proper visual functioning is reflected by the fact that these are the only retinal neurons that form connections with targets of the midbrain, namely the lateral geniculate nucleus (LGN) and the superior colliculus (SC) (Isenmann et al., 2003). Due to the fact that RGCs are the primary transmitting cells between the eye and the brain, the death of RGCs results in irreversible vision loss (Levin, 2003). RGC death is present in a variety of optic neuropathies including arteritic and non-arteritic anterior ischemic neuropathy, Leber's hereditary optic neuropathy and glaucomatous optic neuropathy (GON), with GON being the most prevalent RGC disorder (Levin & Gordon, 2002).

**Figure 1.2 Schematic of the retina.**

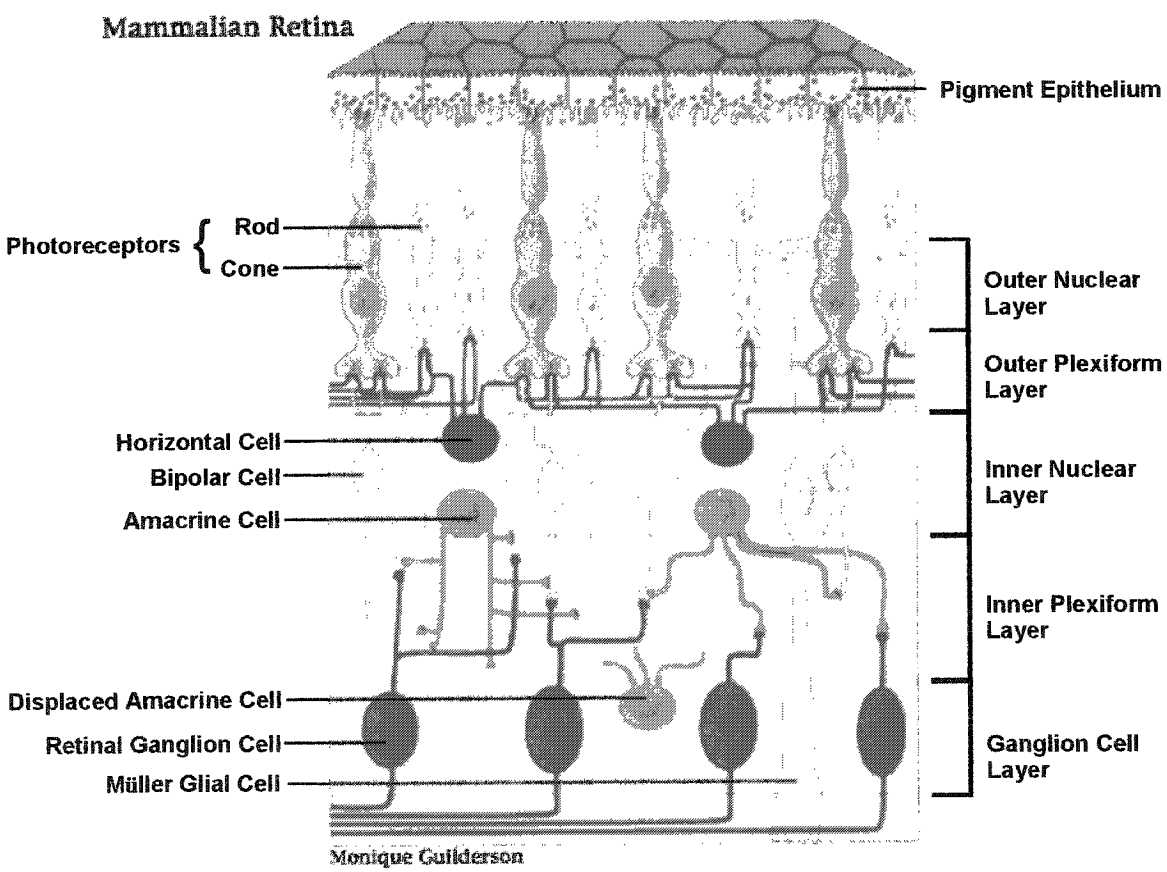
Mammalian Retina
Pigment Epithelium
Photoreceptors
Rod
Cone
Outer Nuclear Layer
Outer Plexiform Layer
Horizontal Cell
Bipolar Cell
Amacrine Cell
Inner Nuclear Layer
Inner Plexiform Layer
Displaced Amacrine Cell
Retinal Ganglion Cell
Müller Glial Cell
Ganglion Cell Layer
Monique Guilderson

Figure 1.2

The glaucomas are a collection of optic neuropathies that occur in a high prevalence amongst elderly populations. Glaucoma has an insidious onset and is associated with a progressive decline in peripheral vision, often associated with elevated pressures within the eye (intraocular pressure; IOP) (Levin & Gordon, 2002). Elevated IOP is thought to lead to mechanical stress, ischemia and loss of trophic support, all of which may contribute to RGC loss in GON. However, while current ocular pressure-reducing therapies decrease IOP, they may not prevent glaucomatous progression (Weinreb & Levin, 1999; CNTGSG, 1998a). Patients may also present with glaucomatous damage despite having IOPs within the normal range and persons with elevated IOPs may not go on to develop glaucoma. Taken together, it is likely that pressure-dependent and pressure-independent factors are involved in the pathogenesis of GON.

The specific mechanism(s) responsible for the induction of glaucomatous damage remain unclear. However, it is widely accepted that RGCs undergo apoptotic death in glaucoma (Garcia-Valenzuela et al., 1995; Kerrigan et al., 1997; Nickells, 1999; Farkas & Grosskreutz, 2001). Apoptosis is a biochemically controlled "suicide" event. All cells in the body have the capacity to activate apoptosis once they are no longer required or once they have sustained injury beyond the point of repair (McKinnon, 1997). Apoptosis or programmed cell death is implicated in maintaining the steady-state kinetics of healthy adult tissues and accounts for the focal deletion of cells during normal embryonic development and metamorphosis (Kerr et al., 1972). A variety of CNS degenerative disorders including Parkinson's disease (PD), Alzheimer's disease (AD), autoimmune deficiency syndrome (AIDS) dementia and stroke all have apoptosis implicated within

their respective etiologies (Leist & Nicotera, 1998). The occurrence of apoptosis provides a critical period during which therapeutic interventions may be applied to rescue the cell (Larner, 2000).

Neuroprotection represents a strategy to either save or preserve neurons, which are susceptible to death following a primary insult or to enhance survival mechanisms intrinsic to the neuron (Weinreb & Levin, 1999). This approach is applicable even when all risk factors are not known because it is designed to rescue the neuron without altering underlying etiological factors. Neuroprotective objectives for GON may include: reducing or neutralizing cytotoxic mediators (glutamate, nitric oxide (NO) and reactive oxygen species (ROS)) within the retinal environment or alternatively reducing the sensitivity of RGCs to these cytotoxic mediators (Schwartz &Yoles, 1999); enhancing the expression of pro-survival factors (Ishii et al., 2003); blocking glutamate-induced increases in intracellular calcium concentrations ($[Ca^{2+}]_i$) (Lipton, 2003); inhibiting proteolytic pathway activation (Isenmann et al, 2003); manipulating inflammatory responses (Bakalash et al., 2002; Schwartz, 2003).

Experimental models designed to study the efficacy and mechanism of action of drugs capable of rescuing injured RGCs and/or preventing the death of healthy RGCs exposed to noxious stimuli, are necessary in order to develop candidate retinal neuroprotective agents which are suitable for adjunctive therapy in combination with pressure lowering modalities for the therapeutic management of GON. The ideal neuroprotective drug should be one that can reach the retina following topical or systemic administration in the most effective concentration to protect RGCs and which exerts the least adverse effects (Osborne et al., 1999b). In addition, where the etiology of glaucoma

is likely multi-factorial, the ideal neuroprotectant should be able to target more than one component of the RGC death cascade (De Keyser et al., 1999).

## *1.2. Epidemiology, Etiology & Risk Factors for Glaucoma*

GON is considered to be the third largest cause of blindness worldwide after cataract and age-related macular degeneration and is responsible for an estimated 5.2 million cases (Thylefors & Negrel, 1994; Congdon et al., 2003). Estimates prepared by the World Health Organization (1997) put the total number of suspect cases of glaucoma at around 105 million. The crisis in North America is that there are likely more than 15 million people affected with GON, yet roughly half of this population are unaware they have it (Tielsch et al., 1991; Raymond, 1997).

The glaucomas may be generally classified into different subtypes according to their etiology, anatomy of the anterior chamber angle or time of disease onset (Quigley, 1999). The most prevalent form of the glaucoma subtypes is primary open angle glaucoma (POAG) (Sheffield et al., 1993). POAG presents with a normal configuration of the irido-corneal angle in the anterior chamber of the eye (Vaughan & Riordan-Eva, 1999) and usually arises in individuals greater than 40 years of age, but may also occur in earlier years of life (Coleman, 1999). POAG itself is considered as a heterogeneous disorder because patients may present with elevated IOPs in association with optic nerve (ON) pathologies, whereas others may have characteristic glaucomatous injury yet exhibit IOPs within the normal accepted range of 10-21 mm mercury (Hg) (Racette et al., 2003; CNTGSG, 1998a; CNTGSG, 1998b). Current global estimates for POAG cases are now at 37 million people (Ray et al., 2003). In 2003, an estimated 600,000 Canadians had POAG and it is predicted that they collectively cost the healthcare system an annual

$300 million (Iskedjian et al., 2003). With no cure currently available, efforts to better understand the etiology of POAG and to develop improved therapies remain a focus of glaucoma research.

The hypothesis that increased pressure within the vitreous chamber of the eye accounts for the ON damage associated with glaucoma was put forward in the mid 1800's by Heinrich Müller and Albrecht von Graefe (Kronfeld, 1974). Through studying post-mortem eyes, these researchers were the first to describe funnel-shaped depressions within the ON that signal a loss of ON fibers. Elevated IOPs may be a considerable risk for glaucomatous damage (Vaughan & Riordan-Eva, 1999). Moreover, the risk for visual field loss increases exponentially with increases in IOP (Quigley, 1993). Despite the linkage between IOP and visual field loss, IOP is no longer regarded as the definitive factor for POAG (Colman, 2003). However, ocular pressure cannot be ruled out of the pathogenesis of NTG entirely due to the fact that a clinical trial demonstrated that a 30% reduction in IOP reduced glaucomatous progression in comparison to non-treated NTG eyes (CNTGSG, 1998a; CNTGSG, 1998b). However, at present, IOP represents the only treatable risk factor in the pathogenesis of glaucoma. Other risk factors for POAG may include advanced age, race, family history and genetics.

## *1.3. The Optic Nerve & Pathologic Change with Glaucomatous Progression*

The ON, which is formed by 777,000-1,679,000 million RGC axons, is the primary site for glaucomatous damage in the eye (Jonas et al., 1992). The ON can be divided into four anatomical layers: (1) retinal nerve fiber layer; (2) prelamina; (3) lamina cribosa; (4) retrolamina. The retinal nerve fiber layer houses the unmyelinated RGC

axons that become organized within papillomacular, nasal radial and arcuate nerve fiber bundles as they converge on the optic disc. The prelamina ON is where the axon nerve fibers are separated into ON head bundles supported by surrounding astrocyte processes (Trivino et al., 1996). Connective sclera plates with pores providing the primary support for ON head bundles, form the lamina cribosa (Elkington, 1990). Astrocytes remain in contact with the bundles and may supply metabolic support (Quigley, 1977) and contribute to the structural integrity of the ONH (Hernandez et al., 1994). The retrolamina marks the beginning of axon myelination. Within the retrolaminar ON, oligodendrocytes generate myelin sheaths to surround the axons *en route* to their targets, the lateral geniculate nucleus and the SC.

GON in adult-onset POAG is characterized by a slowly progressive loss of RGCs and their axons in the ON (Quigley, 1993). The damage within the ON is characterized by a loss of nerve fibers, within the superior and inferior ON poles and this loss matches the pattern of glaucomatous visual field loss (Quigley et al., 1981). Surrounding astrocytes contribute to the pathogenesis of glaucoma by becoming activated to increase the production of basement membrane (type IV) collagen (Hernandez et al., 1994) and elastin (Quigley et al., 1991; Pena et al., 2001), all of which function to make the ON more rigid and likely more susceptible to injury (Zeimer & Ogura, 1989). Knowledge of the exact order of events that lead to the death of RGCs in glaucoma is important for the development of neuroprotective treatments. To date several putative mechanisms have been proposed to underlie RGC death in GON and these may be divided into mechanical, vascular or immunological theories.

The mechanical theory proposes that elevated IOP is an important factor involved in glaucomatous damage. Increased IOP compresses ON bundles at the level of the lamina cribosa, either through misalignment of the connective laminar beams causing the bundles of ON axons to kink (McKinnon, 1997) or via the increased pressure directly compressing the axons. In either case, it has been hypothesized that damage to the axons may lead to blockade of vital transport of trophic factors derived from brain targets to RGC somas, ultimately leading to ganglion cell apoptosis (Nakla et al., 2003). This hypothesis fits well with the pattern of glaucomatous degeneration and visual field loss which is generally observed in GON. Although greater glaucomatous damage occurring within areas of the ON supported by the thinnest laminar beams suggests that these are areas where lamina cribosa plates are more easily misaligned upon increases in IOP. However, the mechanical theory does not completely explain why fewer beams present within the superior and inferior poles of the ONH still give way to increased axonal loss (Nakla et al., 2003). With fewer beams present and thus greater pore size for axons to pass through the lamina cribosa, one would expect axonal bundles to be compressed to a lesser extent. Alternatively, GON resulting from the mechanical theory may occur first at the level of the RGC body rather than at the RGC axons. Transient periods of elevated IOP may compromise Müller glia function to regulate extracellular glutamate levels within the retina (Tanihara et al., 1997). In support of this hypothesis, it has been demonstrated that elevations in IOP, induced through laser treatment of the trabecular meshwork to impede aqueous humor (AH) outflow in the rodent eye, resulted in decreased expression of the Müller glial glutamate transporter EAAT-1 (or GLAST) (Martin et al., 2002). RGCs are known to be selectively susceptible to glutamate

excitotoxicity (Lucus & Newhouse, 1957) and the above mechanism may explain findings of elevated glutamate within the vitreous body of humans with glaucoma (Dreyer et al., 1996).

The vascular theory argues that increased IOP or systemic factors contributing to a compromised blood flow to the ON, explain axonal damage and RGC death in the glaucomatous eye (Hayreh, 1999). The primary source for blood in the ONH arrives via the posterior ciliary arteries (Morgan & Morrison, 2003). Increased IOP-mediated misalignment of lamina cribosa plates, abnormal blood pressure, local vasospasm, haemorrhage or alterations in the physiological and or physical characteristics of retinal blood vessels themselves may all indirectly influence the quality of ONH blood supply (Osborne et al., 2001). A variety of techniques have been developed to assess ocular blood flow in glaucoma patients. These include: angiography, observing the passage of fluorescent dyes through ocular vessels; laser Doppler principles, using optical light waves to detect the passage of red blood cell velocity through a specified blood vessel; measurement of corneal temperature, an indirect measure used to assess ocular blood flow (Flammer et al., 2002). Although the use of these techniques has noted reductions in ocular blood flow in glaucoma patients, it is not known whether alterations in ocular blood flow are a primary insult causing GON or whether these changes result secondary to elevated IOP (Flammer et al., 2002). In either event, reductions in blood supply to the ON can result in retinal ischemia and RGC death.

Ischemic events usually include a necrotic core where the injury originates and a surrounding penumbra of cells undergoing secondary apoptotic death due to the release of injurious substances from cells residing in the epicenter of damage (Dirnagl et al.,

1999). Experimental evidence supports the occurrence of ischemic events following ON compression (Yoles & Schwartz, 1998). These are associated with increased levels of extracellular glutamate, which arise due to energy failure and disruption of normal glutamate reuptake mechanisms (Rothstein et al., 1992; Rothstein et al., 1995; Milton et al., 1997; Massieu & Garcia, 1998; Naskar et al., 2000).

Following subcutaneous injections of L-glutamate in mice, Lucus and Newhouse were the first to observe the toxic effects of glutamate on the inner layers of the retina (Lucus & Newhouse, 1957). In 1969, Olney described this form of neuronal death as a process of over-excitation and coined the term excitotoxicity. Glutamate-mediated neuropathology has been noted in a variety of CNS disorders including stroke, amyotrophic lateral sclerosis (ALS; Rothstein et al., 1992), AD (Mattson, 1994), PD and Huntington's disease (HD; Olney et al., 1990; Lipton & Rosenberg, 1994). Elevations in extracellular glutamate concentrations lead to excessive activation of glutamate receptors (GluRs) including the three ionotropic GluRs: (1) N-methyl-D-aspartate (NMDA); (2) 2-amino-3-(3-hydroxy-5-methylisoxazol-4-yl) proprionate (AMPA); and (3) kainate (KA) receptor subtypes. Activation of the ionotropic GluR subtypes leads to increased intracellular concentrations of $Ca^{2+}$, sodium ($Na^{+}$) and chloride ($Cl^{-}$) ions (Choi, 1987). Increases in these ions contribute to neuronal death through the activation of proteases (Leist, et al., 1997), the uncoupling of mitochondrial oxidative phosphorylation and the release of ROS (Rego & Oliveira, 2003). Inhibition of the NMDA receptors (NMDARs) has been demonstrated to provide neuroprotection following ischemic insults both *in vitro* (Pringle et al., 1997) and *in vivo* (Stuiver et al., 1996). Moreover, RGCs express NMDARs in addition to other types of ionotropic and metabotropic GluRs (Massey &

Miller, 1990). Dreyer and colleagues (1996) noted that the glaucomatous eye has elevated levels of glutamate in the vitreous, which could potentially trigger RGC apoptosis. Dysfunctional glutamate transporters were suggested to be the prevailing mechanism for the increased vitreal glutamate (Maguire et al., 1998; Vorwerk et al., 2000; Martin et al., 2002). However, several different research groups have as yet failed to demonstrate evidence for elevated glutamate within the vitreous of human and experimental glaucomatous eyes (Honkanen et al., 2003; Carter-Dawson et al., 2002; Levkovitch-Verbin et al., 2002a). Regardless of whether glutamate excitotoxicity is involved in the pathogenesis of glaucoma, a number of studies have demonstrated that glutamate antagonists can protect RGCs following increases in IOP (Mosinger et al., 1991).

The hypothesis that ischemic and excitotoxic events play a role in the pathogenesis of POAG supports the potential for NO to also contribute to RGC apoptosis. Moreover, NO-mediated RGC death has been implicated in the pathogenesis of glaucoma (Chao et al., 2000). NO has been described as being a 'double edged sword' capable of being neurotoxic and neuroprotective (Bonne et al., 1998). NO is produced by one of three isozymes of nitric oxide synthase (NOS): (1) neuronal NOS (nNOS); (2) endothelial NOS (eNOS); or (3) inducible NOS (iNOS) (Bonne et al., 1998). The nNOS and eNOS isozymes are also referred to as constitutive NOS (cNOS). The expression of cNOS is believed to be neuroprotective in the retina as post-ischemic inhibition of cNOS has been shown to increase ischemic-reperfusion damage (Hangai et al., 1999). On the other hand, selective inhibition of iNOS, which is located within macrophages, neutrophiles, Müller

glia and MG, was found to provide retinal neuroprotection from elevated IOP-induced retinal ischemia (Geyer et al., 1995).

Support for involvement of the immune system in GON comes from immunohistochemical analysis of sections of human post-mortem glaucomatous ONs revealing activated MG co-localized with transforming growth factor-β2 (TGF-β2), cyclooxygenase-2 (COX-2), TNF-α and proliferating cell nuclear antigen (PCNA) (Yuan & Neufeld, 2001). In contrast, sections from normal eyes showed little evidence of increased expression of these mediators (Yuan & Neufeld, 2001). The simultaneous presence of TGF-β2 and TNF-α within the glaucomatous retina and the exact contribution of MG are not clear. For example, TNF-α and TGF-β2 can have opposing functions in inflammatory and immune reactions in the CNS (Yuan & Neufeld, 2001). Apart from the recent discovery of the protective role TNF-α can play through the NF-κB signalling pathway (Chen & Goeddel, 2002), TNF-α was first recognized for its toxic effects on neurons (Downen et al., 1999) and oligodendrocytes (Selmaj & Raine, 1988). In contrast, TGF-β2 antagonizes MG proliferation and down-regulates inflammatory activities within the glaucomatous ONH (Yuan & Neufeld, 2001). MG in the CNS are thought to function as immune surveillance cells that become activated in response to neuronal injury (Kreutzberg, 1996). Once activated these phagocytes proliferate, present antigens and produce neurodestructive and inflammatory molecules such as NO, eicosanoids and cytokines (Dickson et al., 1993). Activated MG also secrete enzymes that potentially alter the microenvironment (Dickson et al., 1993). In the ONH, activated MG redistribute within the parapapillary chorioretinal region (Neufeld, 1999) and may

become activated either directly or indirectly via mechanical or vascular stress to cause damage to RGCs and the ON.

An alternate view, supporting a contribution of immune factors to the pathogenesis of GON, comes from analysis of sera from glaucoma subjects. Blood samples from NTG patients have been shown to contain increased monoclonal paraproteinemias, a clonal expansion of antibodies specific to B lymphocytes (Wax, 2000). The current hypothesis presented to explain the above finding is that pre-existing immune-related disorders, such as rheumatoid arthritis, have immunopathogens with common antigenic epitopes to that found within the ON, retinal vessels or RGCs, leading to a cross reactivity-mediated GON (Wax, 2000). The idea that auto-antibodies are present in the glaucomatous retina and ON is consistent with findings in other neurodegenerative disorders of the CNS, including encephalomyelitis, multiple sclerosis (MS) and myasthenia gravis (Pluchino et al., 2003).

## *1.4. Current Drug Treatments for Primary Open Angle Glaucoma*

The current therapeutic strategy for managing the glaucomatous eye is to reduce IOP, with the goal in mind that ON damage, RGC death and visual field loss will be arrested once IOP is managed to within a specified target level (Hoyng & van Beek, 2000). If POAG is identified early and managed appropriately, the disease is amenable to therapy (Alward, 1998). Unfortunately due to the insidious progression of POAG, patients are often unaware they are afflicted with the disease and go unidentified until substantial glaucomatous damage has occurred (Colman, 1999). Treatment of IOP relies in large part on ocular hypotensive agents and/or surgery. Surgical approaches primarily include argon laser trabeculoplasty (ALT) of the chamber angle around the scleral spur

and trabecular meshwork to augment aqueous flow and reduce IOP (Spaeth & Baez, 1992).

Present ocular hypotensive treatments for POAG include the following pharmacologic classes: (1) parasympathomimetics; (2) sympathomimetics; (3) sympatholytics; (4) carbonic anhydrase inhibitors; and (5) prostaglandins. Treatment for glaucoma is usually chronic (Hoyng & van Beek, 2000). All of the current hypotensive treatments modify AH dynamics, namely AH production and AH outflow, within the eye. AH is a transparent fluid responsible for nourishing the lens, cornea and trabecular meshwork, via supplying glucose, oxygen and amino acids (Figure 1.1). Flow of AH also functions to remove waste products such as lactic acid and carbon dioxide ($CO_2$), as well as maintaining eye pressure (Green & Pederson, 1973). However, defects in AH outflow can result in an elevated IOP (Cantor, 2003).

Most ocular hypotensive therapies are administered to the eye topically in the form of eye drops; however some hypotensive treatments may be given systemically. Topical hypotensive formulations are at an advantage in comparison to systemic drugs and tend to produce greater intraocular concentrations, while generating fewer unwanted systemic side effects (Hoyng & van Beek, 2000). However, excess topical drug may drain through the nasolacrimal duct into the nose where it can be absorbed into the systemic circulation (Alward, 1998).

In 1864 pilocarpine, a parasympathomimetic/cholinergic agent became the first ocular hypotensive therapy to be prescribed for the management of glaucoma (Cantor, 2003). The parasympathomimetics can interact either directly with muscarinic receptors in the eye or indirectly to prolong the actions of acetylcholine through the inhibition of

endogenous cholinesterase (Hoyng & van Beek, 2000). Factors that provide resistance to AH outflow include IOP, ciliary muscle tone, trabecular meshwork cell activity and the extracellular matrix of both the trabecular meshwork and ciliary body (Morrison & Acott, 2003). As IOP is increased, it is believed that the trabecular meshwork collapses under pressure to retard outflow of AH through Schlemm's canal (Johnstone & Grant, 1973; Brubaker, 2003). Pilocarpine stimulation of muscarinic receptors causes the ciliary muscle to contract resulting in reduced outflow resistance to the trabecular meshwork and Schlemm's canal (Alward, 1998). Ciliary spasm, myopia due to forward displacement and thickening of the lens, blurred vision, conjunctival hyperaemia, retinal detachment, vomiting and nausea, diarrhea, bradycardia, bronchospasm and sweating are all potential adverse effects associated with pilocarpine use (Pape & Forbes, 1978). While pilocarpine was once considered to be a mainstay for treating glaucoma, the associated ocular adverse effects and the drug's multiple dosing regimen currently limit its use (Distelhorst & Hughes, 2003).

The miotic, carbachol, has the ability to both directly stimulate muscarinic receptors and to act as an indirect parasympathomimetic by inhibiting cholinesterase (Hoyng & van Beek, 2000). Inhibition of cholinesterase results in the prolonged duration of action of endogenous acetylcholine within neuromuscular junctions (Alward, 1998). Although the IOP reducing effect of carbachol is greater than that of pilocarpine, its adverse effects are more pronounced and more frequent (Reichert et al., 1988), making its use in the management of POAG limited. Cholinesterase inhibitors, such as echothiophate, are long-acting agents capable of producing serious ocular and systemic

adverse effects (Lesar, 2002). Due to their ability to generate cataracts, the cholinesterase inhibitors are reserved for aphakia or pseudophakia patients (Lesar, 2002).

The sympathomimetics can be divided into two separate divisions; (1) epinephrine-like drugs, those that stimulate the α- and β-adrenergic receptors (ARs); or (2) clonidine-like drugs, those that stimulate only α-ARs (Lewis et al., 1999). Stimulation of ARs allows for increased AH outflow through both the conventional and unconventional routes (Townsend & Brubaker, 1980). In the conventional route, AH exits the eye through the trabecular meshwork and Schlemm's canal (Morrison & Acott, 2003). In contrast, the unconventional route for AH exit, is through the anterior uvea and canals of the sclera into the episcleral space (Morrison & Acott, 2003). Epinephrine, which was introduced as a glaucoma treatment in 1899 (Cantor, 2003), decreases AH production through agonist interactions with α-ARs on the ciliary body, resulting in vasoconstriction and decreased AH production (Serle & Castelbuono, 2003). Epinephrine may also facilitate conventional AH outflow (Wang et al., 2002). Frequent adverse effects are associated with epinephrine use, including blurred vision, vasoconstriction of conjunctival vessels, tachycardia, arrhythmia, high blood pressure, anxiety and anxiousness. These side effects limit the use of epinephrine in managing GON (Hoyng & van Beek, 2000). Dipivefrin, an epinephrine pro-drug, produces fewer ocular and systemic side effects than epinephrine due to its improved intraocular penetrance. However, with the emergence of safer glaucoma medications, dipivefrin is rarely used today (Distelhorst & Hughes, 2003).

The α-AR agonists, brimonidine and apraclonidine, were derived from the systemic antihypertensive agent, clonidine (Alward, 1998), all of which function to

reduce IOP by decreasing AH production and increasing drainage through the uveoscleral route (Toris et al., 1995). In addition, experimental findings also support a neuroprotective role of the α2-AR agonists in the retina, possibly through the induction of basic fibroblastic growth factor (bFGF) expression (Wen et al., 1996; Chao et al., 2000). Adverse effects associated with the use of α-AR agonists include allergic reactions such as blepharitis and conjunctivitis, hyperaemia, staining of the cornea, dry mouth, fatigue and headache (Schuman, 1996). Since brimonidine is more selective for α2-ARs, side effects associated with α1-AR stimulation are less pronounced in comparison to the other α-AR agonists (Hoyng & van Beek, 2000). Brimonidine is capable of achieving a 27% reduction in IOP and is considered a first-line or an adjunctive agent in the treatment of POAG (Serle & Castelbuono, 2003).

Since the late 1970's, the sympatholytics or the β-AR blockers have become the most widely prescribed glaucoma medication and continue to be the benchmark to which newer therapies are compared (Rafuse, 2003). The β-AR blockers are either selective for β1-AR antagonism (e.g. betaxolol) or non-selective, blocking both β1- and β2-ARs (e.g. timolol). Block of β-ARs within the ciliary body reduces IOP through inhibiting AH production (Coakes & Brubaker, 1978). The mechanism for this inhibition is believed to occur via down-regulation of adenylyl cyclase within the ciliary processes (Hoyng & van Beek, 2000). In comparison to the miotics and sympathomimetics, β-AR blockers produce fewer ocular side effects (Hoyng & van Beek, 2000). However, the systemic adverse effects of the non-selective β-AR antagonists are serious due to blockade of β1-ARs of the heart causing bradycardia, arrhythmia and congestive heart failure (McMahon et al., 1979). Interactions with β2-ARs in the lungs can also cause bronchospasm and

status asthmaticus in patients with chronic obstructive pulmonary disease or asthma (McMahon et al., 1979). Since the ciliary body is relatively devoid of β1-ARs, the ability of betaxolol to decrease AH production may be due to nonspecific interactions with β2-ARs in the ciliary body (Reiss & Brubaker, 1983). While the IOP-reducing efficacy of betaxolol is less than that of timolol, betaxolol has been demonstrated to preserve visual field better (Messmer et al., 1991). The improved functional vision observed with betaxolol treatment compared to timolol may be best explained by the ability of betaxolol to directly inhibit $Ca^{2+}$, $Na^{+}$ and potassium ($K^{+}$) influx in RGCs (Hoste & Sys, 1998; Baptiste et al., 2002; Hirooka et al., 2000). However, it remains debatable as to whether or not betaxolol is superior to timolol in the treatment of glaucoma as no statistically significant difference was observed between betaxolol- and timolol-treated patients either in improvements in the changes in mean retinal sensitivity or in the change in localized scotomatous areas (Vainio-Jylha & Vuori, 1999). While the ocular side effect profile for betaxolol is similar to that of the non-selective β-AR antagonists, the reduced frequency of cardiovascular systemic adverse effects associated with betaxolol may increase the likelihood of its indication in treating patients with GON.

The enzyme, carbonic anhydrase, catalyzes the conversion of $CO_2$ to bicarbonate (Alward, 1998). Within the ciliary body, bicarbonate is required for the formation of AH. The carbonic anhydrase inhibitors (CAIs) function to block endogenous carbonic anhydrase enzymes and work to lower IOP through decreasing AH production (Wistrand et al., 1986). The systemic CAI formulations (e.g. acetazolamide) have very few ocular side effects, but it is their systemic adverse effects that limit their use. These include paresthesia, fatigue, depression, renal stones, nausea and vomiting. The topical CAIs

avoid the frequent systemic effects of the oral or intravenous formulations, although they can produce stinging and burning, temporarily blurred vision, itching and tearing (Hoyng & van Beek, 2000).

The prostaglandins are $F_2\alpha$ analogs that work to decrease IOP through facilitating AH outflow via the uveoscleral route (Mishima et al., 1997). All of the prostaglandin analogs are pro-drugs that are hydrolyzed by corneal esterases into biologically active free acid molecules that easily penetrate the cornea (Hylton & Robin, 2003). Latanoprost was the first prostaglandin analog to be marketed and is capable of producing a 25-35% reduction in IOP (Hylton & Robin, 2003). Ocular adverse effects with latanoprost use include burning, tearing, punctuate keratitis, blurred vision, foreign body sensation and the possibility for increased pigmentation of the iris and eyelashes (Johnstone, 1997). Since long-term studies have not reported systemic adverse effects, prostaglandins are regarded as a first line therapy for the therapeutic management of glaucoma (Hylton & Robin, 2003).

## *1.5 Rationale for Development of Neuroprotective Strategies in Glaucoma*

The modulation of AH dynamics in order to reduce IOP can aid in the preservation of ON integrity and vision. The reduction of IOP can itself be considered as a neuroprotective strategy in glaucoma management. Even NTG patients benefit from reductions in IOP (CNTGSG 1998a; CNTGSG 1998b; Heijl et al., 2002). Unfortunately, there is no guarantee that ON damage and accompanying visual field loss will be arrested following reductions in IOP (Brubaker, 1996). In the above study, 12% of patients receiving IOP reducing therapy demonstrated glaucomatous progression (CNTGSG

1998a). In addition, issues of patient compliance and adverse effects associated with ocular hypotensive therapies may limit the effectiveness of IOP reduction in certain patients (CNTGSG 1998b). The best suited therapy for preventing glaucomatous deterioration may be one that incorporates IOP reduction in conjunction with a non-pressure related neuroprotective strategy.

Attempts have been made to apply neuroprotective strategies to a variety of CNS degenerative disorders (Ritch, 2000). Similarities in the mechanism(s) of neuronal loss between several CNS degenerative disorders and that occurring in GON, suggest a paradigm shift towards neuroprotective therapy should be considered for preventing glaucomatous damage (Ritch, 2000).

RGCs represent the output neurons of the retina that connect to visual centers in the brain via RGC axons (Levin, 2003). The irreversible vision loss, which occurs in glaucoma, is a direct result of the apoptosis of RGCs (Garcia-Valenzuela et al., 1995; Kerrigan et al, 1997; Nickels, 1999; Farkas & Grosskreutz, 2001). Apoptosis is a genetically regulated biochemical event that initiates the expression of genes, which trigger cell death and removal without activating an inflammatory response (Kerr et al., 1972). Apoptosis differs from necrosis both biochemically and morphologically. Necrosis, unlike apoptosis, does not require active gene expression to be induced (Wyllie et al., 1980). Furthermore, necrosis involves cell swelling, with eventual rupture of the cell membrane to release intracellular proteolytic enzymes into the extracellular environment, thus generating an inflammatory reaction (Wyllie et al., 1980). The process of apoptosis can be divided into 4 different stages: (1) initiation, the activation of immediate early genes responsible for regulating the expression of pro-apoptotic genes;

(2) commitment, the point in time where removal of the initial trigger does not affect the outcome of apoptotic neuronal death; (3) execution, activation of effector cysteine-dependent aspartate-dependent proteases (caspases) leading to the digestion of integral cellular components; (4) elimination, apoptotic cells are removed from the CNS by phagocytosis (Larner, 2000). Cellular insults implicated in the etiology of glaucoma, including trophic insufficiency and ischemia with associated excitotoxicity, have been shown to initiate apoptosis in neurons (Tatton et al., 2001). Confirmation that RGCs die via apoptosis suggests that applied neuroprotective strategies targeting key proteins in the RGC apoptotic death cascade may be successful in diverting this death (Nickells, 1999). Three putative neuroprotective strategies in POAG are: (1) enhancement of survival mechanisms innate to RGCs; (2) protection of RGCs from ischemic or excitotoxic events; (3) protection of the axons of the ON (Johnson & Morrison, 2003).

Enhancement of RGC innate survival mechanisms represents a direct neuroprotective approach. This may occur by altering the expression of genes involved in regulating apoptosis, such as p53, B-cell lymphoma (leukaemia)-2 (Bcl-2) family members or supplying trophic factors to the RGCs (Johnson & Morrison, 2003), all of which ultimately affect the release of apoptogenic factors from the mitochondria (Tatton et al., 2001). Neuronal mitochondrial-dependent apoptosis signalling has been linked to trophic factor deprivation (TFD), ischemia and glutamate-induced excitotoxicity, where levels of ATP are not completely abolished (Fiskum et al., 2003). Mitochondrial release of pro-apoptotic factors occurs either through the opening of mitochondrial permeable transition pores (Marzo et al., 1998) or through disruption of the outer mitochondrial membrane itself (Fiskum et al., 2003). The p53 tumor suppressor protein, along with

members of the Bcl-2 gene family, is intricately involved in mitochondrial-dependent apoptosis signalling. The role of p53 is to function as the guardian to the cell genome, determining cell cycle progression (Lin et al., 2002). If genomic DNA is sufficiently damaged the p53 transcription factor can arrest the cell cycle by increasing the expression of the cyclin dependent kinase inhibitor, $p21^{Ras}$ (Liu et al., 2003). In addition, p53 increases the synthesis of the pro-apoptotic Bcl-2-associated X protein (Bax), while concomitantly depressing the expression of anti-apoptotic Bcl-2 (Nickells, 1999). The Bcl-2-related proteins share conserved regions designated as the Bcl-2 homology (BH) domains BH1, BH2, BH3 and BH4 (Kelekar & Thompson, 1998). Members of the Bcl-2 family interact via BH domains allowing for the proteins to form homo- and heterodimers (Larner, 2000). The interactions between pro- and anti-apoptotic Bcl-2 members sets a cellular 'apoptostat' that determines the propensity of the cell to undergo apoptosis (Larner, 2000). In addition, Bax homodimers are believed to form mitochondrial channels allowing the release of cytochrome c (cyt c) to the cytoplasm, ultimately leading to the generation of the apoptosome and apoptosis mediated through the activation of a caspase cascade (Nickells, 1999). Therefore, compounds capable of increasing the expression of anti-apoptotic Bcl-2 family members or decreasing p53 and pro-apoptotic Bcl-2 related proteins are potentially neuroprotective. Cao and colleagues (2002) recently used recombinant gene technology to develop a bioactive Bcl-$x_L$ fusion protein, derived from the human immunodeficiency TAT protein, which could be administered systemically to effectively reduce brain infarction following occlusion of the central cerebral artery. Intravitreal injections of brain derived trophic factor (BDNF) and ciliary neurotrophic factor (CNTF) have also been shown to protect RGCs from ON axotomy-

mediated apoptosis (Mey & Thanos, 1993). Mitogenic factors (Finkbeiner & Greenberg, 1996) and $Ca^{2+}$/calmodulin are believed to increase $p21^{Ras}$ expression, which in turn stimulates phosphatidylinositol 3-kinase (PI-3K) to phosphorylate protein kinase B (also referred to as Akt) (Tatton et al., 2001). Phosphorylated Akt is activated to phosphorylate the pro-apoptotic Bcl-2 family member, Bcl-2 associated death protein (Bad), which in turn, interacts with 14-3-3 proteins instead of forming Bad-Bcl-2 or Bad-Bcl-xL heterodimers, ultimately inhibiting Bad-mediated apoptosis (del Peso et al., 1997; Tatton et al., 2001; Steelman et al., 2004). Activated Akt may also contribute to neuronal survival through the activation of NFκB (Lilienbaum & Israël, 2003).

Heat shock proteins (Hsps) can be intrinsically expressed in the retina after ischemia and or excitotoxic events, to functionally protect cells (Lewden et al., 1998). Hsps function as molecular chaperones to prevent protein aggregation and facilitate refolding of dysfunctional proteins necessary for the viability of the cell (Morimoto & Santoro, 1998). The proposed mechanisms for survival promotion by the Hsps are through the suppression of immediate early pro-apoptotic gene, c-Jun N-terminal kinase (JNK) activation, prevention of mitochondrial cyt c release, disruption of apoptosome formation, inhibition of apoptosis protease activating factor (Apaf)-1 and suppression of pro-caspase recruitment (Ishii et al., 2003). Recently it has been demonstrated that systemically administered geranylgeranylacetone (GGA) can protect RGCs in a chronic elevated rat IOP model of glaucoma by inducing the expression of Hsp72 (Ishii et al., 2003). GGA is an acyclic polyisoprenoid developed and used clinically in Japan for treatment of ulcers through the expression of gastric mucosal cell Hsps (Hirakawa et al., 1996).

The family of neurotrophins is comprised of fibroblast growth factor (FGF), CNTF, nerve growth factor (NGF), BDNF and the neurotrophins 3 and 4/5 (NT-3, NT-4/5) (Dawbarn & Allen, 2003). NT-6 has only been identified in fish (Gotz et al., 1994). Neurons that fail to synapse to targets supplying trophic support die through an apoptotic route (Dawbarn & Allen, 2003). Neurotrophins are retrogradely transported in the CNS (Distefeno et al., 1992) and in the retina it is believed that RGCs receive trophic support through retrograde axonal transport from the SC and LGN (Fournier et al., 1997; Ma et al., 1998). In addition, RGCs and amacrine cells represent internal trophic stores within the retina (Cusato et al., 2002). It has been demonstrated previously that if the source of trophic support to RGCs is depleted, rescue may occur, albeit transiently, upon supplementation of trophic factors (Mey & Thanos, 1993). Temporary rescue of RGCs with neurotrophins may be explained by an ability of BDNF to induce the expression of both protective cNOS and injurious iNOS (Klöcker et al., 1999). However, the success of applying neurotrophins as a neuroprotective strategy may be hindered clinically due to their poor pharmacokinetic profiles and current lack of effective methods for their administration into the retina (Dawbarn & Allen, 2003). Recently, some success has been obtained using viral-mediated transfer of trophic factors to delay RGC death after ON transection or following elevated IOP in animal models (van Adel et al., 2003; Martin et al., 2002).

The use of GluR antagonists and $Ca^{2+}$ channel blockers as a neuroprotective strategy for glaucoma is consistent with ischemia and excitotoxic theories (see Introduction, section 1.3.). In a recent double-blind, parallel-group clinical trial where patients with moderate-to-severe AD were randomly assigned to memantine, a non-

competitive NMDAR antagonist, or to an identical placebo, memantine was shown to effectively reduce symptoms associated with AD without having a significant association with increased adverse effects (Reisberg et al., 2003). At present, memantine is being evaluated for its potential in managing GON (Lipton, 2003). Glutamate, the most prominent neurotransmitter in the CNS, is implicated in the visual signal processing within the vertical retinal pathway following phototransduction (Bloomgren & Dowling, 1985a; Bloomgren & Dowling, 1985b; Thoreson & Witkovsky, 1999; Aarts & Tymianski, 2003). Moreover, glutamate is required for cognition, memory, movement and sensation (Lipton & Rosenberg, 1994). This then poses a problem with the use of GluR blockers, because the same processes that contribute to excitotoxic neuronal death are required for normal retinal function (Lipton, 2003). The non-competitive NMDA antagonists, amantidine and memantine have exhibited positive effects in stabilizing dementia and PD (Ikonomidou & Turski, 2002). Despite the above findings, clinical trials for stroke and traumatic brain injury, with second and third generation NMDAR blockers have failed (Ikonomidou & Turski, 2002). Recently, Hardingham and coworkers (2002) demonstrated that contradictory biologic functions exist between synaptic and extra-synaptic NMDARs. Glutamate stimulation of synaptic NMDARs triggers neuroprotective $Ca^{2+}$-dependent cAMP-response element binding protein (CREB)-mediated BDNF expression in neurons, while stimulation of extra-synaptic NMDARs mediates a $Ca^{2+}$-dependent CREB shut off to block BDNF expression, leading to mitochondrial dysfunction and neuronal apoptosis (Hardingham et al., 2002). Thus the current failure with NMDAR blockers may be due to the inappropriate use of non-

specific NMDAR antagonists that antagonize synaptic NMDARs. It therefore seems fitting to direct a search for extrasynaptic NMDAR antagonists.

$Ca^{2+}$ channel blockers are already prescribed in the treatment of systemic hypertension, coronary artery disease, stroke, cardiac arrhythmias and vasospasm (Ritch, 2000). Vasospasm characteristically presents in association with cold hands, low blood pressure, migraine, myocardial ischemia and high plasma levels of endothelin-1 (ET-1) (Flammer et al., 2002). ET-1 is a potent vasoconstrictor produced by vascular endothelial cells and has been shown to be to be elevated within the AH from glaucomatous dogs (Källberg et al., 2002) and humans (Tezel et al., 1997; Noske et al., 1997). Moreover, while ET-1 basal plasma levels were demonstrated to be similar between glaucomatous patients and control subjects, patients with GON have ET-1 abnormally increased following body cooling (Nicolela et al., 2003). In addition, administration of ET-1 to the retina causes activation of astrocytes and glaucomatous-like ON damage in animal models (Prasanna et al., 2002; Chauhan et al., 2004). Thus, $Ca^{2+}$ channel blockade is hypothesized to be beneficial in the management of POAG (Flammer et al., 2001; Toriu et al., 2001). Additionally, $Ca^{2+}$ channel blockers may be useful in combating excessive glutamate-induced $Ca^{2+}$ influx through NMDARs during ischemia-reperfusion insults of the CNS. Multiple voltage-dependent $Ca^{2+}$ channels (VDCCs) exist, namely, L-, N-, P-, Q-, R- and T-types that can be distinguished based on their individual pharmacologic properties and voltage-dependent kinetics (Kobayashi & Mori, 1998). Retinal neurons predominantly have L-, N-, P- and T-type VDCCs (Hartwick, 2001). Early administration of nimodipine, an L-type $Ca^{2+}$ channel blocker and flunarizine, primarily a T-type $Ca^{2+}$ channel blocker, have been demonstrated to reduce infarct size after focal

cerebral ischemia (De Keyser et al., 1999). Although some success has been reported using certain $Ca^{2+}$ channel blockers in ET-1/ischemic animal models (O'Neill et al., 2001; Toriu et al., 2001; Stuiver et al., 1996; Sun et al., 1999), this strategy has proven to be unsuccessful in clinical trials (Kobayashi & Mori, 1998; De Keyser et al., 1999).

In the retina $Ca^{2+}$ channels are found on RGC somas and ON axons. ON axons are rich in L- and N-type $Ca^{2+}$ channels, as well as $Na^{+}/Ca^{2+}$ exchangers (Sun & Chiu, 1999; Fern et al., 1995). Elevations in intra-axonal $Ca^{2+}$ following insults of mechanical compression, ischemia or excitotoxicity can activate calpains, a proteinase implicated in myelin and cytoskeletal protein degradation in white matter (Ray et al., 1999). Calpains are present within the mammalian ON (Blomgren & Karlsson, 1990); however, the inhibition of these proteases has not been proven experimentally to provide functional ON preservation (Jiang & Stys, 2000). Moreover, the effects of systemic $Ca^{2+}$ antagonists on calpain-induced ON axon damage have not yet been assessed. Furthermore, although the use of $Ca^{2+}$ channel blockers may decrease RGC apoptosis in GON, a double masked placebo controlled study conducted on patients with POAG demonstrated that systemically administered nifedipine is not well tolerated and there were no obvious beneficial effects on visual fields or ocular perfusion (Rainer et al., 2001). Further clinical studies on different $Ca^{2+}$ channel blockers are still required to validate this approach.

## *1.6. Overall Hypothesis*

*Drugs capable of decreasing glutamate-induced increases in intracellular calcium concentration and inhibiting proteolytic pathways that lead to pro-apoptotic gene expression will enhance retinal neuron viability following excitotoxicity, trophic factor deprivation or optic nerve transection.*

## *1.7. Objectives of Study*

The overall objectives of this research are:

1. **To compare the efficacy of various β-AR antagonists, α2-AR agonists and tetracycline derivatives to protect retinal neurons in cell culture or animal models of excitotoxicity, TFD or ON transection and**
2. **To determine the pharmacological mechanism(s) underlying the retinal neuroprotective actions of AR drugs and tetracycline derivatives.**

# CHAPTER 2

# GENERAL METHODS

## 2.1. Cell Culture

### *2.1.1. Primary Retinal Cells*

Primary cultures consisting of retinal neurons and glia were obtained from Long Evans rat pups, 6-10 days of age. All procedures were carried out in accordance with the ARVO statement for the use of Animals in Ophthalmic and Vision Research and the Canadian Council for Animal Care. Rat pups were anaesthetized using halothane inhalation, sacrificed by decapitation and the eyes were enucleated. In a laminar flow hood, each eye was placed in a 35 mm diameter Petri dish and washed with 10% fetal bovine serum (FBS) and 1% gentamicin, in Dulbecco's Modified Eagle's Medium (D-MEM(+); Sigma, St. Louis, MO). With the aid of a dissecting microscope, the globes were bisected along the equator just above the ora serrata. The posterior eye-cup with the retina attached was placed in fresh D-MEM(+) and the anterior portions of the eye, including the cornea, lens, iris and vitreous were discarded. The retina was then gently dissected free using fine forceps. Isolated retinas were collected in a 15 ml test tube containing fresh D-MEM(+) and centrifuged at 1,000 rpm for 3 min. The contaminating RPE, which appears as a black layer overlaying the white neural retina precipitate, was removed by gentle suction through a fire-polished Pasteur pipette. The resulting neural retinal pellet was dissociated by incubation with 1 ml of 0.125% trypsin in D-MEM at 37 °C for 3 min. The trypsin action was terminated by adding 2 ml of D-MEM(+). The resulting retinal cell suspension was then centrifuged at 1,000 rpm for 3 min and the

**Primary retinal cell media compositions (ml)**

| | GM(+) | GM(-) | TM | TMG | DMEM(+) |
|---|---|---|---|---|---|
| D-MEM | 89.84 | 94.84 | - | - | 89.5 |
| D-MEM with Ham's F12 | - | - | 89.84 | 88.84 | - |
| FBS | 5 | - | 5 | 5 | 10 |
| L-glutamine (200 mM) | 0.25 | 0.25 | 0.25 | 0.25 | - |
| N-2 Supplement (100X) | 1 | 1 | 1 | 1 | - |
| Sodium Pyruvate (110 mg/ml) | 1 | 1 | 1 | 1 | - |
| Taurine (375 µg/ml) | 1 | 1 | 1 | 1 | - |
| Tri-iodo-L-thyronine (200 µg/ml) | 0.01 | 0.01 | 0.01 | 0.01 | - |
| Cytidine 5`-Diphospho-ethanolamine (1.28 mg/ml) | 0.1 | 0.1 | 0.1 | 0.1 | - |
| Cytidine 5`-Diphospho-choline (2.56 mg/ml) | 0.1 | 0.1 | 0.1 | 0.1 | - |
| Hydrocortisone (200 µg/ml) | 0.1 | 0.1 | 0.1 | 0.1 | - |
| BDNF (1 mg/ml) | 1 | 1 | 1 | 1 | - |
| CNTF (1 mg/ml) | 0.1 | 0.1 | 0.1 | 0.1 | - |
| L-glutamate (10 mM) | - | - | - | 1 | - |
| Gentamycin | 0.5 | 0.5 | 0.5 | 0.5 | 0.5 |

**Table 2.1**

supernatant was aspirated. A volume of 4 ml primary retinal cell growth media (GM(+) see Table 2.1.) was then added to the retinal cell pellet. The resulting cell suspension was homogenized by triturating with a narrow bore fire-polished Pasteur pipette to create a suspension of single cells. An aliquot of the cell suspension (50 µl) was then combined with an equal volume of 4% trypan blue (Sigma) for determination of cell viability and cell density. Viable cells exclude the trypan dye and appear phase-bright under an inverted light microscope. Conversely, compromised or dying cells take up trypan blue and appear blue. Viable cells were counted by applying 10 µl aliquots onto the grids of a hemocytometer and viewed with an inverted light microscope. Cells, at a density of $2.5x10^5$ cells/ml, were then seeded in 24 well culture dishes pre-coated with laminin (2 µg/ml) and poly-$_D$-lysine (10 µg/ml) and maintained in a humidified incubator at 37 °C with an atmosphere of 5% $CO_2$/95% $O_2$. For maintenance of primary retinal cell cultures half of the GM(+) was replaced with fresh GM(+) every 2-3 days.

### *2.1.2. E1A-NR.3 Retinal Cell Line*

Sub-culture of the E1A-NR.3 retinal cells was carried out using methods previously described (Tezel & Wax, 1999; Xu et al., 1999). Cells growing in 50 ml flasks were incubated at 37 °C with 2 ml calcium magnesium free-ethylenediaminetetraacetic acid (CMF-EDTA) containing 0.0625% trypsin-EDTA for 5 min. E1A-NR.3 cells were then triturated with a narrow bore fire-polished Pasteur pipette and transferred into a fresh 15 ml test tube. The trypsin reaction was stopped by adding 5 ml of E1A-NR.3 GM(+) (see Table 2.2.). The resulting cell suspension was centrifuged at 1,000 rpm for 3 min to obtain a cell pellet. The supernatant was then aspirated and replaced with another 5 ml of GM(+). The cell pellet was then homogenized by triturating

**E1A-NR.3 cell line media compositions (ml)**

| | GM(+) | GM(-) | TM | TMG | DMEM(+) |
|---|---|---|---|---|---|
| D-MEM | 83.875 | 93.875 | - | - | 89.5 |
| D-MEM with Ham's F12 | - | - | 83.875 | 82.875 | - |
| FBS | 10 | - | 10 | 10 | 10 |
| L-glutamine (200 mM) | 1 | 1 | 1 | 1 | - |
| Sodium bicarbonate (7.5%) | 3 | 3 | 3 | 3 | - |
| MEM non-essential amino acids (100X) | 1 | 1 | 1 | 1 | - |
| MEM vitamins (100X) | 1 | 1 | 1 | 1 | - |
| L-glutamate (10 mM) | - | - | - | 1 | - |
| Gentamycin | 0.125 | 0.125 | 0.125 | 0.125 | 0.5 |

**Table 2.2**

with a narrow bore fire-polished Pasteur pipette to yield single cells in suspension. The volume of the cell suspension was adjusted to achieve a cell density of $1x10^5$ cells/ml. Cells were then seeded into 24 well culture dishes, 35 mm culture dishes or 50 ml flasks and maintained in a humidified incubator at 37 °C with an atmosphere of 5% $CO_2$/95% $O_2$. The GM(+) was replaced with fresh GM(+) every 2-3 days.

### *2.1.3. C6 Glioma Cell Line*

Sub-culture of the C6 glial tumor cells was carried out using methods previously described (Koufali et al., 2003). For cells growing in 50 ml flasks, growth media was first aspirated and cells were dissociated by adding 2 ml 0.25% trypsin-EDTA for 15 min. The cells were then triturated with a narrow bore fire-polished Pasteur pipette and then transferred to a 15 ml test tube. The trypsin reaction was stopped by adding 6 ml of D-MEM(+) (see Table 2.1.). The resulting cell suspension was centrifuged at 1,000 rpm to obtain a cell pellet. The supernatant was aspirated and replaced with 4 ml of D-MEM(+). The cell pellet was then homogenized by triturating with a narrow bore fire-polished Pasteur pipette to yield single cells in suspension. The volume of the cell suspension was adjusted to achieve a cell density of $1x10^5$ cells/ml. Cells were then seeded in 24 well culture dishes and maintained in a humidified incubator at 37 °C with an atmosphere of 5% $CO_2$/95% $O_2$. The D-MEM(+) was replenished with fresh D-MEM(+) every 2-3 days.

### *2.1.4. Pheochromocytoma Cell Line*

Culture and differentiation of pheochromocytoma (PC12) cells was carried out using a previously defined protocol (Greene, 1978). Undifferentiated PC12 cells were maintained in 50 ml flasks containing D-MEM supplemented with 10% horse serum

(Gibco), 5% FBS (Gibco), 2 mM L-glutamine (Gibco) and 100 μg/ml penicillin-streptomycin (Sigma) (GM; see Table 2.4.). To differentiate PC12 cells, GM was removed and the cells were washed 3X with 4 ml of Hank's Balanced Salt Solution (HBSS; Gibco). The cells were then triturated in HBSS using a narrow bore fire-polished Pasteur pipette. The resulting cell suspension was centrifuged at 1,000 rpm for 5 min, the supernatant was aspirated and the cell pellet was re-suspended in another 4 ml of HBSS. The above steps of centrifugation and aspiration were repeated once more and the cell pellet was then resuspended in 2 ml of GM containing 100 ng/ml nerve growth factor (7S NGF; Collaborative Research Inc., Bedford, MA; GM(+) (see Table 2.4.)). The cell suspension was triturated to obtain a homogeneous solution before assessment of cell viability and cell density, as described previously. The PC12 cell suspension was added at a density of $6x10^4$ cells/ml to 35 mm diameter culture dishes pre-coated with rat-tail collagen (1 mg/ml). Both undifferentiated and differentiated PC12 cultures were maintained in a humidified atmosphere of 5% $CO_2$/95% $O_2$ and replenished with fresh GM or GM(+) respectively, every 2-3 days.

## 2.2. Immunocytochemistry

### *2.2.1. Identification of Neurons and Glia*

A double-labelling technique previously described (Baptiste et al., 2002) was used to identify retinal neurons and glia in primary retinal cultures. Primary retinal cultures were grown on glass coverslips pre-coated with laminin and poly-$_D$-lysine in 24 well culture plates for 3-7 days. The cells were first washed with phosphate buffered saline (PBS; Sigma) and then fixed in 100% methanol for 5 min at 20 °C. Cells were permeabilized with 0.3% Triton-X (Sigma) for 20 min at room temperature. The

permeabilized cells were washed 3X with PBS and background staining minimized by blocking non-specific binding of the secondary antibodies with PBS containing 10% normal sheep serum for 1 hr at room temperature. Following removal of the blocking solution, a mixture of the primary antibodies, including a 1:200 dilution of mouse β-tubulin (TUJ1; Babco, Richmond, CA) and 1:50 dilution of glial fibrillary acidic acid protein (GFAP) was added. β-tubulin is a specific marker for neuronal microtubules and GFAP labels glial cells. The cells were incubated with the primary antibodies overnight at 4 °C. Negative control experiments had primary antibodies omitted. Subsequently, the cells were washed in PBS with agitation on an orbital shaker 3X for 5 min. They were then incubated with a 1:500 dilution of goat anti-mouse IgG conjugated to Alexa Fluor 546 and goat anti-rabbit IgG conjugated to Alexa Fluor 488 secondary antibodies (both secondary antibodies from Molecular Probes, Eugene, OR) for 1 hr at room temperature. The cells were then washed once with distilled water and 3X with PBS. The coverslips were mounted with aqueous mount (glycerol/PBS 1:1) and the cells were viewed with a Nikon C1 microscope equipped for epifluorescence with filters for G-1B (excitation 546 nm; barrier 590 nm; emission 575 nm) and FITC (excitation 450-490 nm; barrier 520-560 nm; emission 505 nm).

## 2.3. Retinal Cell Death Models

### *2.3.1. Glutamate-induced Excitotoxicity*

Glutamate-induced cell death was carried out using primary retinal cell cultures and the E1A-NR.3 retinal cell line. Primary retinal cells were grown in 24 well culture dishes for 7 days before being divided into groups of 3-4 wells. Each group was treated with one of the following treatments: (1) treatment media (TM); (2) TM + L-glutamate

(TMG); (3) TMG + drug (see Tables 2.1. and 2.2.). Standard formulations of D-MEM contain 0.8 mM magnesium. At this concentration, magnesium is capable of antagonizing the NMDAR (Hahn et al., 1988; Zeevalk & Nicklas, 1992) and for this reason standard D-MEM formulations are not suitable for *in vitro* studies of glutamate excitotoxicity. To circumvent this problem, we used the Ham's F12 formulation of D-MEM, which contains no magnesium, includes supra-physiological concentrations of calcium (10 mM $CaCl_2$) and has 50 μM endogenous glutamate (see Table 2.3.) (Pellegrini & Lipton, 1993). Thus, the final glutamate concentrations for the groups TM and TMG are 50 and 150 μM respectively. Following treatment, both retinal cell types were incubated in a humidified atmosphere of 5% $CO_2$/95% $O_2$ and maintained at 37 °C. After 24 hr incubation retinal cell survival was quantified using the Zap-Oglobin cell lysis technique, as described in the General Methods, section 2.4.1.

### *2.3.2. Trophic Factor Deprivation-induced Cell Death*

Trophic factor deprivation (TFD) was carried out using cultures of primary rat retinal cells, the E1A-NR.3 retinal cell line and the NGF-differentiated PC12 cell line. All cell types were grown for 3-5 days in 35 mm diameter culture dishes. After 3-days of culture the GM(+) was aspirated and the cells were gently washed with PBS (3X) to remove trace amounts of trophic factors and divided into one of 3 groups: (1) GM(+); (2) GM(-), which received GM minus serum and trophic factors; (3) GM(-) + various concentrations of drugs (see Tables 2.1., 2.2. and 2.4. for cell-type specific media composition). Upon division into their various treatment groups, cells were returned to their 37°C incubator and maintained in a humidified atmosphere of 5% $CO_2$/95% $O_2$ until further analysis. Cell survival was assayed in primary retinal cells using the Zap-Oglobin

**D-MEM Ham's F12 formulation**

| | |
|---|---|
| Distilled water | 500 ml |
| D-MEM with Ham's | 0.074 g (10 mM) |
| Calcium chloride | 0.555 g (10 mM) |
| Sodium bicarbonate | 1.6 g (14 mM) |
| Magnesium | - |

*pH to 7.4 with 1N HCl or 1N NaOH

**Table 2.3**

**PC12 cell line media compositions (ml)**

| | GM | GM(+) | GM(-) |
|---|---|---|---|
| D-MEM | 83 | 82 | 98 |
| Horse serum | 10 | 10 | - |
| FBS | 5 | 5 | - |
| L-glutamine (200 mM) | 1 | 1 | 1 |
| NGF 7S (10,000 ng/ml) | - | 1 | - |
| Penicillin-streptomycin (10,000 μg/ml) | 1 | 1 | 1 |

**Table 2.4**

cell lysis technique following 24 hr of TFD (Gupta et al., 1997). Cell viability of the PC12 and E1A-NR.3 cultures were assessed at 24 or 48 hr following TFD, respectively. Viable and apoptotic cells were quantified using the acridine orange/ethidium bromide (AO/EB) assay (Bertolesi et al., 2002).

## 2.4. Cell Survival Assays

### *2.4.1. Zap-Oglobin Cell Lysis*

To determine the number of viable cells per treatment group the cells from individual wells of a 24 well culture plate were triturated and transferred into individually numbered 15 ml culture tubes. Cells, which retained anchorage to the bottom of the plate, were removed using a 5 min incubation with 500 µl of 1X trypsin-EDTA in D-MEM at room temperature. The enzymatic reaction was terminated with an equal volume of D-MEM+ (see Table 2.1.). The cell suspensions were centrifuged at 1,000 rpm for 3 min and the supernatant was removed. The resulting cell pellets were lysed with 200 µl of a 1:10 dilution of Zap-Oglobin detergent made up in PBS. Nuclear membranes differ from cellular membranes in that the former include extensions of the endoplasmic reticulum. Healthy cells have intact nuclear membranes, which resist the lytic effects of detergents and therefore under light microscopy these appear as both circular and phase bright. Conversely, cells, which are undergoing cell death, have weaker, more fragile nuclear membranes, hence in the presence of a detergent the nuclear membrane becomes disassembled and the dying cells present either as irregularly shaped intact nuclei or as cellular debris. Two 10 µl aliquots of each well were counted on a hemocytometer, with at least three separate wells included for each treatment group.

### *2.4.2. Acridine Orange-Ethidium Bromide*

The viability of retinal cells and PC12 cells following TFD was quantified using AO/EB dye exclusion (Bertolesi et al., 2002). Briefly a mixture of 100 μg/ml AO and 100 μg/ml EB was made in PBS. Both AO and EB are DNA intercalating dyes, however, only EB is excluded from incorporating into the nucleus of viable cells. Dying cells allow the incorporation of both dyes. Cells were then visualized with a Nikon C1 microscope equipped for epifluorescence with filters for UV-2A (excitation 330-380 nm; barrier 420 nm; emission 400 nm). Therefore, the type of cell death can be determined based upon nuclear color and morphological criteria (Bertolesi et al., 2002). For example healthy viable cells take up AO within their DNA to display large green nuclei, whereas cells undergoing cell death take up both AO and EB within their DNA. Dying cells in turn exhibit one of two predominant patterns: (1) condensed or pyknotic orange/red nuclei, which are indicative of cells undergoing apoptotic cell death; or (2) large orange/red nuclei, equivalent in size to viable nuclei, characteristic of cells undergoing necrotic cell death. Following TFD, the media was removed and the cells were washed 2X with PBS. Following this, 1.5 ml of the AO/EB solution was applied to the culture dishes for 3 min at room temperature, after which the cells were washed with PBS. Nuclei derived from live and apoptotic cells were quantified using epifluorescence microscopy upon placing a micrometer grid with an optical field area of 0.23 $mm^2$ under the view of a 20X objective. Color pictures were captured with a Nikon FDX 35 mm digital camera through a Nikon Multi-Point Sensor System U-III using either a 20X objective or a 100X oil immersion objective.

### *2.4.3. Retrograde Labelling of Retinal Ganglion Cells*

Using adult Long Evans male rats weighing 225-275 g RGCs were retrogradely-labelled via the SC with the stable vital tracer, Fluoro-Gold (FG 2% in 0.9% NaCl). Rats used for labelling were maintained in a 12 hr light: 12 hr dark cycle (7 am: 7 pm) and were anesthetized by intraperitoneal injection with 1mg/kg body weight of anesthetic cocktail consisting of 1 mg/kg ketamine hydrochloride (Vetalar; Vetrepharm, Belleville, ON), 1mg/kg xylazine (Rompun; Bayer Inc., Toronto, ON) and 1mg/kg acepromazine (Atravet; Ayerst Veterinary Laboratories, Guelph, ON). The rat heads were shaved, wiped with gauze soaked in 70% ethanol to sterilize the area and remove excess hair and the animal was secured with ear bits to a stereotaxic apparatus. A 1 mg/kg dose of bupenephrine was administered prior to surgery to ensure effective analgesic action immediately upon completion of the labelling procedure. Using a binocular microscope, an oval shaped hole was drilled into the skull at the midpoint between Bregma and Lambda to expose both lobes of the cerebellum. Overlying pia was carefully dissected so as not to rupture major blood vessels and a blunted 25 5/8 gauge needle attached to a suction apparatus was used to remove the overlying cerebellum and expose the SC. A single small piece of gelfoam soaked in 2% FG (made in 0.9% NaCl) was placed over the top of each SC. The incision was sealed with staples and Polysporin ointment was then applied to the wound. Animals were given 0.6 ml 0.9% NaCl by intraperitoneal injection to account for blood loss. Upon completion of the labelling procedure, animals were returned to fresh cages and allowed to recover under a heat lamp.

### *2.4.4. Optic Nerve Transection*

Animals were maintained for 5-7 days after FG-labelling to allow retrograde transport of the dye to the RGC somas in the retina before intraorbital axotomy of the ON. FG-labelled rats were anesthetized and secured within a stereotaxic apparatus as previously described (see section 2.4.3.). Using a binocular microscope the skull was wiped with gauze soaked in 70% ethanol and the right superior conjunctiva was sutured and weighted with forceps to retract the ON into a more accessible position for transection. The skin overlying the skull was also sutured and pulled down over the eye. The second suture was held in place with tape. Using a number 10 razor, an incision in the conjunctiva was made close to the orbital rim and lateral to the cornea. The orbit was opened, lacrimal glands were moved out of view to the side and extra-ocular muscles were separated to expose the ON. After removing the overlying dura, complete transection of the ON was made at a distance of 1-2 mm from the back of the globe using micro-scissors. Care was taken not to interfere with the blood supply via the central retinal artery. Following transection of the ON, the characteristic arbor of blood vessels for the operated right eye was fundoscopically checked with an ophthalmoscope. The contralateral unoperated left eye served as control. Animals were returned to their cages and allowed to recover under a heat lamp.

### *2.4.5. Retinal Whole-mounts*

Five to fourteen days after ON transection, rats were sacrificed with a $CO_2$ overdose and the eyes were enucleated and placed in vials containing 0.9% NaCl. Enucleated eyes were then transferred to a dissecting dish and, using binocular microscopy, the lens was removed. The remaining ocular tissues were then placed in

small jars containing 4% paraformaldehyde and fixed for 3 hr on a mechanical shaker. Following fixation, the retinas were carefully dissected, cut into quadrants and whole-mounted in mounting media (Sigma) on glass slides. The slides were covered with a 22x22 $mm^2$ cover-slip and sealed with nail polish. All slides were labelled with water-soluble marker and given to an independent investigator for recoding to mask the identification of retinal tissue from the initial investigator. The slides were examined using a Nikon C1 microscope equipped for epifluorescence with filters for UV-2A (excitation 330-380 nm; barrier 420 nm; emission 400 nm). Black and white images of retinal whole-mounts were captured with a COHU High Performance CCD camera using a 20X objective (standard area of 0.23 $mm^2$). Experimental and control retinas had FG-positive cells quantified at eccentric distances of 1, 2 and 3 mm from the optic disc for each quadrant. The FG-loaded SC results in selective retrograde labelling of RGCs, as these are the only retinal cells that synapse with the SC. Retinal MG become visible following damage to retrogradely-labelled RGCs because these activated phagocytes engulf the surrounding FG-positive RGC debris and dying RGCs. However, the two cell types can be easily distinguished from each other based on morphological criteria. RGCs are recognized by their large circular cell bodies, conversely MG present as small rod shaped cells, which are often, aligned parallel to the retinal vasculature (Thanos et al., 1994; Naskar et al., 2002).

## 2.5. Caspase-3 Analyses

### *2.5.1. Reverse Transcription Polymerase Chain Reaction*

Total cellular RNA was obtained from the E1A-NR.3 retinal cell line using TRIzol™ reagent according to the manufacturer's protocol. The RNA concentration,

absorption and ratio of RNA:DNA were determined spectrophotometrically using a GeneQuant ™II RNA/DNA calculator (Amersham Biosciences, Piscataway, NJ). The RNA samples (10 μg) were then DNase I-treated and used to generate single-stranded complementary DNA (cDNA) with the Moloney Murine Leukemia Virus Reverse Transcriptase. All PCR amplifications were carried out in a total volume of 25 μl with 2 ng of cDNA, 0.4 μM primers, 50 mM KCl, 10 mM Tris-HCl, pH 8.8, 1.5 mM $MgCl_2$, 0.2 mM dNTP and 2.5 units of recombinant Taq DNA polymerase (Denovan-Wright et al., 1999). Primer sequences have been previously published for cyclophilin (Hirooka et al., 2002) and caspase-3 (Harrison et al., 2001) (see Table 2.5.). To compare caspase-3 messenger ribonucleic acid (mRNA) levels of expression between the various TFD treatment groups (GM(+), GM(-) and GM(-) + drug; see Table 2.2.), the number of PCR cycles was determined to be in the linear range to ensure that the differences in noted amplification efficiencies did not arise due to the depletion of the reaction components listed above (Bustin, 2000; Freeman et al., 1999). The number of cycles and annealing temperatures for each gene investigated were 20 cycles at 50 °C for cyclophilin and 30 cycles at 55 °C for caspase-3. The duration for annealing was 40 sec. Denaturation and extension temperatures occurred at 94 °C for 30 sec and 72 ° C for 1 min 10 sec respectively for each primer. The PCR products were resolved by staining with EB and by electrophoresis in a 1.5% agarose gel. PCR products were visualized under UV illumination using a Geldoc imaging system (Bio-Rad, Mississauga, ON, Canada). Images of the PCR bands were subjected to densitometry using Molecular Analyst image software version 1.5 (Bio-Rad, Hercules, CA).

**Primer sequences used in RT-PCR reactions**

| Gene | Accession No. | PCR Product Size (base pairs) | Sequence 5'-3' |
|---|---|---|---|
| Caspase-3 | U49930 | 636 | ACC TCA GAG AGA CAT TCA TGG<br>CCC ACT CCC AGT CAT TCA TTT |
| Cyclophilin | Y00052 | 371 | TGG TCA ACC CCA CCG TGT TCTT<br>GCC ATC CAG CCA CTC AGT CTTG |

**Table 2.5**

### *2.5.2. Western Blot*

E1A-NR.3 cells were washed with PBS and transferred to 1.5 ml Eppendorf tubes and centrifuged at 1,000 rpm for 5 min. The tubes were then placed on ice and 100 µl of Cell Lysis Buffer (Cell Signalling Technology Inc., Beverly, MA) was added. After 20 min the pellets were sonicated briefly and centrifuged for 10 min at 5,000 rpm at 4 °C. The resulting supernatants were transferred to fresh 1.5 ml Eppendorf tubes and the protein concentrations were determined using the bicinchoninic acid (BCA) protein assay kit (Novagen, Pierce, Rockford, IL) with bovine serum albumin (BSA) as a calibration standard. Protein samples were then diluted to equivalent concentrations with aliquots of sodium dodecyl sulphate (SDS) buffer and heated at 95 °C for 5 min. The application of the anionic detergent, SDS, together with heating serves to denature the protein while still providing a negative surface charge. The protein mass can be determined with SDS-polyacrylamide gel electrophoresis (SDS-PAGE; 12%) because the amount of SDS bound to the protein is proportional to the molecular weight of the protein (Sambrook et al., 1989). Proteins were electro-transferred to a nitrocellulose membrane at 95 volts for 1 hr. The membranes were dried for 2 hr and then incubated on an orbital shaker with a 1:1,000 dilution of primary rabbit anti-rat caspase-3 monoclonal antibody overnight at 4 °C. Membranes receiving only the primary antibody skim milk diluent served as negative controls. Membranes were then washed 3X with PBS-Tween 80 for 5 min before incubation with secondary antibody horse radish peroxidase (HRP) conjugated goat anti-rabbit IgG at a dilution of 1:2,000 for 1 hr at 37 °C. Following this, membranes were washed 3X with PBS-Tween 80 at 37 °C on an orbital shaker for 20 min. Protein bands were visualized with the enhanced chemiluminescence detection system (ECL System;

Super Signal, Pierce, Rockford, IL) and exposed to film (XAR; Kodak). Negative controls were conducted in experiments by excluding primary antibodies.

## 2.6. Statistical Analysis

### *2.6.1. Statistical Tests*

All *in vitro* data were analyzed by with one-way analysis of variance (ANOVA) followed by parametric post-test analysis with either a Dunnett Multiple Comparison test to allow assignment of one treatment group to be set as a control group to which all other test groups were compared (Pan & Kupper, 1999) or a Bonferroni Multiple Comparison test when only two groups were compared. *In vivo* data were analyzed by the non-parametric two-tailed Mann-Whitney Rank Sum test. On normalization to contralateral controls, *in vivo* data were tested for normality with the Kolmogorov-Smirnov test followed by a parametric ANOVA with a Dunnett Multiple Comparison post-test. All statistics were computed using GraphPad Instat version 3.00 Software for Windows 95 (San Diego, CA). The criterion for noting a significant difference was $p<0.05$, a probability conventionally thought to minimize type one and type two errors simultaneously (Zar, 1999).

# CHAPTER 3

# AN EVALUATION OF THE NEUROPROTECTIVE EFFECTS OF ADREONCEPTOR DRUGS IN RETINAL CELL CULTURES

## 3.1. Introduction

Glutamate, the predominant excitatory amino acid neurotransmitter in the vertebrate CNS, has diverse actions on post-synaptic receptors due to the actions of a variety of ionotropic and metabotropic classes of GluRs (Thoreson & Witkovsky, 1999). Glutamate's actions in the CNS can be both physiological and pathological. Glutamate is responsible for neuronal plasticity, memory, growth, survival and differentiation, and following phototransduction glutamate acts as an important neurotransmitter for visual signal processing within the vertical retinal pathway (Bloomgren & Dowling, 1985a; Bloomgren & Dowling, 1985b; Thoreson & Witkovsky, 1999; Aarts & Tymianski, 2003). In direct contrast, elevations in extracellular glutamate arising from traumatic or ischemic events, leads to over excitation of GluRs, increased $Ca^{2+}$ influx and a heightened activation of $Ca^{2+}$-dependent enzymes, including iNOS, which ultimately results in the accumulation of NO and ROS. This in turn causes lipid peroxidation, mitochondrial dysfunction, caspase activation, genomic cleavage and ultimately neuronal death (El-Remessy et al., 2003). Apoptosis-mediated excitotoxic neuronal death is believed to be very important in the etiology of many degenerative disorders of the CNS (Lipton, 2003). Apoptotic RGC death has been reported in several ON disorders including GON (Garcia-Valenzuela et al., 1995; Kerrigan et al, 1997; Nickels, 1999), the most common of the optic neuropathies (Levin & Gordon, 2002). Although controversy

exists surrounding the involvement of excitotoxic events in the pathogenesis of GON, excessive stimulation of GluRs leads to selective damage to the inner layers of the retina and ultimately RGC death (Lucus & Newhouse, 1957; Li et al., 1999). Furthermore, GluR antagonists have been demonstrated to rescue RGCs following axonal damage (Calzada et al., 2002; Schuettauf et al., 2000; Kikuchi et al., 2000). The therapeutic potential of GluR antagonists has not yet been realized in clinical trials for human disease, largely due to the adverse effects associated with the large doses required to provide neuroprotection (Ikonomidou & Turski, 2002; De Keyser et al., 1999). Memantine, an NMDAR open channel blocker, is currently in phase III clinical trials for use in GON (Kilpatrick & Tilbrook, 2002) and continued research is underway for the development of safer neuroprotective compounds which have the ability to prevent excitotoxic neuronal death without the associated adverse effects.

Currently, medical management for GON is focused largely on targeting sites within the ciliary body and various outflow routes, in order to decrease AH secretion and facilitate AH outflow which in turn can help in reducing IOP (Cantor, 2003). However, because GON likely has a multi-factorial etiology, additional pressure-independent factors are expected to be involved (Halpern & Grosskreutz, 2002). In addition to their IOP reducing qualities, the selective β1- AR antagonist, betaxolol (Agarwal et al., 2002; Woo Cheon et al., 2002; Cheon et al., 2003; Wood et al., 2003) and the α2-AR agonist, brimonidine (Lafuente López-Herrera et al., 2002; Ahmed et al., 2001; Donello et al., 2001; Levkovitch-Verbin et al., 2000), have previously been reported to be neuroprotective for retinal neurons. Although increased RGC survival was observed in *in vivo* experiments, it was not possible to differentiate whether the protective effects were

targeted directly to retinal neurons and /or to the retinal vasculature itself. An *in vitro* cell culture system would permit the neuroprotective mechanism(s) of betaxolol and brimonidine to be studied in a controlled experimental system devoid of vasculature.

After a review of the current literature in this area, we hypothesized that the neuroprotective effects of betaxolol and brimonidine may occur via the inhibition of GluR-induced increases in $[Ca^{2+}]_i$ in retinal neurons. This research compares the neuroprotective efficacy and possible mechanism(s) of action for the β-AR antagonists: betaxolol, metoprolol and timolol; and the α2-AR agonist, brimonidine, in a retinal cell culture model of excitotoxic injury.

## 3.2. Materials & Methods

### *3.2.1. Cell Cultures*

Primary cultures consisting of retinal neurons and glia were obtained from Long Evans rat pups, 6-10 days of age. Rat pups were anaesthetized with halothane, sacrificed by decapitation and the eyes were enucleated as previously described (see General Methods, section 2.1.1.). Retinal cells at a density of $2.5x10^5$ cells/ml were seeded in 24 well culture dishes pre-coated with laminin and poly-$_D$-lysine and maintained in a humidified incubator at 37 °C with an atmosphere of 5% $CO_2$/95% $O_2$. For maintenance of primary retinal cell cultures half of the GM(+) was replaced with fresh GM(+) every 2-3 days.

Sub-culture of the C6 glial tumor cells was performed using methods previously described (see General Methods, section 2.1.3.). C6 cells were seeded at density of $1x10^5$ cells/ml in 24 well culture dishes and maintained in a humidified incubator at 37 °C with

an atmosphere of 5% $CO_2$/95% $O_2$. The D-MEM(+) was replenished with fresh D-MEM(+) every 2-3 days.

### *3.2.2. Immunocytochemistry*

Neurons and glia within mixed primary rat retinal cell cultures were identified using the generalized protocol outlined in section 2.2.1. Neurons were labelled with a primary mouse monoclonal anti-β-tubulin antibody (used at a 1:200 dilution in PBS), whereas glia were identified by staining with a rabbit polyclonal antibody specific for GFAP (used at a 1:50 dilution in PBS). The secondary antibodies used were goat anti-mouse IgG conjugated to Alexa Fluor 546 and goat anti-rabbit IgG conjugated to Alexa Fluor 488, both at a dilution of 1:500. The coverslips were mounted with aqueous mount (glycerol/PBS 1:1) and the cells were viewed with a Nikon C1 microscope equipped for epifluorescence with filters for G-1B (excitation 546 nm; barrier 590 nm; emission 575 nm) and FITC (excitation 450-490 nm; barrier 520-560 nm; emission 505 nm).

### *3.2.3. Cell Survival Assays*

Glutamate-induced excitotoxicity was carried out using primary retinal cell cultures or the C6 glioma cell line by replacing the normal growth media with an alternative media which contained 50 μM glutamate, no magnesium and was supplemented with 10 mM $Ca^{2+}$ (see General Methods, section 2.3.1. and Tables 2.1., 2.2. and 2.3.). Cell cultures grown in 24 well culture plates were divided into treatment groups consisting of the following media: (1) treatment media (TM); (2) TM + L-glutamate (TMG); or (3) TMG + drug (see Tables 2.1. and 2.2.). Following treatment, retinal cells were incubated in a humidified atmosphere of 5% $CO_2$/95% $O_2$ and maintained at 37 °C for 24 hr. Retinal cell survival was then quantified using the Zap-

Oglobin cell lysis technique, as previously described (see General Methods, section 2.4.1.). Mean cell counts were obtained from 3-4 wells per treatment group and expressed as a percentage of the number of intact nuclei derived from viable cells in the control TM group. Mean percentage data ± SD were obtained from 3-6 separate experiments. The drugs used were betaxolol, timolol and metoprolol (β-AR antagonists) and brimonidine (α2-AR agonist), and the effect of each drug was tested over the range of concentrations from 1-1,000 μM. The specificity of the effect of brimonidine was further investigated with the α2-AR antagonist yohimbine at 1 and 10 μM. Solutions of brimonidine were prepared from stocks dissolved in dimethyl sulfoxide (DMSO; 1%). Therefore, in experiments in which brimonidine was used; equivalent amounts of DMSO were also added to the other treatment solutions (i.e. TM and TMG). All other drugs were prepared from stocks dissolved in PBS free of $Ca^{2+}$ and magnesium.

### *3.2.4. Statistical Analysis*

All data generated were analyzed using one-way ANOVA followed by parametric post-test analysis with either Bonferroni or Dunnett Multiple Comparison tests (GraphPad Instat version 3.00; San Diego, CA). The criterion for noting a significant difference was $p<0.05$.

## 3.3. Results

### *3.3.1. Immunocytochemical Identification of Retinal Neurons & Glia*

Neuronal and glial cells were identified in retinal cultures via immunocytochemistry with antibodies specific for neuron specific β-tubulin and glia selective GFAP (Figure 3.1). β-tubulin-labelled retinal neurons, which frequently grow on top of a glial monolayer, had defined cell bodies with processes (neurites) longer than

**Figure 3.1 Double–labelled epifluorescence photomicrograph of the primary retinal cell culture.** Retinal neurons were identified with an antibody against neuron-specific β-tubulin (TUJ1; red); glial cells were labelled by an antibody against glial fibrillary acidic acid protein (GFAP; green). Scale bar = 10 μm.

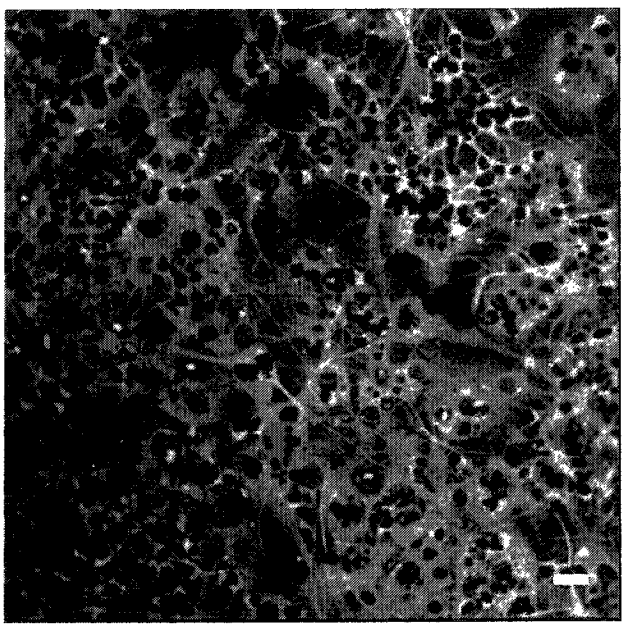

**Figure 3.1**

**Figure 3.2 Effect of excitotoxic media on retinal cell viability.** The number of intact nuclei for primary retinal cell cultures following a 24 hr exposure to media containing D-MEM Ham's F12 formulation (TM); or TM plus an additional 1, 10, 100 or 1000 μM glutamate concentrations (TMG). Cell viability was assessed by counting the density of intact nuclei derived from healthy retinal cells after Zap-Oglobin cell lysis. Data are from 3 separate experiments and are expressed as mean ± SD. $^{**}p<0.01$ compared to the TM control group.

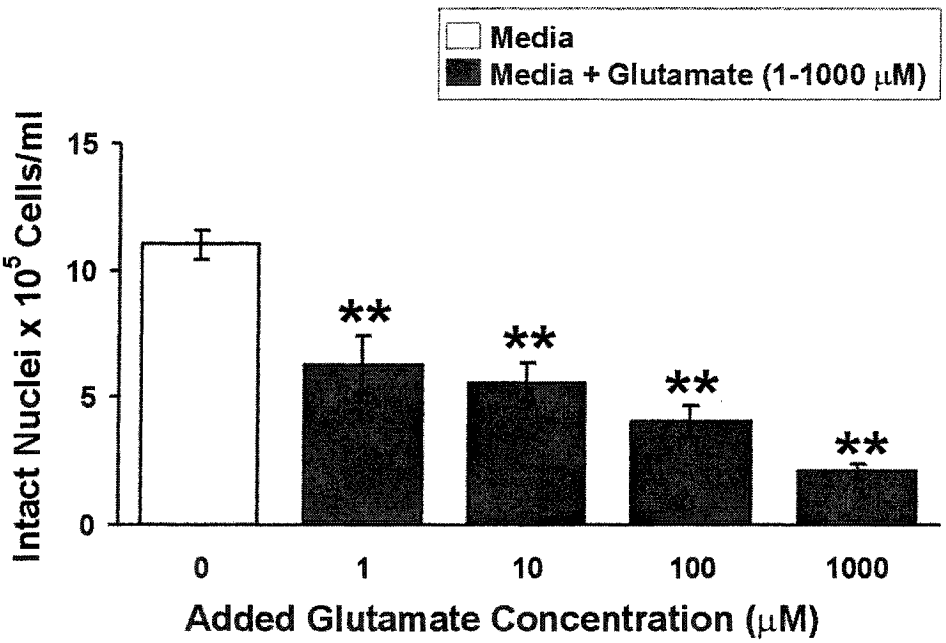
Media
Media + Glutamate (1-1000 μM)
Intact Nuclei x 10^5 Cells/ml
15
10
5
0
**
**
**
**
0
1
10
100
1000
Added Glutamate Concentration (μM)

**Figure 3.2**

twice the cell bodies. On the other hand, GFAP-labelled retinal glial cells exhibited a flattened morphology with less pronounced processes in comparison to β-tubulin-labelled retinal neurons. Co-localization of β-tubulin and GFAP was never observed. In subsequent survival assays, neurite lengths greater than twice the diameter of the corresponding soma were used to distinguish retinal neurons from glia. Estimates of neuronal populations within mixed retinal cultures were approximately 35%-40%.

### *3.3.2. Effect of Glutamate on Retinal Neuron Survival*

The effects of adding increasing amounts of glutamate on cell viability were assessed in mixed retinal cultures of neurons and glia using the Zap-Oglobin cell lysis method. Following 24 hr incubation with exogenously added glutamate (1-1000 μM), retinal cell survival was significantly reduced, in a dose-dependent manner, in comparison to the control group (Figure 3.2). Cell survival declined to 57% ± 10%, 51% ± 7%, 37% ± 6% and 19% ± 3% of the control group at 1, 10, 100 and 1000 μM glutamate, respectively. The decrease in retinal cell viability was significant for all doses of exogenously added glutamate ($p<0.01$). Subsequently, the 100 μM exogenous glutamate concentration was selected as the test dose for all excitotoxic experiments because this dose reliably produced approximately 50% or greater reductions in mixed retinal cell culture viability.

To further determine the viability of both neurons and glia following excitotoxic challenge, the number of neurite-bearing and non-neurite bearing cells was quantified in 10 successive 680 x 460 μm high-power (40x objective) fields, under phase contrast inverted light microscopy, before and after 24 hr incubation in 150 μM glutamate (Figure 3.3). At the end of the 24 hr exposure, the survival of neurite-bearing cells was reduced

**Figure 3.3 Morphological analysis of retinal neurons & glia after excitotoxic insult.** The number of neurite-bearing neuronal cells (processes greater than twice the diameter of the corresponding cell body) and non–neurite-bearing glial cells counted in 10 successive 680 x 460 μm high-power (40x objective) fields, before and after 24 hr of exposure to 150 μM glutamate. Data are from 3 separate experiments and are expressed as the mean ± SD. ***$p<0.001$ compared to control TM.

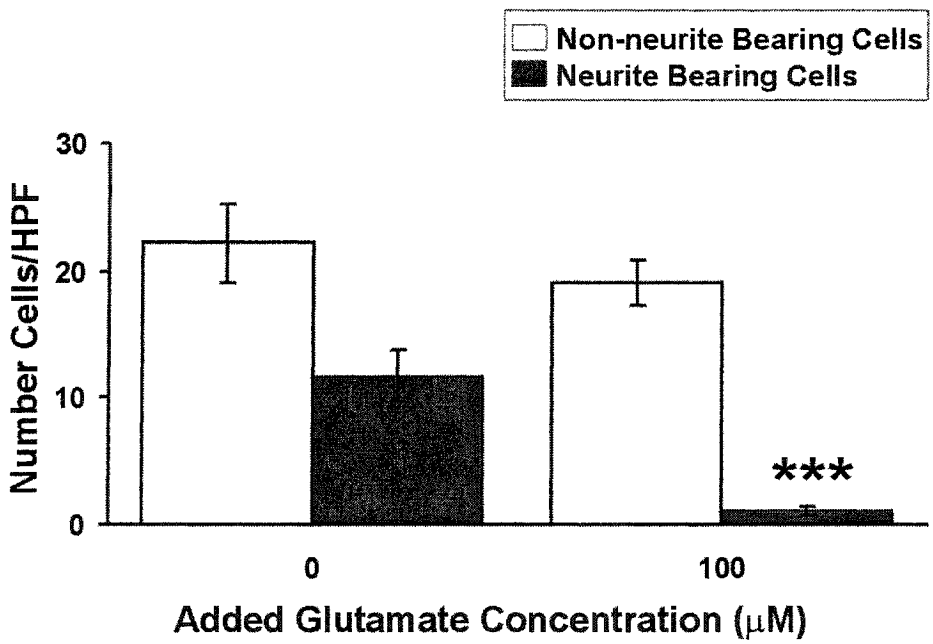
Non-neurite Bearing Cells
Neurite Bearing Cells
Number Cells/HPF
30
20
10
0
***
0
100
Added Glutamate Concentration (μM)

**Figure 3.3**

**Figure 3.4 Effect of excitotoxic media on C6 glioma cell viability.** The number of intact nuclei for C6 glioma cell line cultures following 24 hr of exposure to media containing D-MEM Ham's F12 formulation (TM); or TM plus an additional 10 or 100 μM glutamate concentrations (TMG). Cell viability was assessed by counting the density of intact nuclei derived from healthy C6 glioma cells after Zap-Oglobin cell lysis. Data are derived from 4 separate experiments and are expressed as the mean ± SD.

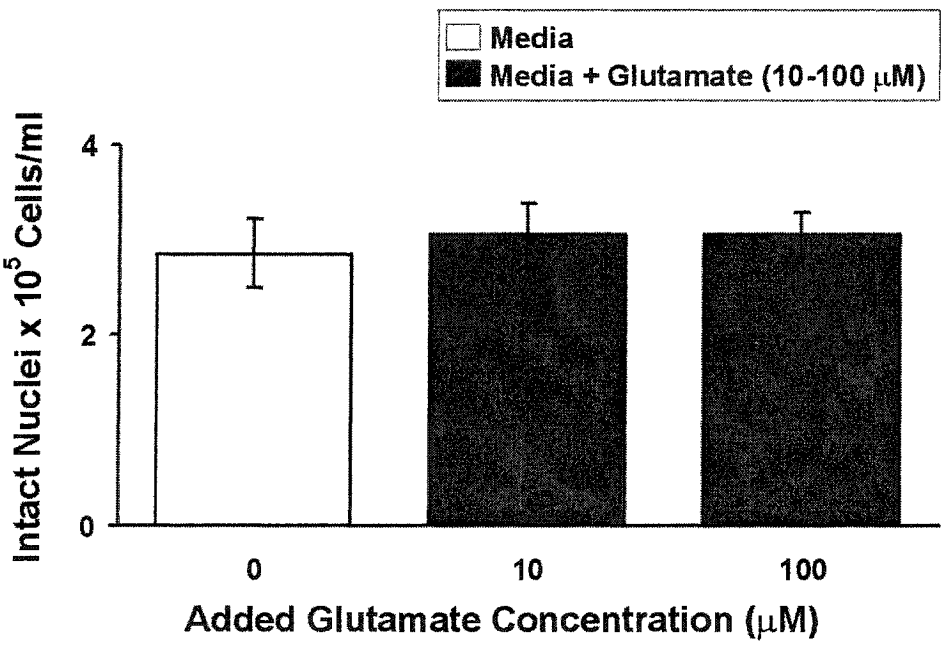
Media
Media + Glutamate (10-100 μM)
Intact Nuclei x 10^5 Cells/ml
4
2
0
0
10
100
Added Glutamate Concentration (μM)

**Figure 3.4**

by 91% ($p<0.001$). In comparison, the viability of non-neurite bearing cells was only reduced by 14% ($p>0.05$). Analysis of the effects of glutamate excitotoxicity in a pure glial cell line culture, C6 glioma, revealed no significant decrease in cell viability (Figure 3.4). Addition of 10 and 100 μM glutamate to C6 glioma cultures for 24 hr did not significantly alter the number of viable cells (107% ± 12% and 107% ± 8% of the control group, respectively ($p>0.60$)). These results corroborate those of others in that elevations in extracellular glutamate concentrations result primarily in a significant decline in retinal neuron viability. In direct contrast, C6 glial cultures, which are known to support NMDA-mediated currents (Liu et al., 1997), exhibited no reduction in cell survival when exposed to similar glutamate levels.

### *3.3.3. Effects of β-Adrenoceptor Antagonists on Retinal Neuron Survival*

The first class of drugs tested for survival promoting effects following excitotoxic challenge were the β-AR antagonists. Following a 24 hr incubation with 100 μM added glutamate, retinal cell viability was reduced to 53% ± 7% of the control group. In contrast, addition of increasing doses of the selective β1-AR blocker, betaxolol, simultaneously with 100 μM glutamate resulted in a dose-dependent increase in viability from 56% ± 17%, 78% ± 3%, 92% ± 26% and 86% ± 52% for 1, 10, 100 and 1000 μM betaxolol concentrations, respectively (Figure 3.5). This increase in cell survival was significant at 100 μM betaxolol ($p<0.05$) with increased variability at the higher 1000 μM dose limiting the significance ($p>0.05$), possibly due to inconsistency in responses of neuronal and glial populations within test wells or non-specific drug-receptor actions at higher concentrations.

**Figure 3.5 Effect of betaxolol on retinal cell viability following exposure to excitotoxic media.** Percent intact nuclei for primary retinal cells treated with the selective β1-AR blocker, betaxolol, following 24 hr of glutamate excitotoxicity. Cell viability was assessed by counting the density of intact nuclei derived from healthy retinal cells after Zap-Oglobin cell lysis. Treatment groups consisted of: media containing D-MEM Ham's F12 formulation (TM); TM plus an additional 100 μM glutamate (TMG); or TMG plus various doses of betaxolol (1-1000 μM). Data are from 3 separate experiments and are expressed as the mean ± SD (%) of the TM control group (100%). *$p<0.05$ compared to the TMG-only group.

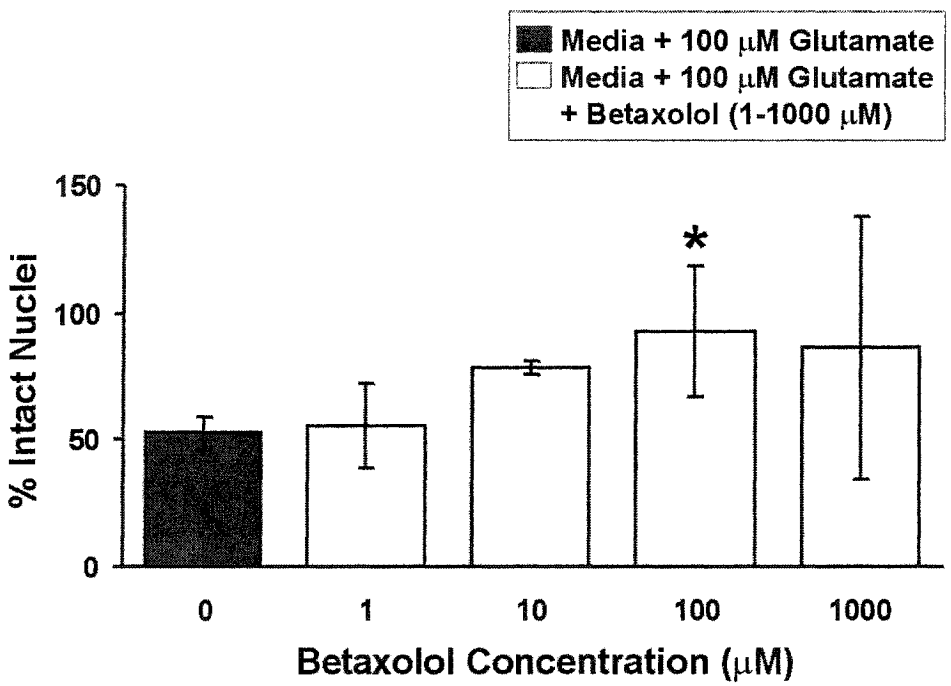
Media + 100 μM Glutamate
Media + 100 μM Glutamate
+ Betaxolol (1-1000 μM)
150
100
50
0
% Intact Nuclei
*
0
1
10
100
1000
Betaxolol Concentration (μM)

**Figure 3.5**

**Figure 3.6 Effect of timolol on retinal cell viability following exposure to excitotoxic media.** Percent intact nuclei for primary retinal cells treated with the non-selective β-AR blocker, timolol, following 24 hr of glutamate excitotoxicity. Cell viability was assessed by counting the density of intact nuclei derived from healthy retinal cells after Zap-Oglobin cell lysis. Treatment groups consisted of: media containing D-MEM Ham's F12 formulation (TM); TM plus an additional 100 μM glutamate (TMG); or TMG plus various doses of timolol (1-1000 μM). Data are from 3 separate experiments and are expressed as the mean ± SD (%) of the TM control group (100%).

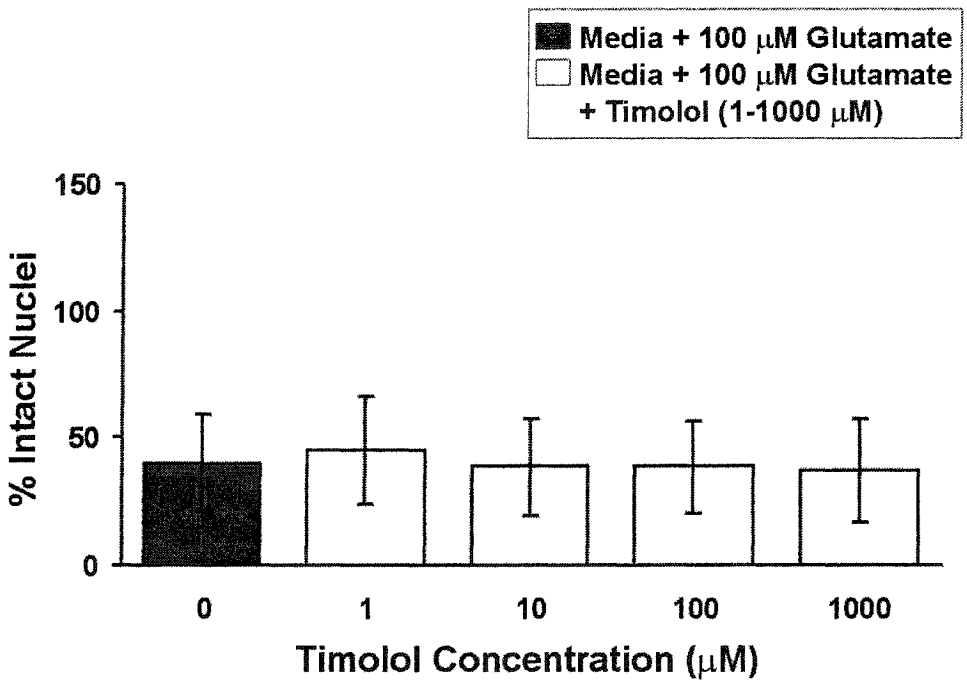
Media + 100 μM Glutamate
Media + 100 μM Glutamate
+ Timolol (1-1000 μM)
150
100
50
0
% Intact Nuclei
0
1
10
100
1000
Timolol Concentration (μM)

**Figure 3.6**

**Figure 3.7 Effect of metoprolol on retinal cell viability following exposure to excitotoxic media.** Percent intact nuclei for primary retinal cells treated with the selective β1-AR blocker, metoprolol, following 24 hr of glutamate excitotoxicity. Cell viability was assessed by counting the density of intact nuclei derived from healthy retinal cells after Zap-Oglobin cell lysis. Treatment groups consisted of: media containing D-MEM Ham's F12 formulation (TM); TM plus an additional 100 μM glutamate (TMG); or TMG plus various doses of metoprolol (1-1000 μM). Data are from 3 separate experiments and are expressed as the mean ± SD (%) of the TM control group (100%).

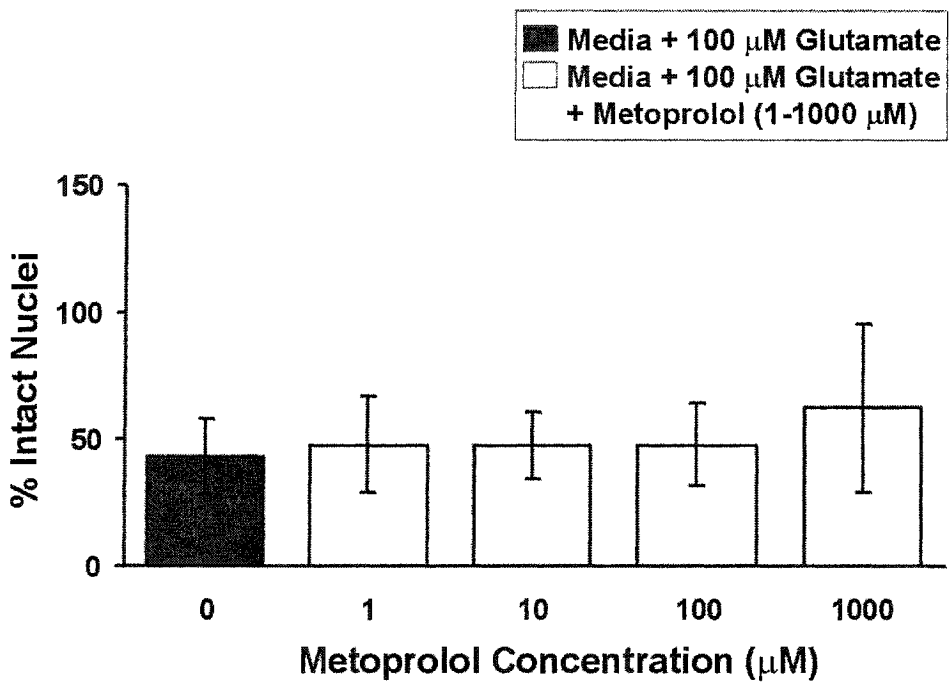
Media + 100 μM Glutamate
Media + 100 μM Glutamate
+ Metoprolol (1-1000 μM)
% Intact Nuclei
150
100
50
0
0
1
10
100
1000
Metoprolol Concentration (μM)

**Figure 3.7**

To determine whether the protective properties of betaxolol were mediated through interactions with β-ARs we next tested the ability of a non-selective β-AR blocker, timolol, to protect retinal neurons from glutamate excitotoxicity (Figure 3.6). The effect of 24 hr exposure to 150 μM glutamate concentration was a reduction in viability to 40% ± 19% relative to the control group. Timolol at 1, 10, 100 and 1000 μM failed to provide a significant increase in cell survival at all doses tested, resulting in 45% ± 21%, 39% ± 19%, 38% + 18% and 37% ± 20% survival compared to the control group ($p$>0.90). We also investigated the ability of another selective β1-AR blocker, metoprolol, to protect retinal neurons from glutamate-induced excitotoxicity (Figure 3.7). The effect of 24 hr exposure to 150 μM glutamate was a reduction in viability to 43% ± 15% relative to the control group. Like timolol, metoprolol failed to provide significant ($p$>0.80) retinal neuroprotection for all doses tested. In the presence of 1, 10, 100 and 1000 μM metoprolol neuronal survival was only 48% ± 19%, 48% ± 13%, 48% ± 16% and 62% ± 33% of the control group, respectively. Taken together these results demonstrate that the protective effects provided by betaxolol occur independently of interactions with β-ARs.

### *3.3.4. Effect of α2-Adrenoceptor Agonist Stimulation on Retinal Neuron Survival*

The neuroprotective properties of the selective α2-AR agonist, brimonidine, were investigated in our *in vitro* model of retinal excitotoxicity (Figure 3.8). In the presence of an exogenously added 100 μM glutamate, retinal neuron survival was reduced to 62% ± 6% of the control group. Brimonidine, at doses of 1, 10, 100 and 1000 μM, increased retinal cell survival to 74% ± 24%, 106% ± 37%, 90% ± 21% and 91% ± 22% of the control group, respectively. Survival was significant ($p$<0.05) at 10 μM brimonidine and

**Figure 3.8 Effect of brimonidine on retinal cell viability following exposure to excitotoxic media.** Percent intact nuclei for primary retinal cells treated with the selective α2-AR agonist, brimonidine, following 24 hr of glutamate excitotoxicity. Cell viability was assessed by counting the density of intact nuclei derived from healthy retinal cells after Zap-Oglobin cell lysis. Treatment groups consisted of: media containing D-MEM Ham's F12 formulation (TM); TM plus an additional 100 μM glutamate (TMG); or TMG plus various doses of brimonidine (1-1000 μM). Data are from 6 separate experiments and are expressed as the mean ± SD (%) of the TM control group (100%). *$p<0.05$ compared to the TMG-only group.

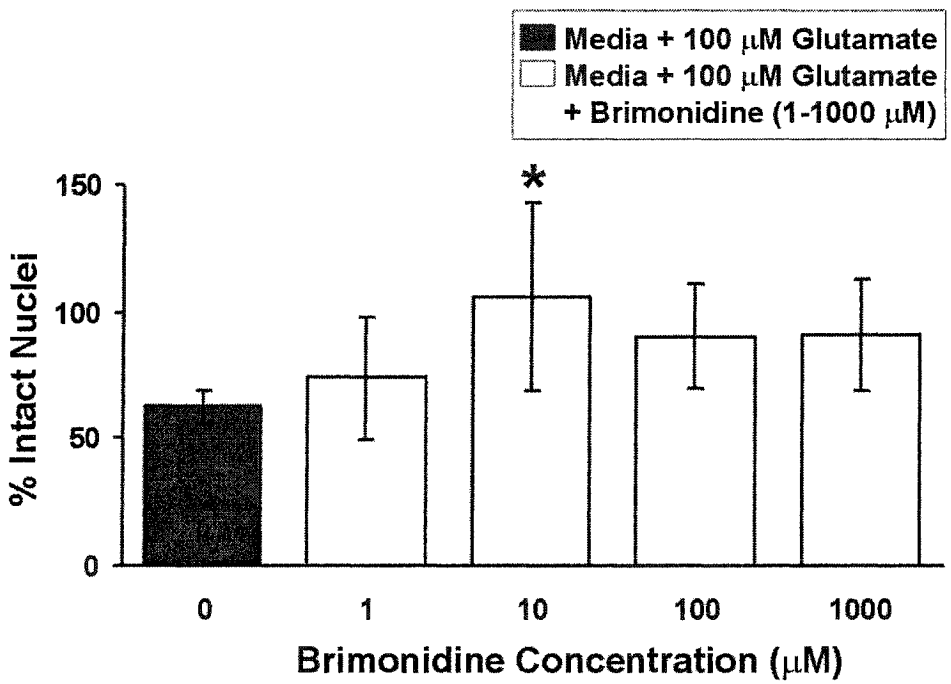
Media + 100 μM Glutamate
Media + 100 μM Glutamate
+ Brimonidine (1-1000 μM)
150
100
50
0
% Intact Nuclei
*
0
1
10
100
1000
Brimonidine Concentration (μM)

**Figure 3.8**

**Figure 3.9 Antagonism of brimonidine-mediated retinal cell protection with yohimbine.** Percent intact nuclei for primary retinal cells treated with the α2-AR agonist, brimonidine and the selective α2-AR blocker, yohimbine, following 24 hr of glutamate excitotoxicity. Cell viability was assessed by counting the density of intact nuclei derived from healthy retinal cells after Zap-Oglobin cell lysis. Treatment groups consisted of: media containing D-MEM Ham's F12 formulation (TM); TM plus an additional 100 μM glutamate (TMG); TMG plus 10 μM brimonidine in combination with 1 or 10 μM of yohimbine. Data are from 3 separate experiments and are expressed as the mean ± SD (%) of the TM control group (100%).

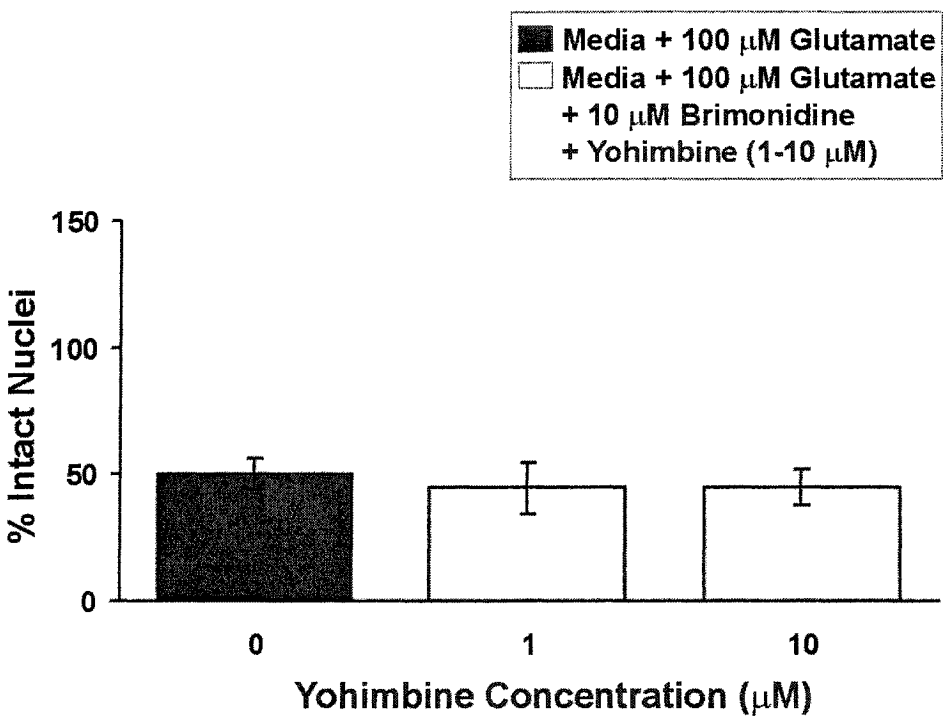
Media + 100 μM Glutamate
Media + 100 μM Glutamate
+ 10 μM Brimonidine
+ Yohimbine (1-10 μM)
150
100
50
0
% Intact Nuclei
0
1
10
Yohimbine Concentration (μM)

**Figure 3.9**

was reduced with higher concentrations (100 and 1000 μM) of the α2-AR agonist, possibly due to receptor desensitization (Diverse-Pierluissi et al., 1996). To determine whether the neuroprotective effect(s) of brimonidine were mediated through interactions with α2-ARs, we used yohimbine, a selective α2-AR antagonist (Figure 3.9). Following 24 hr exposure to 150 μM glutamate, retinal cell viability diminished to 50% ± 6% of the control group. The neuroprotective effect of 10 μM brimonidine was completely abolished in the presence of 1 and 10 μM yohimbine, with cell survival at 45% ± 10% and 45% ± 7% of control, respectively. Taken together, these results suggest that the increase in cell survival observed in the presence of brimonidine required interactions with α2-ARs.

## 3.4. Discussion

The excitotoxic retinal cell culture model used in these studies selectively promotes neuronal death. Previous studies have reported that retinal neuron cultures are only sensitized to elevated extracellular glutamate concentrations once the extracellular $Ca^{2+}$ concentrations are increased to 10 mM and the magnesium content is removed entirely (Hahn et al., 1988). Blockade of excitotoxicity with 0.8 mM magnesium or the selective NMDAR antagonist dizocilpine (MK-801), further supports the hypothesis that glutamate-induced neuronal death in mixed retinal cell cultures occurs largely via activation of NMDARs, as non-NMDARs would still be activated in the presence of 0.8 mM magnesium or with NMDAR blockade (Hahn et al., 1988).

Using the excitotoxic assay with mixed primary rat retinal cell cultures our results demonstrated that betaxolol, a selective β1-AR blocker and brimonidine, a selective α2-AR agonist, promote retinal neuron survival. In support of our findings, other studies

have shown that both betaxolol and brimonidine protect RGCs following chronic elevations in IOP (Cheon et al., 2003; WoldeMussie et al., 2001), transient retinal ischemia-reperfusion (Lafuente López-Herrera et al., 2002) and partial crush of the ON (Yoles et al., 1999).

Betaxolol-mediated neuroprotection in the retina has been reported to occur independently of β-AR blockade (Wood et al., 2003), which corroborates well with the scarce evidence for β1-ARs in the retina (Zarbin et al., 1986). Results from this investigation are in support of this finding. If antagonism of the β-ARs were required to counteract excitotoxic neuronal injury, we would have expected to see similar neuroprotection with the β-AR blockers metoprolol or timolol. $Ca^{2+}$ imaging experiments on isolated rat retinal neurons have now shown that betaxolol can decrease glutamate-induced $Ca^{2+}$ influx (Baptiste et al., 2002). Experiments on isolated RGCs have verified that this decrease in $Ca^{2+}$ influx occurs via actions by betaxolol on L-type dihydropyridine sensitive $Ca^{2+}$ channels (Hirooka et al., 2000). Moreover, in addition to inhibition of L-type $Ca^{2+}$ channels, betaxolol also reduced $Na^{+}$ currents, gamma-aminobutyric acid (GABA) currents and $Ca^{2+}$-activated $K^{+}$ channels suggesting that the net effect of betaxolol is to decrease neuronal excitability (Hirooka et al., 2000). In a recent report, neuroprotection following retinal ischemia-reperfusion was also found with the non-selective β-AR blocker, metipranolol, (Wood et al., 2003). These authors concluded that the neuroprotective abilities mediated by β-AR antagonists correlated directly with their ability to counteract glutamate-induced $Na^{+}$ and $Ca^{2+}$ influx (Wood et al., 2003). Interestingly, timolol was also reported to prevent glutamate-induced ion influx; however this occurred at much higher doses and resulted in weaker effects than

that observed with betaxolol or metipranolol (Wood et al., 2003). Based on these findings the actions of betaxolol on neuronal ion channels and receptors resulting in a reduction in $Ca^{2+}$ influx may be responsible for the increased neuronal survival found in our experiments. Additionally, betaxolol may also exert indirect neuroprotective effects through interactions with glial cells, via stimulation of glial-released diffusible survival factors. More recently, systemically administered betaxolol has been shown to up-regulate bFGF and CNTF mRNA levels in a rat photic-induced retinopathy model (Agarwal et al., 2002).

In this study, unlike betaxolol, neuroprotection by brimonidine appeared to be dependent upon interactions with α2-ARs, as the selective α2-AR antagonist, yohimbine, completely abolished any protective effects mediated by the α2-AR agonist. Radioligand binding studies have revealed the existence of α2-AR isoforms within the mammalian retinas of a variety of species including porcine (Wikberg-Matsson et al., 1996), bovines (Berlie et al., 1995), rodents (Elena et al., 1989) and humans (Bylund & Chacko, 1999). However, only $\alpha 2_A$ and $\alpha 2_C$ have been found within human retinas (Bylund and Chacko, 1999). Systemic and topically administered α2-AR agonists have been reported to increase the expression of bFGF (Lai et al., 2002), BDNF (Gao et al., 2002), Bcl-2 and Bcl-$x_L$, as well as to enhance the level of activation of extracellular signal-regulated kinases (ERKs) and the PI-3K/Akt pathways following an episode of acute retinal ischemia-reperfusion (Lai et al., 2002). Administration of bFGF and BDNF prevents excitotoxicity in cerebellar granule cells, possibly through the down-regulation of the NR2A and NR2C NMDAR subunit expression respectively (Brandoli et al., 1998). The effects of Bcl-2, Bcl-xL and Akt are known to be anti-apoptotic due to the fact that they

block the release of mitochondrial cytochrome c, which prevents the subsequent activation of caspases (Lai et al., 2002). PI-3K/Akt, ERK and CREB pathways can control the cell death machinery by neutralizing the pro-apoptotic effects of Bad. Akt-mediated phosphorylation of Bad, inactivates Bad and maintains its location in the cytosol where Bad is impaired in its ability to antagonize the mitochondrial-protective functions of the anti-apoptotic Bcl-2 family members. In addition, ERK-mediated activation of CREB positively influences the transcription of pro-survival genes including the Bcl-2 family members, Bcl-2 and Bcl-$x_L$ and survival factors such as BDNF (Ballif & Blenis, 2001; Park et al., 2004). Furthermore, the activated ERK pathway, which may be an intrinsic mechanism for cells to combat stress, may be required for trophic factor-induced neuroprotection as Hetman et al. (1999) found that specific ERK inhibitors successfully antagonized the protective effects mediated by BDNF. Our results also indicated that α2-AR agonists decrease glutamate-induced $Ca^{2+}$ influx in isolated retinal neurons (Baptiste et al., 2002). This effect was dependent upon α2-ARs as determined by the fact that the decrease in $[Ca^{2+}]_i$ observed in the presence of the α2-AR agonist, brimonidine, was deleted when the α2-AR antagonist yohimbine was included. This result is consistent with other reports that demonstrate that α2-ARs are negatively coupled through $G_i/G_o$ to adenylyl cyclase to inhibit voltage sensitive $Ca^{2+}$ channels (Ansah et al., 2003). Moreover, brimonidine, as well as betaxolol and dipivefrin, were recently shown to block glutamate-induced $Ca^{2+}$ increases and decrease basal $Ca^{2+}$ concentrations within neuroblastoma cells (Hong et al., 2003).

The major findings of this study are that both the β1-AR antagonist, betaxolol and the α2-AR agonist, brimonidine, can increase survival of isolated retinal neurons *in vitro*.

Our results confirm that these drugs can act as neuroprotectants through actions which are independent of vascular targets. Given the above properties, betaxolol and the α2-AR agonists appear well suited for combating retinal neurodegenerative disorders involving excitotoxicity and or ischemia-reperfusion. Animal studies have provided evidence that these drugs do reach the retina at concentrations comparable to those required for *in vitro* neuroprotection following topical or systemic administration (Wood et al., 2001; Lai et al., 2002). Furthermore, scheduled vitrectomies in phakic, pseudophakic and aphakic patients receiving topical brimonidine have demonstrated measurable vitreous levels of α2-AR agonists at concentrations known to activate α2-ARs (Kent et al., 2001). Currently, only brimonidine is under investigation for use as a neuroprotectant in clinical trials of optic neuropathies related to glaucoma (Wheeler et al., 2003). Results generated from this study support previous and current investigations on the protective mechanisms provided by AR agents in the retina and suggest further consideration of these drugs as neuroprotectants in glaucoma.

# CHAPTER 4

# AN INVESTIGATION OF THE NEUROPROTECTIVE EFFECTS OF THE TETRACYCLINE DERIVATIVES IN CELL CULTURE MODELS OF RETINAL CELL DEATH

## 4.1. Introduction

Apoptosis, although required for successful embryonic development and normal tissue homeostasis, has been linked to the pathogenesis of a variety of neurodegenerative disorders (Heidenreich, 2003). Investigation of human post-mortem brain (Tatton et al., 2003), spinal cord (Dangond et al., 2004) and retina (Wax et al., 1998), as well as cell culture (Otori et al., 2003) and animal models (McKinnon et al., 2002) have all provided evidence supporting a role for apoptosis in CNS disease. Central to the 'execution phase' of the apoptosis program is the activation of caspases (Friedlander, 2003). These proteases comprise a family of at least 14 different members that exist in the cell as latent enzymes or pro-enzymes that become proteolytically activated after cell stress (Tenneti & Lipton, 2000). The caspase family has been divided into two classes, those that target and initiate the activation of other caspases (caspases-1, -2, -4, -5, -8, -9 and -10) and those caspases that are involved in the execution phase of apoptosis, namely caspases-3, -6, -7 and -14 (Schulz et al., 1999). In neurons, evidence exists that caspase-3 activity is seminal in neuronal death following glutamate-induced excitotoxicity (Tenneti & Lipton, 2000; Brecht et al., 2001). Similarly, the withdrawal of small peptides classified either as neurotrophins, neurotrophic factors, cytokines or growth factors can also initiate caspase-3 dependent neuronal death (Vaghefi et al., 2004). Furthermore, excitotoxicity (Dreyer et

al., 1996), TFD (Quigley & Addicks, 1980; Quigley et al., 2000) and caspase-3 activation (McKinnon et al., 2002) may contribute to optic neuropathies related to GON.

The activation of caspase cascades and apoptotic execution may occur either through 'extrinsic' or 'intrinsic' pathways. In the extrinsic pathway, caspases are activated following ligand binding to death receptors of the TNF receptor (TNFR) family (Putcha et al., 2002). In contrast, cellular stresses such as excessive stimulation of GluRs and TFD leading to mitochondrial $Ca^{2+}$ overload are believed to trigger the release of apoptogenic cyt c from the mitochondrial electron transport chain into the cytosol through an unknown mechanism which may involve the regulatory activities of Bcl-2 family members and the opening of the mitochondrial permeable transition pores (Putcha et al., 2002). Once in the cytosol cyt c can assemble with Apaf-1 and procaspase-9 to form the apoptosome. The activated apoptosome then activates other effector caspases, such as caspase-3, to execute the proteolytic destruction of vital components of the cell. Cross-talk can also exist as TNFR-mediated activation of procaspase-8 has been demonstrated to proteolytically activate the pro-apoptotic Bcl-2 member, BH3-interacting homology death domain agonist (Bid), to translocate to the mitochondrial membrane to mediate cyt c release (Putcha et al., 2002). Activated caspase-8 has also been implicated in the direct processing of procaspases-9 and -3 (McDonnell et al., 2003; see Figure 4.1). Recently Oshitari & Adachi-Usami (2003) demonstrated that inhibition of caspase-1, -3, -8 and -9 were all effective in blocking RGC apoptosis following TFD. Intravitreal injection of caspase inhibitors has also prevented apoptosis of axotomized RGCs (Weishaupt et al., 2003). Taken together, the above information suggests that caspases represent a reasonable therapeutic target for retinal neuroprotection.

**Figure 4.1 Schematic of intrinsic & extrinsic cell death pathways.**

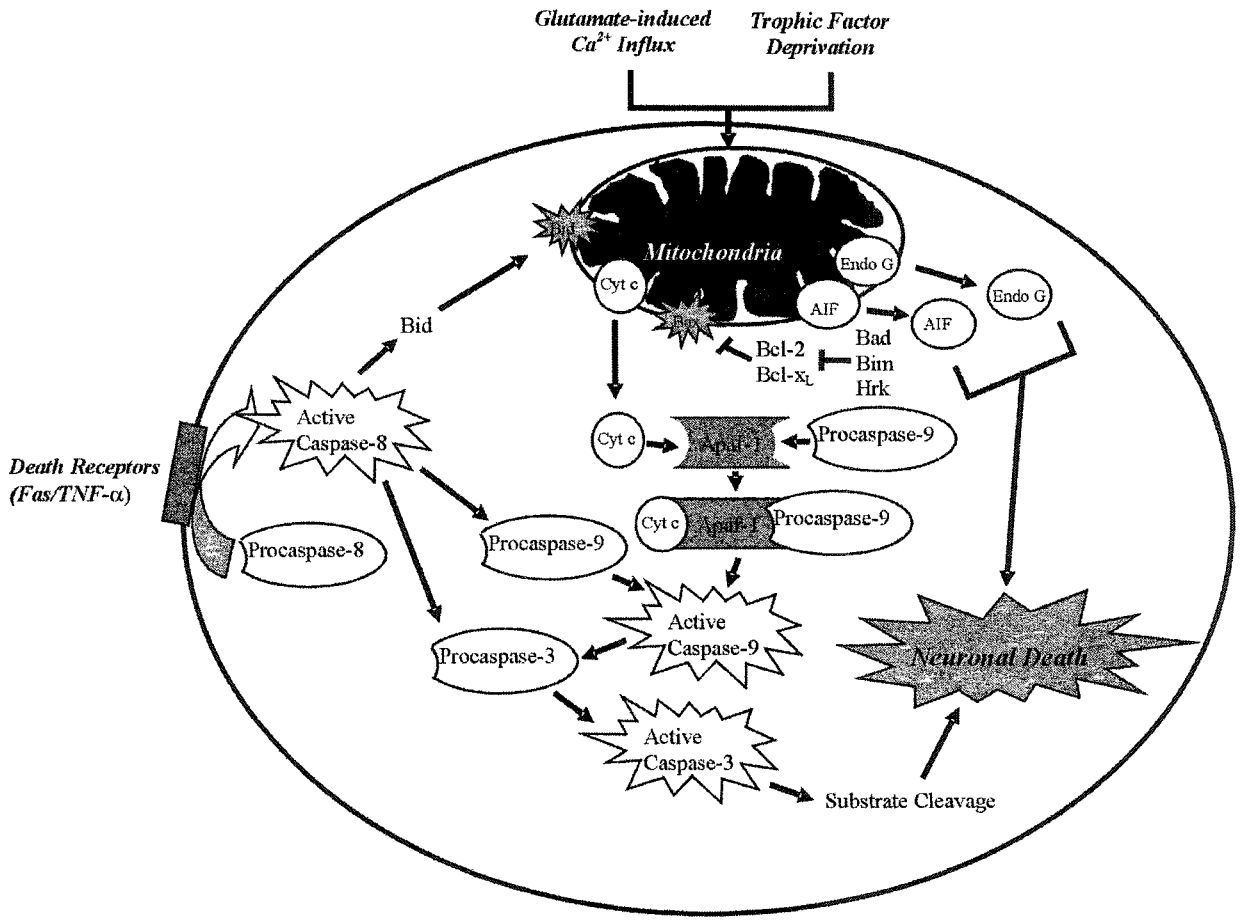
Glutamate-induced
Ca2+ Influx
Trophic Factor
Deprivation
Mitochondria
Cyt c
Endo G
AIF
Endo G
AIF
Bad
Bcl-2
Bcl-xL
Bim
Hrk
Bid
Active
Caspase-8
Death Receptors
(Fas/TNF-α)
Procaspase-8
Cyt c
Apaf-1
Procaspase-9
Procaspase-9
Cyt c
Apaf-1
Procaspase-9
Active
Caspase-9
Procaspase-3
Neuronal Death
Active
Caspase-3
Substrate Cleavage

**Figure 4.1**

Minocycline is a highly lipophilic semi-synthetic derivative of tetracycline and is capable of crossing the blood-brain-barrier (BBB) where its ability to exert anti-inflammatory properties is uniquely distinct from its ability to inhibit bacterial protein synthesis (Yrjänheikki et al., 1999). Moreover, researchers have demonstrated that minocycline can inhibit excitotoxicity (Tikka & Koistinaho, 2001; Tikka et al., 2001; Zhu et al., 2002), oxidative stress (Lin et al., 2003), caspase-dependent- and caspase-independent-mediated pathways of neuronal death (Wang et al., 2003), as well as pro-inflammatory mediators released by activated MG (Tikka et al., 2001). Given its relatively safe track record in humans, minocycline is currently being investigated for use as a neuroprotectant in both HD (Bonelli et al., 2003) and ALS (Friedlander, 2003). The multi-faceted protective effects of this second generation tetracycline derivative are attractive for neuroprotective studies in GON, a disease in which multiple stressors may contribute to RGC loss and ON damage.

In the present study we compared and contrasted the neuroprotective abilities of tetracycline and minocycline, in rat retinal cell cultures following excitotoxic- and TFD-induced stresses. We also investigated whether the resulting neuroprotection provided by minocycline was due to alterations in caspase-3 expression.

## 4.2. Materials & Methods

### *4.2.1. Cell Culture*

Culture of the rat retinal cell line, E1A-NR.3, was carried out using methods previously described (see General Methods, section 2.1.2.). Following removal of the GM(+) (see Table 2.2), E1A-NR.3 cells were dissociated for 5 min at 37 °C in 0.0625% trypsin-EDTA. The trypsin reaction was terminated by adding an equal volume of GM(+).

Cells were centrifuged at 1,000 rpm for 3 min and the resulting cell pellet was triturated in GM(+) to form a homogeneous cell suspension. Cells were then plated at a density of $1x10^5$ cells/ml in 24 well culture dishes, 35 mm culture dishes or 50 ml flasks.

Primary retinal cells were cultured using procedures previously described (see General Methods, section 2.1.1.). Briefly, rat pups were anesthetized using halothane inhalation, sacrificed by decapitation, the eyes were enucleated and the posterior eye-cups with the retina attached were placed in fresh D-MEM(+). The anterior portions of the eye were then discarded and the retinas were gently dissected free and dissociated by incubation with 0.125% trypsin in D-MEM at 37 °C for 3 min. The trypsin action was terminated by adding D-MEM(+). Cells were centrifuged, washed with fresh media and resuspended in D-MEM (+). The resulting retinal cell suspension was then adjusted to achieve a cell density of $2.5x10^5$ cells/ml and seeded into 24 well culture dishes pre-coated with laminin (2 μg/ml) and poly-$_D$-lysine (10 μg/ml).

Culture and differentiation of PC12 cells was carried out using the protocol defined in the General Methods, section 2.1.4. Briefly, PC12 cells were plated at a density of $6x10^4$ cells/ml in 35 mm diameter culture dishes pre-coated with rat-tail collagen (1 mg/ml). The cells were then differentiated by the addition of 100 ng/ml 7S NGF (Collaborative Research Inc.; GM(+) (see Table 2.4.)) and grown for a further 7 days.

All cell cultures were maintained in a humidified atmosphere of 5% $CO_2$/95% $O_2$ and replenished with their respective fresh GM(+) every 2-3 days.

### *4.2.2. Glutamate-induced Excitotoxicity, Trophic Factor Deprivation, & Cell Quantification*

Glutamate-induced cell death was assayed using the E1A-NR.3 retinal cell line and primary retinal cell cultures (see General Methods, section 2.3.1.). Primary retinal cells were grown in 24 well culture dishes for 7 days and then divided into groups of 3-4 wells. Each group was treated with one of the following treatments: (1) treatment media (TM); (2) TM + L-glutamate (TMG); (3) TMG + drug (see Tables 2.1. and 2.2.). Ham's F12 formulation of D-MEM, which contains no magnesium, 10 mM $CaCl_2$ and 50 μM endogenous glutamate (see Table 2.3.) was used in the TM instead of standard D-MEM formulations. The final glutamate concentrations for the groups TM and TMG were 50 and 150 μM respectively. Following treatment, retinal cells were incubated in a humidified atmosphere of 5% $CO_2$/95% $O_2$ and maintained at 37 °C for 24 hr. Retinal cell survival was subsequently quantified using the Zap-Oglobin cell lysis technique, as described in the General Methods, section 2.4.1.

TFD was carried out using cultures of primary rat retinal cells, the E1A-NR.3 retinal cell line and the NGF-differentiated PC12 cell line, as described previously in the General Methods, section 2.3.2. All cell types were grown for 3-5 days in 35 mm diameter culture dishes. After 3 days of culture the GM(+) was aspirated and the cells were gently washed with PBS (3X) to remove trace amounts of trophic factors and divided into one of 3 groups: (1) GM(+); (2) GM(-), which received GM with no serum or trophic factors; (3) GM(-) + various concentrations of drugs (see Tables 2.1., 2.2. and 2.4. for cell-type specific media composition). Cells were then returned to a 37°C incubator and maintained under a humidified atmosphere of 5% $CO_2$/95% $O_2$ until further

analysis. Cell survival was assayed in primary retinal cells using the Zap-Oglobin cell lysis technique following 48 hr of TFD. Cell viability of the E1A-NR.3 and PC12 cultures was assessed at 24 or 48 hr following TFD. The number of viable and apoptotic cells were quantified using the AO/EB assay.

To determine the number of viable cells per treatment group the cells were removed from the 24 well culture dishes with 1X trypsin-EDTA in D-MEM at room temperature. The enzymatic reaction was terminated with an equal volume of D-MEM(+) (see Table 2.1.). The cell suspensions were centrifuged for 3 min and resuspended in 200 µl of a 1:10 dilution of Zap-Oglobin lysing solution. Viable nuclei were counted with a hemocytometer under inverted light microscopy. Mean cell counts were obtained from at least three separate wells per treatment group (TM, TMG, TMG + drug) and expressed as a percentage of the number of viable nuclei in the control TM group. Mean percentage data ± SD were obtained from 3-6 separate experiments. The drugs tested were MK-801 (a selective noncompetitive NMDAR antagonist), tetracycline and minocycline (a second generation tetracycline derivative), and the effects of each drug were tested over the range of concentrations from 0.002-200 µM. All drugs were prepared in stocks dissolved in PBS free of $Ca^{2+}$ and $Mg^{2+}$.

The viability of E1A-NR.3 retinal and PC12 cell lines following TFD were quantified using AO/EB dye exclusion (General Methods, see section 2.4.2.). Following TFD, the media was removed and the cells were washed with PBS. A mixture of 100 µg/ml AO and 100 µg/ml EB made in PBS was applied to the culture dishes for 3 min at room temperature, after which the cells were washed with PBS. AO-positive green nuclei and AO/EB-positive orange/red pyknotic nuclei derived from live and apoptotic

cells, respectively, were then visualized using a Nikon C1 microscope equipped for epifluorescence with filters for UV-2A (excitation 330-380 nm; barrier 420 nm; emission 400 nm) and quantified by placing a micrometer grid with an optical field area of 0.23 $mm^2$ under the view of a 20X objective. Color pictures were captured with a Nikon FDX 35 mm digital camera through a Nikon Multi-Point Sensor System U-III using both a 20X objective and a 100X oil immersion objective.

### *4.2.3. Caspase-3 Analysis*

Caspase-3 expression was analyzed in the E1A-NR.3 retinal cell line following TFD using both RT-PCR and Western blot techniques (see General Methods, sections 2.5.1. and 2.5.2.). Briefly, total cellular RNA was obtained from the E1A-NR.3 retinal cell line using TRIzol™ reagent according to the manufacturer's protocol. The RNA samples were then DNase I-treated and used to generate single-stranded cDNA with the Moloney Murine Leukemia Virus Reverse Transcriptase. Primer sequences have been previously published for cyclophilin (Hirooka et al., 2002) and caspase-3 (Harrison et al., 2001) (see Table 2.5.). To compare caspase-3 mRNA levels of expression between the various TFD treatment groups (GM(+), GM(-) and GM(-) + drug; see Table 2.2.), the number of PCR cycles was determined to be in the linear range. PCR was performed as follows: denaturation, 94 °C 30 sec; annealing 40 sec; extension 72 °C 1 min 10 sec. The PCR products were resolved by staining with ethidium bromide and by electrophoresis in a 1.5% agarose gel. PCR products were visualized under UV illumination using a Geldoc imaging system (Bio-Rad, Mississauga, ON, Canada). Images of the PCR bands were subjected to densitometry using Molecular Analyst image software version 1.5 (Bio-Rad, Hercules, CA).

E1A-NR.3 cells were washed with PBS and lysed on ice with 100 µl of Cell Lysis Buffer (Cell Signalling Technology Inc., Beverly, MA). Protein concentration was determined using the BCA protein assay kit (Novagen, Pierce, Rockford, IL) and the samples were boiled in SDS buffer for 5 min. Protein samples (25 µg) were separated in 12% SDS-PAGE at 95 volts for 1 hr and electro-transferred to a nitrocellulose membranes. The membranes were dried for 2 hr and then incubated on an orbital shaker with a 1:1,000 dilution of primary rabbit anti-rat caspase-3 monoclonal antibody overnight at 4 °C. Membranes receiving only the primary antibody skim milk diluent served as negative controls. Membranes were then washed 3X with PBS-Tween 80 for 5 min before incubation with secondary antibody HRP-conjugated goat anti-rabbit IgG at a dilution of 1:2,000 for 1 hr at 37 °C. Following this, membranes were washed 3X with PBS-Tween 80 at 37 °C on an orbital shaker for 20 min. Protein bands were visualized with the ECL System (Super Signal, Pierce, Rockford, IL) and exposed to film (XAR; Kodak). Negative controls were conducted in experiments by excluding primary antibodies.

#### *4.2.4. Statistical Analysis*

All data were analyzed using a one-way ANOVA followed by parametric post-test analysis with a Dunnett Multiple Comparison test (GraphPad Instat version 3.00; San Diego, CA). The criterion for noting a significant difference was $p<0.05$.

## 4.3. Results

#### *4.3.1. Effect of Glutamate on E1A-NR.3 Retinal Cell Survival*

In this study, we first investigated E1A-NR.3 cell survival following glutamate-induced excitotoxicity (Figure 4.2). After a 24 hr incubation with additions of exogenous

**Figure 4.2 Effect of excitotoxic media on E1A-NR.3 cell viability.** Percent intact nuclei for E1A-NR.3 retinal cell line cultures following 24 hr exposure to media containing D-MEM Ham's F12 formulation (TM); TM plus an additional 10 or 100 μM glutamate concentration (TMG). Cell viability was assessed by counting the density of intact nuclei derived from healthy retinal cells after Zap-Oglobin cell lysis. Data are from 6 separate experiments and are expressed as the mean ± SD (%) of the TM control group (100%).

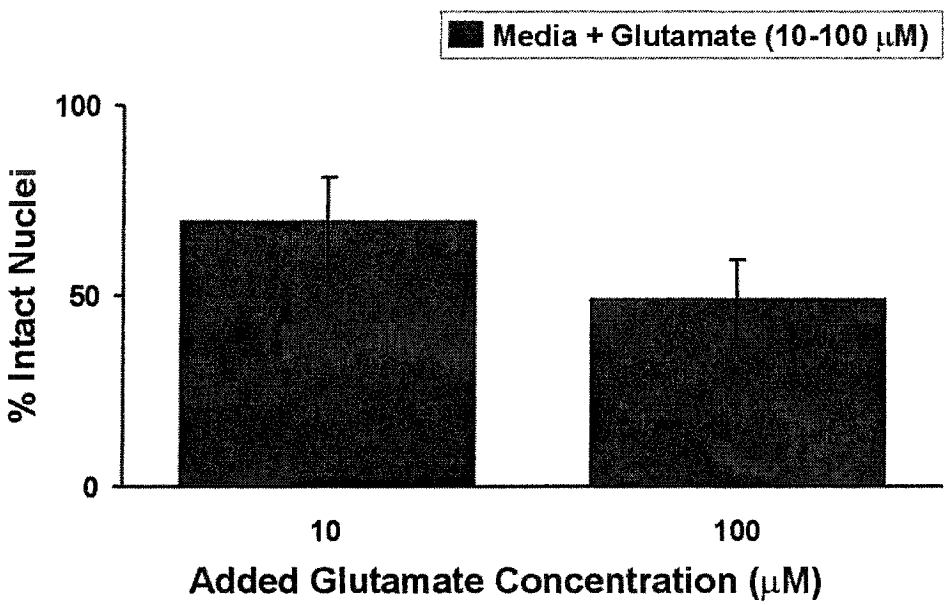
Media + Glutamate (10-100 μM)
100
50
0
% Intact Nuclei
10
100
Added Glutamate Concentration (μM)

**Figure 4.2**

glutamate (10-100 μM), retinal cell survival was reduced in a dose-dependent manner compared to the control group, which did not receive additional glutamate. Cell survival declined from 69% ± 12% to 49% ± 10% of the control group at 10 and 100 μM glutamate, respectively. Subsequently, the 100 μM exogenous glutamate concentration was selected as the test dose for all further excitotoxicity experiments with E1A-NR.3 cultures because this dose reliably produced approximately 50% or greater reductions in mixed retinal cell culture viability.

To determine whether glutamate-induced excitotoxic death was mediated via NMDARs, we next investigated the potential for the NMDAR antagonist, MK-801 (1-100 μM), to rescue E1A-NR.3 retinal cells (Figure 4.3). Treatment of E1A-NR.3 cells with 100 μM exogenous glutamate reduced viability to 62% ± 10% in comparison to controls, which did not receive additional glutamate. Addition of MK-801 counteracted the excitotoxic effects of glutamate in a dose-dependent manner. At concentrations of 1, 10 and 100 μM MK-801, cell survival in the presence of 100 μM exogenous glutamate was increased to 74% ± 23%, 86% ± 17% and 102% ± 18%, respectively. The increase in cell survival was significant at 100 μM MK-801 ($p<0.01$).

To determine whether excitotoxic retinal cell death involved changes in pro-apoptotic caspase-3 expression we used RT-PCR to examine caspase-3 mRNA expression (Figure 4.4). RT-PCR and gel electrophoresis analysis of the E1A-NR.3 cell line following an 8 hr exposure to excitotoxic conditions revealed a 636 base pair (bp) band corresponding to increased caspase-3 mRNA expression (lane 2). Controls not receiving an additional 100 μM glutamate had a reduced expression of mRNA for caspase-3 (lane 1). Primers for the constitutively expressed gene, cyclophilin, resulted in

**Figure 4.3 Effect of MK-801 treatment on E1A-NR.3 retinal cell viability following exposure to excitotoxic media.** Percent intact nuclei for E1A-NR.3 retinal cell line cultures treated with the NMDAR antagonist, MK-801, following 24 hr of glutamate excitotoxicity. Cell viability was assessed by counting the density of intact nuclei derived from healthy retinal cells after Zap-Oglobin cell lysis. Treatment groups consisted of the following: media containing D-MEM Ham's F12 formulation (TM); TM plus an additional 100 μM glutamate (TMG); TMG plus various doses of the MK-801 (1-100 μM). Data are from 6 separate experiments and are expressed as the mean ± SD (%) of the TM control group (100%). $^{**}p<0.01$ compared to the TMG-only group.

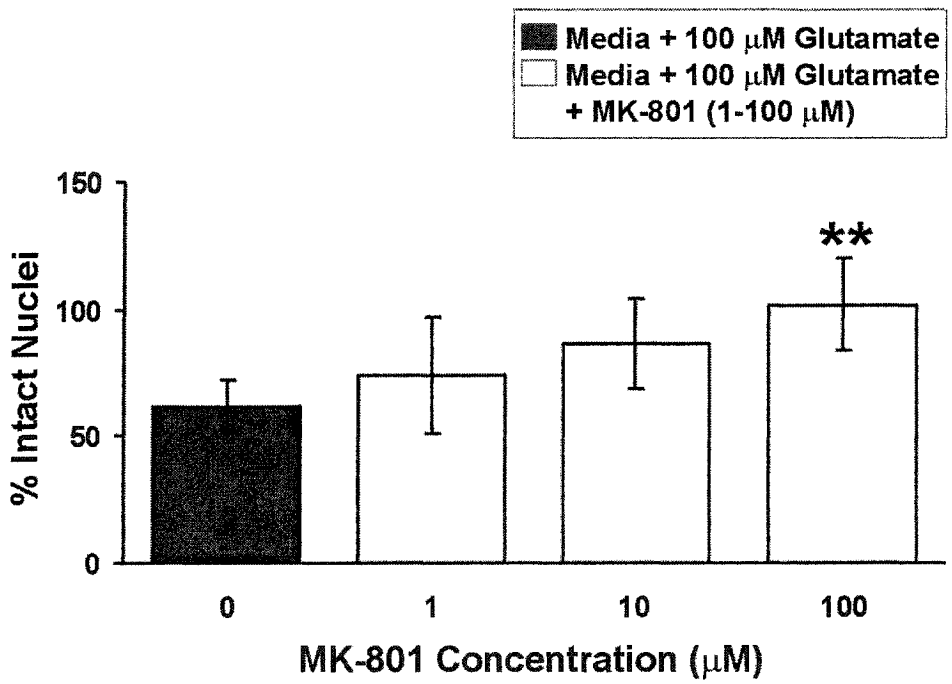
Media + 100 μM Glutamate
Media + 100 μM Glutamate
+ MK-801 (1-100 μM)
150
100
50
0
% Intact Nuclei
**
0
1
10
100
MK-801 Concentration (μM)

**Figure 4.3**

**Figure 4.4 Effect of excitotoxic media on caspase-3 expression in E1A-NR.3 retinal cells.** Electrophoresis of RT-PCR products shows bands of expected size for caspase-3 (646 bp) and cyclophilin (371 bp) following an 8 hr incubation in D-MEM Ham's F12 formulation (TM; lane 1) or TM supplemented with an additional 100 μM glutamate (TMG; lane 2).

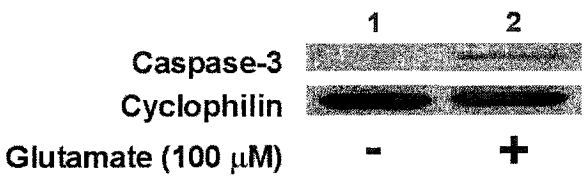


**Figure 4.4**

371 bp band products of approximately equal intensity for cDNA derived from both control (lane 1) and excitotoxic cells (lane 2). Collectively the data obtained from these excitotoxicity experiments demonstrate that the E1A-NR.3 retinal cell line is susceptible to glutamate-induced excitotoxic challenge and that apoptosis following glutamate excitotoxicity is mediated largely through an NMDAR pathway, which leads to an enhanced transcriptional expression of caspase-3.

### *4.3.2. Effect of Tetracycline Derivatives on Retinal Cell Survival Following Excitotoxicity*

Figure 4.5 shows data from experiments examining the survival of E1A-NR.3 retinal cell cultures exposed to excitotoxic conditions alone or in combination with various concentrations of tetracycline (0.002-2 μM). The inclusion of increasing tetracycline concentrations (0.002, 0.02, 0.2 and 2 μM) failed ($p>0.05$) to increase retinal cell survival. Cell viability following tetracycline treatment was 64% ± 10%, 62% ± 9%, 71% ± 4% and 66% ± 12%, respectively, in comparison to the glutamate-only group (69% ± 5%). In contrast, minocycline produced a dose-dependent increase in viable E1A-NR.3 cells (Figure 4.6). At concentrations of 0.002, 0.02 and 0.2 μM minocycline, cell viability was increased to 77% ± 9%, 83% ± 13% and 85% ± 10%, respectively, in comparison to the glutamate-only group (60% ± 11%). Furthermore, the increases in cell survival were significant at concentrations of 0.02 μM ($p<0.05$) and 0.2 μM ($p<0.05$) of minocycline. However, the addition of 2 μM minocycline resulted in a mean survival of only 67% ± 15%. This relative increase in cell viability was not significantly different from the glutamate-only group. Similar neuroprotection by minocycline was observed in primary retinal cell cultures following excitotoxicity (Figure 4.7). Following a 24 hr

**Figure 4.5 Effect of tetracycline treatment on E1A-NR.3 retinal cell viability following exposure to excitotoxic media.** Percent intact nuclei for E1A-NR.3 retinal cell line cultures treated with tetracycline following 24 hr of glutamate excitotoxicity. Cell viability was assessed by counting the density of intact nuclei derived from healthy retinal cells after Zap-Oglobin cell lysis. Treatment groups consisted of the following: media containing D-MEM Ham's F12 formulation (TM); TM plus an additional 100 μM glutamate (TMG); TMG plus various doses of tetracycline (0.002-2 μM). Data are from 3 separate experiments and are expressed as the mean ± SD (%) of the TM control group (100%).

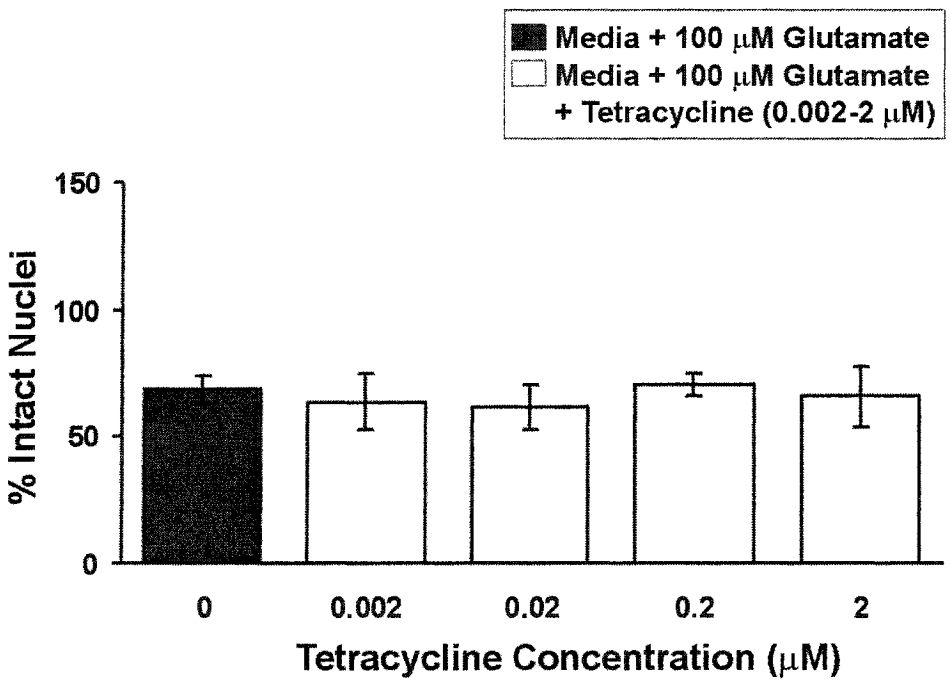
Media + 100 μM Glutamate
Media + 100 μM Glutamate
+ Tetracycline (0.002-2 μM)
% Intact Nuclei
150
100
50
0
0
0.002
0.02
0.2
2
Tetracycline Concentration (μM)

**Figure 4.5**

**Figure 4.6 Effect of minocycline treatment on E1A-NR.3 retinal cell viability following exposure to excitotoxic media.** Percent intact nuclei for E1A-NR.3 retinal cell line cultures treated with minocycline following 24 hr of glutamate excitotoxicity. Cell viability was assessed by counting the density of intact nuclei derived from healthy retinal cells after Zap-Oglobin cell lysis. Treatment groups consisted of the following: media containing D-MEM Ham's F12 formulation (TM); TM plus an additional 100 μM glutamate (TMG); TMG plus various doses of minocycline (0.002-2 μM). Data are from 4 separate experiments and are expressed as the mean ± SD (%) of the TM control group (100%). *$p<0.05$ compared to the TMG-only group.

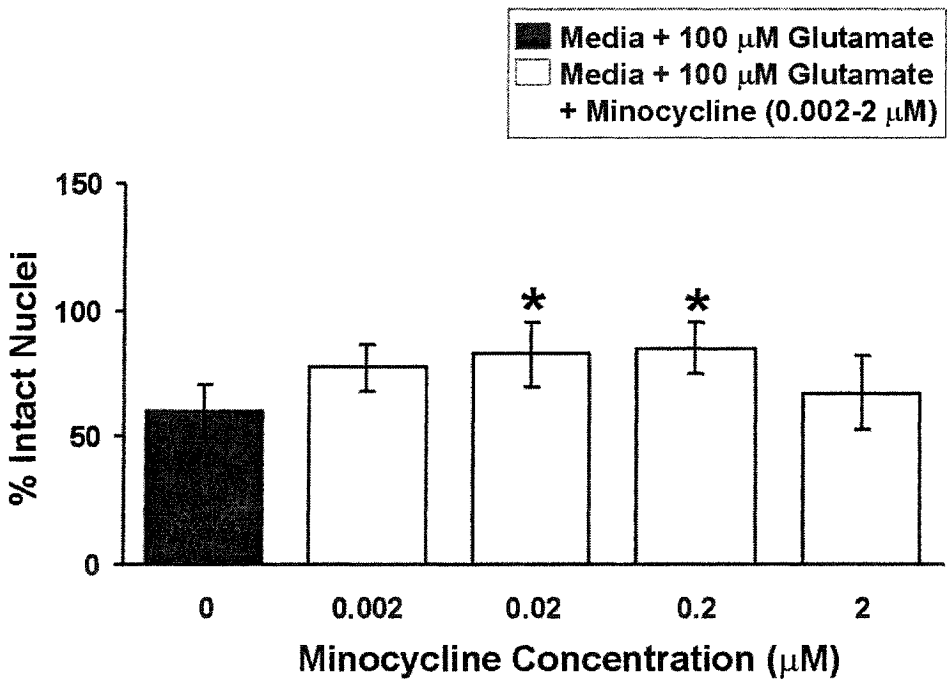
Media + 100 μM Glutamate
Media + 100 μM Glutamate
+ Minocycline (0.002-2 μM)
150
100
50
0
% Intact Nuclei
*
*
0
0.002
0.02
0.2
2
Minocycline Concentration (μM)

**Figure 4.6**

**Figure 4.7 Effect of minocycline treatment on primary retinal cell viability following exposure to excitotoxic media.** Percent intact nuclei for primary retinal cells treated with minocycline following 24 hr of glutamate excitotoxicity. Cell viability was assessed by counting the density of intact nuclei derived from healthy retinal cells after Zap-Oglobin cell lysis. Treatment groups consisted of the following: media containing D-MEM Ham's F12 formulation (TM); TM plus an additional 100 μM glutamate (TMG); TMG plus various doses of minocycline (2-200 μM); TM plus minocycline (20 μM) in the absence of exogenous glutamate. Data are from 3 separate experiments and are expressed as the mean ± SD (%) of the TM control group (100%). *$p<0.05$ compared to the TMG-only group.

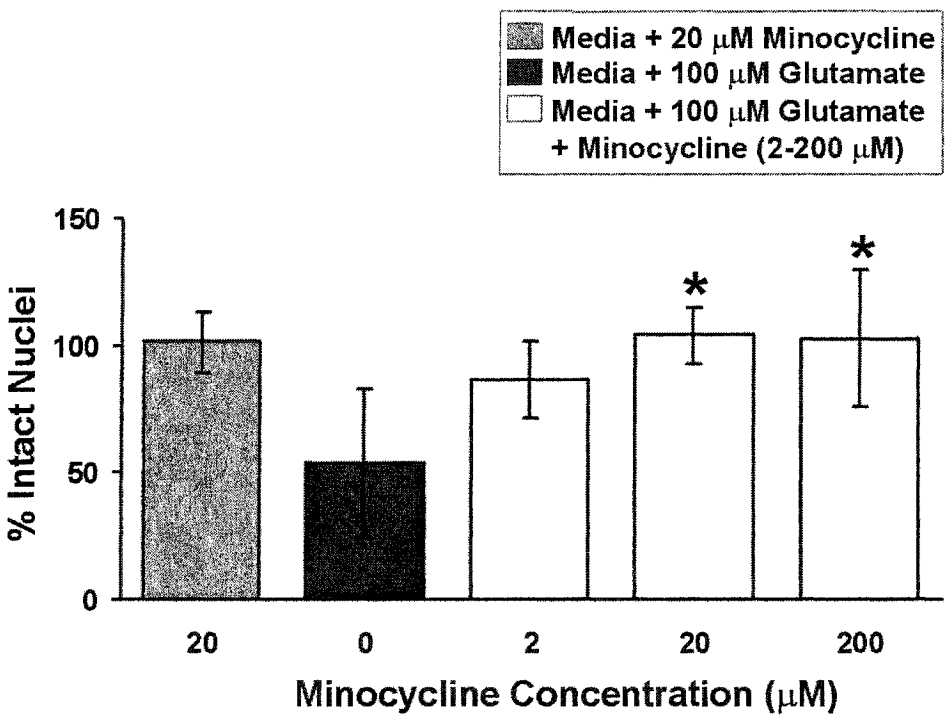
Media + 20 μM Minocycline
Media + 100 μM Glutamate
Media + 100 μM Glutamate
+ Minocycline (2-200 μM)
% Intact Nuclei
150
100
50
0
*
*
20
0
2
20
200
Minocycline Concentration (μM)

**Figure 4.7**

challenge with an additional 100 μM glutamate, primary retinal cell viability was reduced to 54% ± 29%. Minocycline, 2-200 μM, produced a dose-dependent increase in the percentage of viable cells. In the presence of 2, 20 and 200 μM minocycline, viability was increased to 86% ± 15%, 104% ± 11% and 103% ± 27%. The increase in cell survival was significant ($p<0.05$) at the 20 and 200 μM minocycline concentrations. Higher doses of minocycline failed to provide further neuroprotection over that observed with 200 μM minocycline. As an internal control, 20 μM minocycline was added to wells receiving treatment media only. No decrease in cell viability for this group was noted, with survival at 101% ± 12% of the control media. Collectively, these data demonstrate that of the tetracycline derivatives tested only minocycline is capable of decreasing retinal cell death triggered by glutamate excitotoxicity.

To determine whether the protective effects mediated by minocycline were due to the blockade of NMDAR-mediated signalling we next investigated the effect of combining sub-maximal concentrations of MK-801 and minocycline (0.002 μM) under excitotoxic conditions in E1A-NR.3 cultures (Figure 4.8). Following a 24 hr incubation, in the presence of 100 μM exogenous glutamate, cell viability was reduced to 68% ± 7%. On their own, neither 1 μM MK-801 nor 0.002 μM minocycline significantly protected these retinal cells from excitotoxic death with cell survival of 72% ± 7% and 68% ± 6% of the media-only control group, respectively. On the other hand, synergistic survival was observed upon combining sub-maximal concentrations of MK-801 and minocycline. The combination of these drugs completely counteracted the excitotoxic effects of 100 μM glutamate resulting in a significant ($p<0.01$) increase in viability to 99% ± 10% of the media-only control group. The effect of adding PBS without the drugs to the

**Figure 4.8 Effect of MK-801 and minocycline on E1A-NR.3 retinal cell viability following exposure to excitotoxic media.** Percent intact nuclei for E1A-NR.3 retinal cell line cultures treated concurrently with sub-maximal doses of the NMDAR blocker, MK-801 and minocycline, following 24 hr of glutamate excitotoxicity. Cell viability was assessed by counting the density of intact nuclei derived from healthy retinal cells after Zap-Oglobin cell lysis. Treatment groups consisted of the following: media containing D-MEM Ham's F12 formulation (TM); TM plus an additional 100 μM glutamate (TMG); TMG plus 1 μM MK-801; TMG plus 0.002 μM minocycline; TMG with 1 μM MK-801 plus 0.002 μM minocycline. Data are from 3 separate experiments and are expressed as the mean ± SD (%) of the TM control group (100%). $^{**}p<0.01$ compared to the TMG-only group.

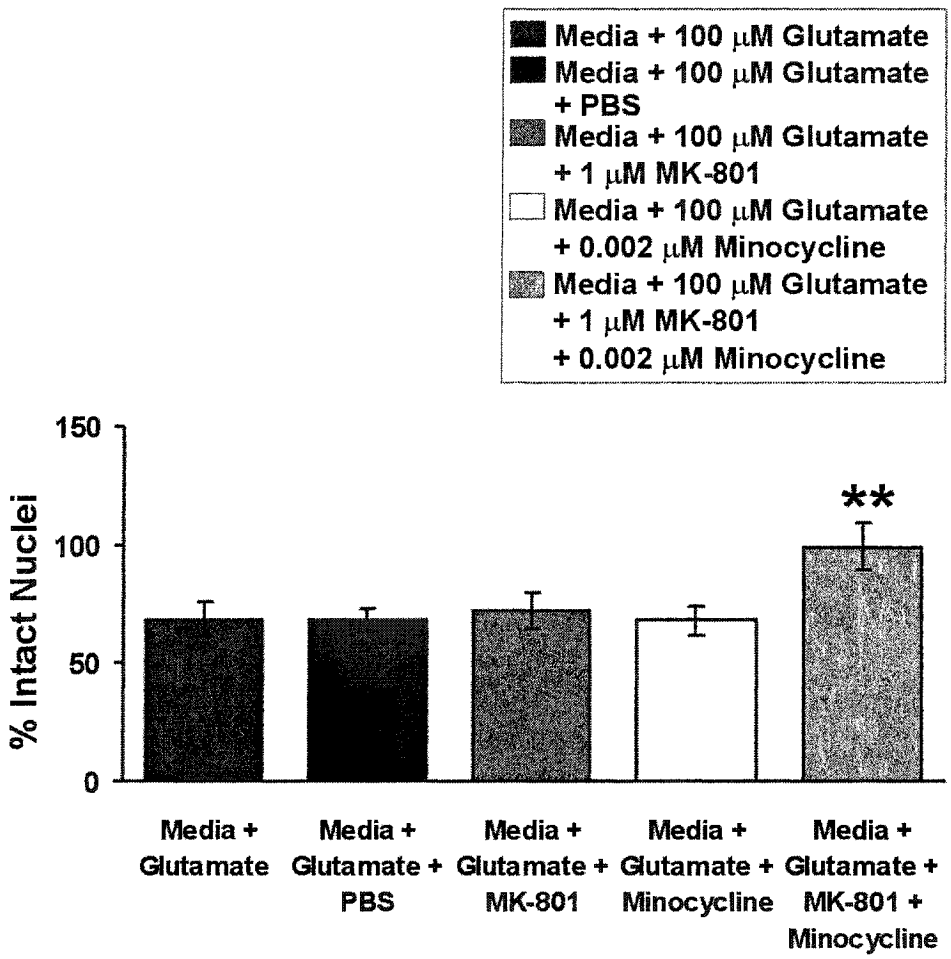
Media + 100 μM Glutamate
Media + 100 μM Glutamate + PBS
Media + 100 μM Glutamate + 1 μM MK-801
Media + 100 μM Glutamate + 0.002 μM Minocycline
Media + 100 μM Glutamate + 1 μM MK-801 + 0.002 μM Minocycline
% Intact Nuclei
150
100
50
0
**
Media + Glutamate
Media + Glutamate + PBS
Media + Glutamate + MK-801
Media + Glutamate + Minocycline
Media + Glutamate + MK-801 + Minocycline

Figure 4.8

excitotoxic media resulted in a mean E1A-NR.3 viability percentage of 69% ± 5%, which was not significantly different from the survival occurring in the glutamate-only group. Taken together, this result supports the conclusion that minocycline provides neuroprotection following excitotoxic insult independent of interactions with NMDARs.

### *4.3.3. Effect of Minocycline on Trophic Factor Deprivation-induced Retinal Cell Apoptosis*

Experiments using a cell viability assay with AO/EB allowed morphological analysis of E1A-NR.3 retinal cell death following TFD. In this assay healthy cells intercalate AO within their genomic DNA and appear green under UV epifluorescence. In contrast, apoptotic cells have both AO and EB intercalate within their genomic DNA and are easily distinguished due to their condensed or pyknotic nuclei when viewed under UV epifluorescence. Figure 4.9 (A-D) shows fluorescent photomicrographs taken 48 hr after treatment of E1A-NR.3 cells with media containing: serum (GM(+)) (A), no serum (GM(-)) (B), GM(-) + 0.02 μM minocycline (C) or GM(-) + 0.2 μM minocycline (D). Mean data from the AO/EB assay are shown in (E). The greatest proportion of pyknotic nuclei (39% ± 4%) was seen with GM(-) conditions. In contrast, control cells receiving GM(+) had a pyknotic nuclei ratio of 15% ± 5%, which was significantly lower than the pyknotic nuclei ratio in GM(-) treated cells ($p<0.01$). GM(-) E1A-NR.3 cells treated with minocycline had a similar reduction in the number of pyknotic nuclei following TFD. At 0.02 and 0.2 μM minocycline the pyknotic/live nuclei ratios were 16% ± 7% and 21% ± 4%, respectively, which were significantly less than the GM(-) group ($p<0.01$). Minocycline-mediated neuroprotection following TFD was also observed in primary retinal cell cultures (Figure 4.10). Following 24 hr of TFD, viable cell numbers for

**Figure 4.9 Effect of minocycline treatment on trophic factor deprivation-induced apoptosis in E1A-NR.3 retinal cells.** Cell viability assay with AO/EB dye exclusion in E1A-NR.3 cells treated for 48 hr with growth media containing: serum (GM(+)) (**A**), no serum (GM(-)) (B), GM(-) plus 0.02 μM minocycline (C) or GM(-) plus 0.2 μM minocycline (D). AO-positive nuclei derived from healthy retinal cells stain green (arrows), while nuclei derived from retinal cells undergoing apoptosis have both AO and EB intercalate within genomic DNA to display orange/red pyknotic nuclei (arrowheads in A-D). (E) Histogram of the ratio of pyknotic to live nuclei observed from five high-powered fields (area = 0.23 $mm^2$) per treatment group in 3 separate experiments. $^{**}p<0.01$ compared to the GM(-) group. Scale bar = 10 μm.

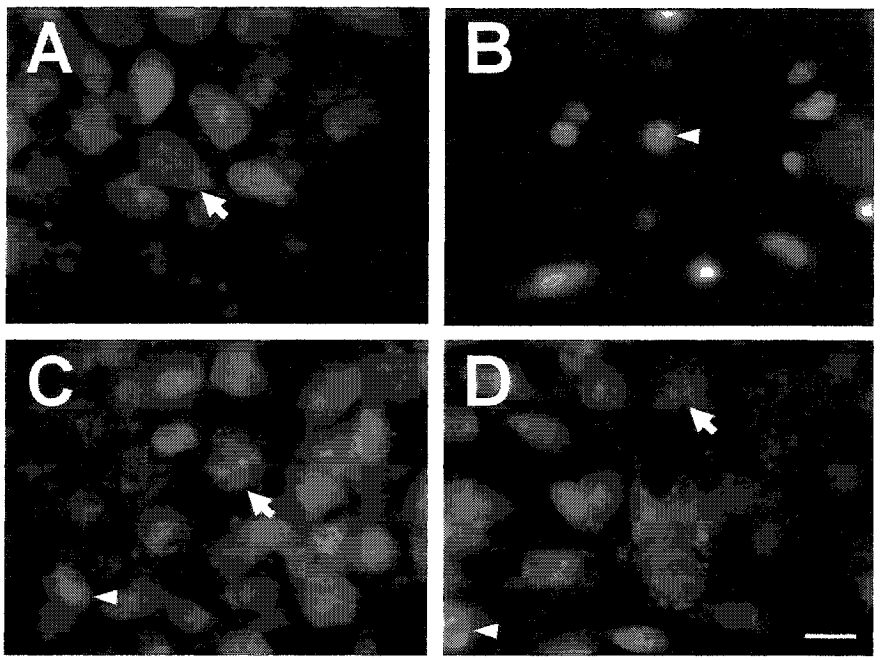
A
B
C
D

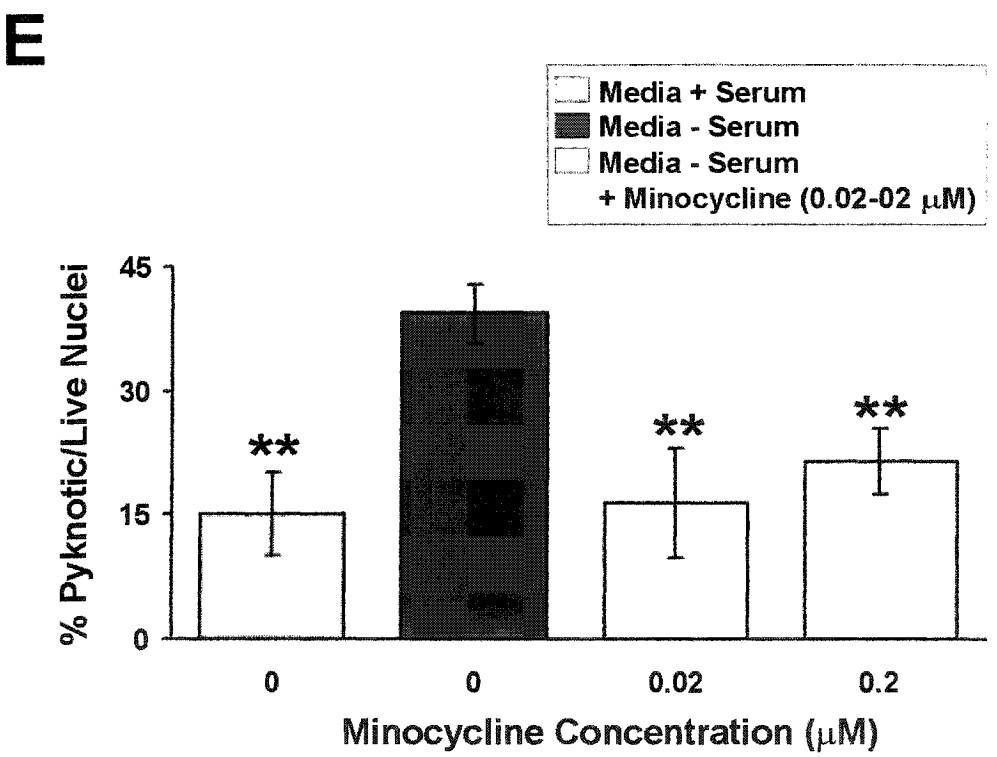
E
Media + Serum
Media - Serum
Media - Serum
+ Minocycline (0.02-02 μM)
% Pyknotic/Live Nuclei
45
30
15
0
**
**
**
0
0
0.02
0.2
Minocycline Concentration (μM)

Figure 4.9

primary retinal cell cultures were reduced to 52% ± 8% of control. Addition of minocycline produced a dose-dependent increase in cell viability. Viable cell numbers for TFD cultures supplemented with 0.002, 0.02, 0.2, 2 and 20 μM minocycline were 53% ± 7%, 53% ± 1%, 66% ± 8%, 78% ± 17% and 61% ± 14%, respectively. The increase in cell viability noted at 2 μM minocycline was significant ($p<0.05$) compared to the GM(-) group. As an internal control 20 μM minocycline was also included in GM(+) and resulted in a viability of 97% ± 10%, which was not significantly different from the control GM(+) group.

#### *4.3.4. Effect of Minocycline on Caspase-3 Expression Following Trophic Factor Deprivation*

The effects of minocycline on TFD-induced changes of caspase-3 expression were studied with RT-PCR using total RNA isolated from cultures of E1A-NR.3 retinal cells incubated for 18 hr with GM(+), GM(-), GM(-) + 0.02 μM minocycline or GM(-) + 0.2 μM minocycline (Figure 4.11). Primers specific for pro-apoptotic caspase-3 and the constitutive house keeping gene cyclophilin (internal control) generated PCR products that were visualized by UV epifluorescence following gel electrophoresis. In A, an increased caspase-3 mRNA band of 636 bp was observed for E1A-NR.3 cells maintained in GM(-) (lane 2) relative to control cells receiving GM(+) (lane 1). No apparent decrease in caspase-3 mRNA was noted for cells treated with GM(-) + 0.02 μM minocycline. In contrast, mRNA for caspase-3 was reduced in cells treated with GM(-) + 0.2 μM minocycline (lane 4). In B, the resulting densitometric ratio analysis between caspase-3 and cyclophilin (371 bp) PCR products gave values for GM(+), GM(-), GM(-) + 0.02 μM and GM(-)+ 0.2 μM minocycline as 26% ± 13%, 48% ± 19%, 57% ± 37% and

**Figure 4.10 Effect of minocycline treatment on primary retinal cell viability following trophic factor deprivation.** Percent intact nuclei for primary retinal cells treated with minocycline following 24 hr of TFD. Cell viability was assessed by counting the density of intact nuclei derived from healthy retinal cells after Zap-Oglobin cell lysis. Treatment groups consisted of growth media containing: serum, BDNF and CNTF (GM(+)), no serum, BDNF or CNTF (GM(-)), GM(+) plus minocycline (20 μM) or GM(-) plus various concentrations of minocycline (0.002-20 μM). Data are from 3 separate experiments and are expressed as the mean ± SD (%) of the GM(+) control group (100%). *$p<0.05$ and **$p<0.01$ compared to the GM(-) group.

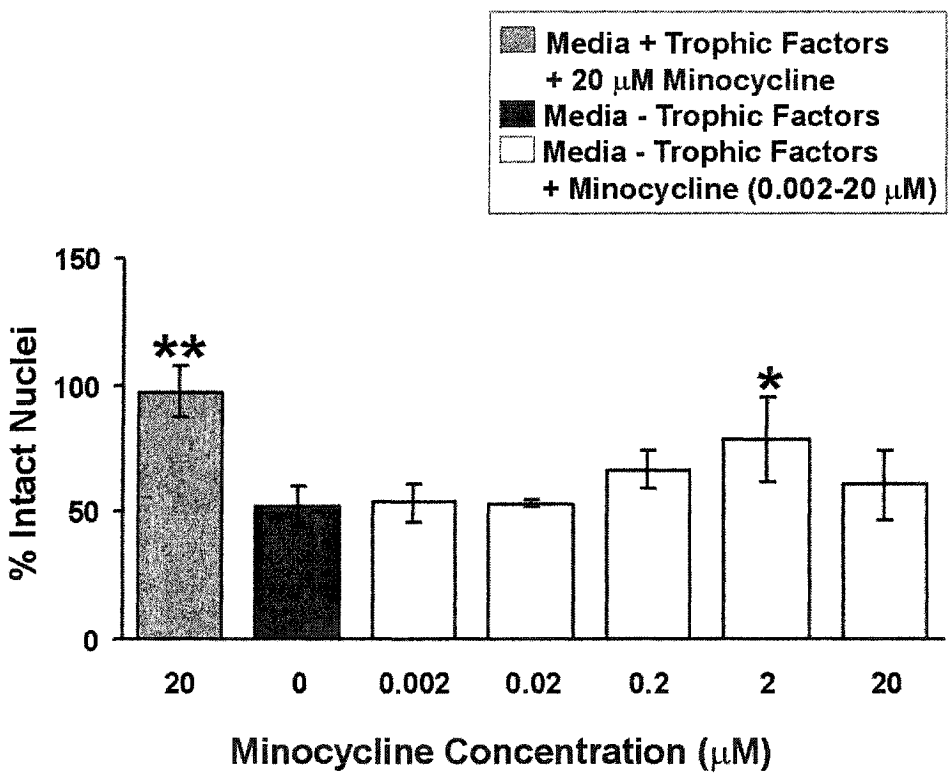
Media + Trophic Factors
+ 20 μM Minocycline
Media - Trophic Factors
Media - Trophic Factors
+ Minocycline (0.002-20 μM)
% Intact Nuclei
150
100
50
0
**
*
20
0
0.002
0.02
0.2
2
20
Minocycline Concentration (μM)

**Figure 4.10**

**Figure 4.11 Effect of minocycline on caspase-3 expression in E1A-NR.3 retinal cells following trophic factor deprivation.** (A) Electrophoresis of RT-PCR products for caspase-3 (646 bp) and cyclophilin (371 bp) following an 18 hr incubation in growth media containing: serum (GM(+); lane 1), no serum (GM(-); lane 2), GM(-) supplemented with 0.02 μM minocycline (lane 3) or GM(-) supplemented with 0.2 μM minocycline (lane 4). (B) Densitometry results of the ratio of caspase-3 PCR products to that of cyclophilin. Data represent the mean ± SD (%) from 3 separate experiments.

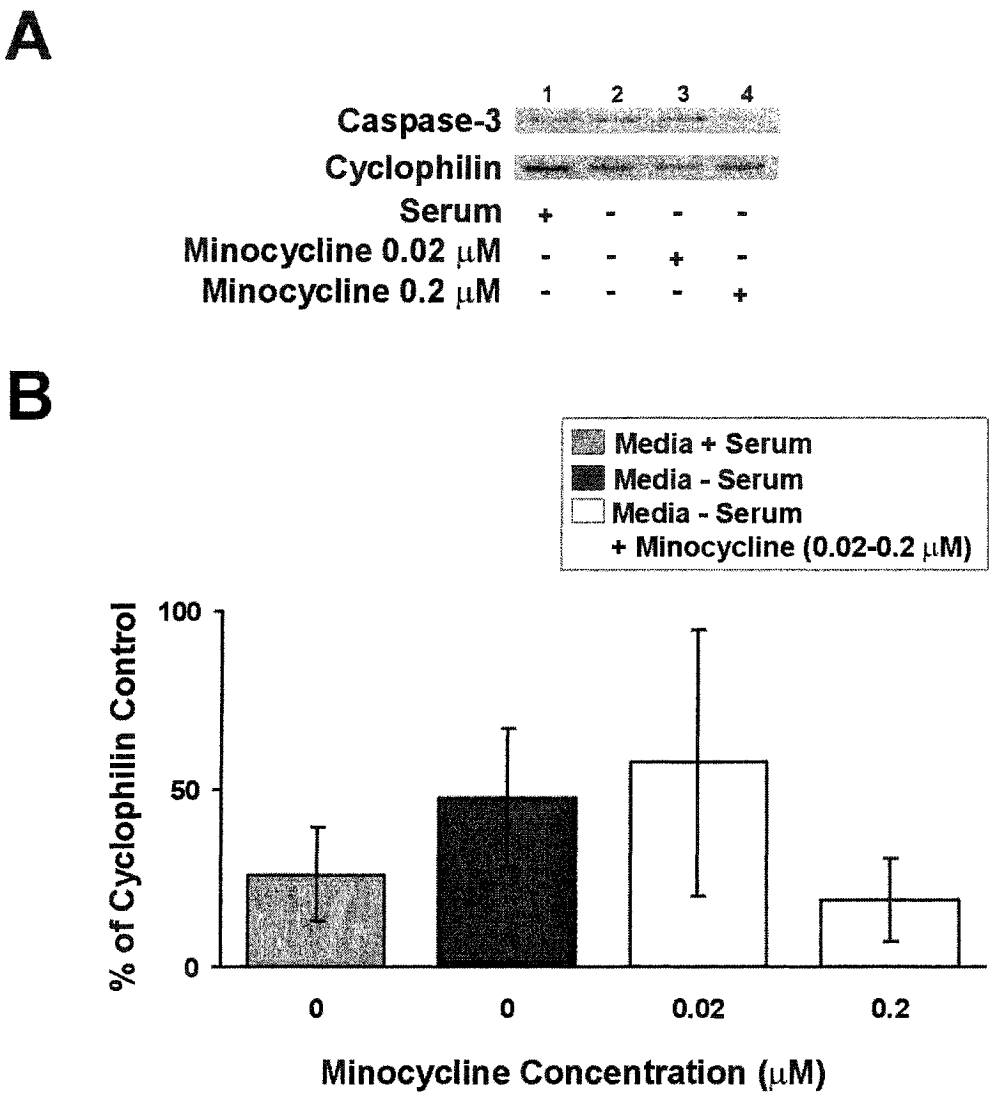
A
1 2 3 4
Caspase-3
Cyclophilin
Serum + - - -
Minocycline 0.02 μM - - + -
Minocycline 0.2 μM - - - +
B
Media + Serum
Media - Serum
Media - Serum
+ Minocycline (0.02-0.2 μM)
% of Cyclophilin Control
100
50
0
0
0
0.02
0.2
Minocycline Concentration (μM)

Figure 4.11

19% ± 12%, respectively.

Figure 4.12 shows Western blot results for caspase-3 protein expression in GM(-) treated E1A-NR.3 after 48 hr treatment with minocycline. The presence of caspase-3 activation was assessed via the expression of the 17 and 19 kDa subunits that were derived from the proteolytic cleavage of the 32 kDa pro-enzyme caspase-3. Similar to the RT-PCR results, minocycline only reduced caspase-3 activation at the higher 0.2 μM concentration.

### *4.3.5. Effect of Minocycline on NGF-differentiated PC12 Cells Following Trophic Factor Deprivation*

NGF-differentiated PC12 cell cultures were grown in the presence (GM(+)) or absence of serum and NGF (GM(-)) for 24 hr (Figure 4.13). PC12 cells exposed to GM(+) displayed extended neurites (A) and incorporated AO within their cellular DNA thereby exhibiting viable green nuclei (B and C). Removal of trophic factor support resulted in the degeneration of neuronal processes (D) and resulted in AO/EB DNA incorporation demonstrated by an increase in the number of orange/red pyknotic nuclei (E and F). PC12 cells treated with 0.02 μM minocycline during TFD showed increased neurite numbers (G) and decreased numbers of apoptotic nuclei (H and I). Graphical representation of the effect of increasing minocycline concentrations (0.002-20 μM) revealed a dose-dependent decrease in the proportion of apoptotic nuclei (J). The observed pyknotic/live nuclei ratios for differentiated PC12 cells receiving GM(+), GM(-) and GM(-) + minocycline (0.002, 0.02, 0.2, 2 and 20 μM) were 1% ± 0%, 48% ± 7%, 43% ± 10%, 29% ± 4%, 26% ± 7%, 26% ± 4% and 34% ± 7%, respectively. The

**Figure 4.12 Effect of minocycline on caspase-3 activation in E1A-NR.3 retinal cells following trophic factor deprivation.** Western blot results using antibodies specific for cleaved 17 and 19 kDa caspase-3 subunits in E1A-NR.3 cells after a 48 hr incubation in growth media containing: serum (GM(+); lane 1), no serum (GM(-); lane 2), GM(-) supplemented with 0.02 μM minocycline (lane 3) or GM(-) supplemented with 0.2 μM minocycline (lane 4).

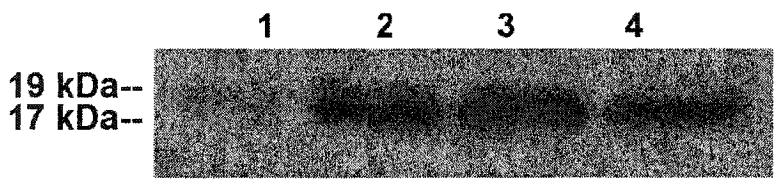


**Figure 4.12**

**Figure 4.13 Effect of minocycline treatment on trophic factor deprivation-induced apoptosis in NGF-differentiated PC12 cells.** Cell viability assessed after 24 hr treatment using AO/EB dye exclusion in NGF-differentiated PC12 cell cultures treated with growth media containing: serum and NGF (GM(+)) (B and C); no serum or NGF (GM(-)) (E and F); GM(-) plus 0.02 μM minocycline (H and I). AO-positive nuclei derived from healthy cells stain green (arrows in C and I), while nuclei derived from cells undergoing apoptosis have both AO and EB intercalate within genomic DNA to display orange/red pyknotic nuclei (arrowheads in C, F and I). The effect of TFD on PC12 neuronal processes can be seen in the phase photomicrographs (A, D and G). (J) Histogram of the ratio of pyknotic to live nuclei obtained from five high-powered fields (area=0.23 $mm^2$) per treatment group in 3 separate experiments. $^{**}p<0.01$ compared to the GM(-) group. Scale bar (G, H and I) = 20 μm.

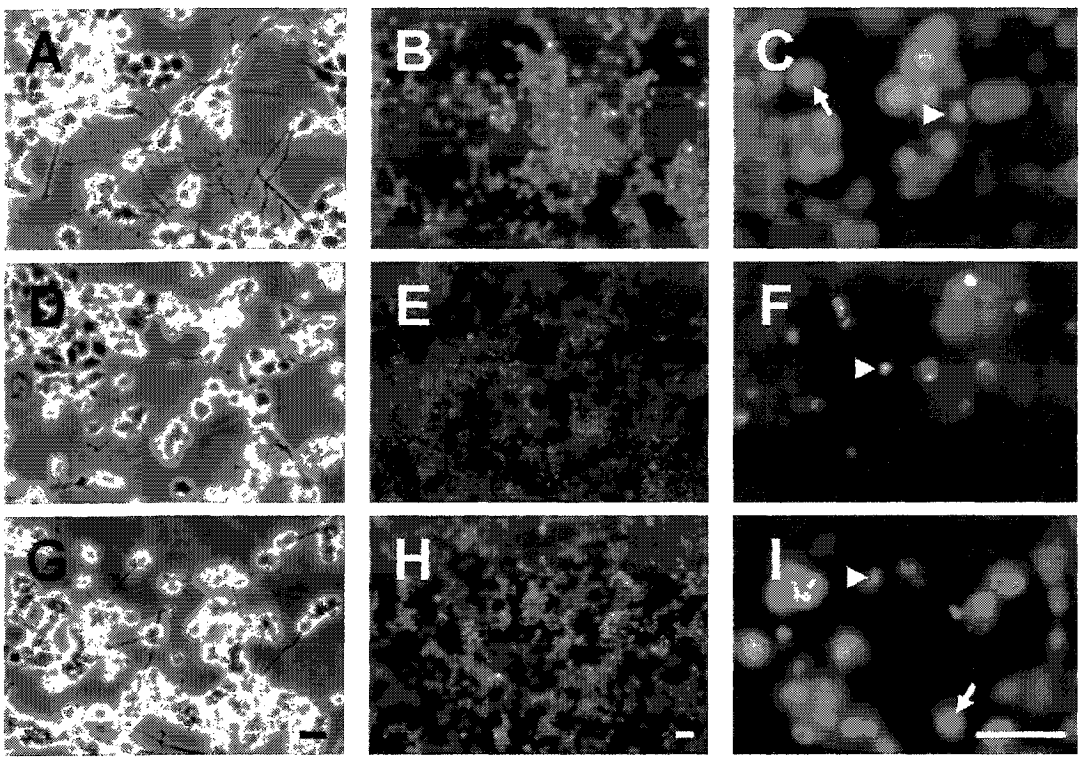
A
B
C
D
E
F
G
H
I

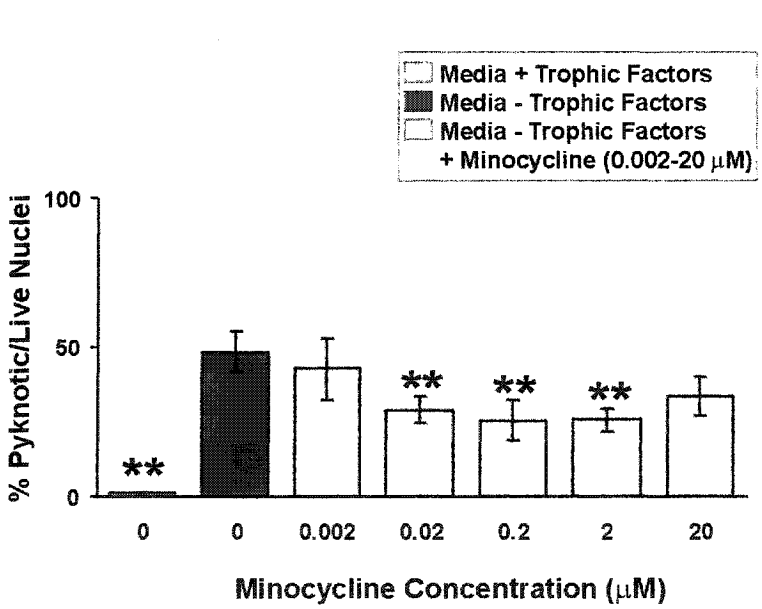
J
Media + Trophic Factors
Media - Trophic Factors
Media - Trophic Factors
+ Minocycline (0.002-20 μM)
% Pyknotic/Live Nuclei
100
50
0
**
**
**
**
0
0
0.002
0.02
0.2
2
20
Minocycline Concentration (μM)

Figure 4.13

reductions in the pyknotic/live nuclei ratio for the minocycline (0.02-2 μM) treatment groups were significant ($p<0.01$). These results suggest that minocycline can inhibit apoptosis by targeting neurons directly.

## 4.4. Discussion

The retina represents an easily accessible organ of the CNS that can be utilized for the study of neuronal death mechanisms and the evaluation of potentially neuroprotective reagents for their use in therapeutic treatment. Yet, to our knowledge, neuroprotective studies with tetracycline derivatives within the retina have not been investigated. In this study, we utilized the immortalized precursor rat retinal cell line, E1A-NR.3, to assess the neuroprotective effects of tetracycline derivatives following excitotoxicity and TFD. This cell line is known to express immunopositive markers for photoreceptors, bipolar cells, RGCs and glia (Seigel, 1996). Moreover, the E1A-NR.3 cell line demonstrates non-transformed qualities as exhibited by its contact-inhibited anchorage-dependent cell growth (Seigel et al., 1998). It has previously been demonstrated to undergo caspase-dependent apoptosis following ischemia, excitotoxicity (Tezel & Wax, 1999) and TFD (Tezel et al., 1999).

The present research examined whether or not tetracycline drugs were neuroprotective in retinal cell cultures following glutamate-induced excitotoxic and TFD-induced stresses. Previous work in our laboratory has demonstrated that primary retinal cell cultures predominantly undergo neuronal death following 24 hr exposure to elevated concentrations of glutamate (Baptiste et al., 2002). In these excitotoxicity experiments, E1A-NR.3 retinal cell viability was consistently reduced following 24 hr incubation with exogenously added 100 μM glutamate. Furthermore, increased E1A-NR.3 retinal cell

survival observed with the selective NMDAR antagonist, MK-801, suggests that such glutamate-induced cell death occurs through a NMDAR-mediated pathway, which results in subsequent upregulation of caspase-3 mRNA. In collaboration with the Baldridge laboratory, ratiometric fura-2 fluorescence experiments demonstrated minocycline (1 μM) was without any significant effect on glutamate-induced increases of $[Ca^{2+}]_i$ in isolated primary retinal neurons, suggesting that minocycline operates downstream of interactions with NMDARs and glutamate-induced $Ca^{2+}$ influx (data not shown). This result is consistent with the finding that minocycline was unable to inhibit $Ca^{2+}$-mediated loss of mitochondrial membrane potential (Zhu et al., 2002). Excitotoxicity experiments combining sub-maximal concentrations of minocycline and MK-801 resulted in enhanced neuroprotective effects, which exceeded the additive effects of each drug alone. Taken together, the above results provide strong evidence that minocycline-mediated neuroprotective actions occur via cellular targets which are distinct from the modulation of NMDAR-mediated $[Ca^{2+}]_i$ increases.

Glutamate is capable of generating mitochondrial instability, which leads to an increased production of ROS within the cell. Recently, minocycline has been shown to significantly reduce 6-hydroxydopamine-induced production of ROS in cerebellar granule neurons (Lin et al., 2003). Therefore, the protective effects observed after minocycline treatments in our retinal cell excitotoxicity experiments may also involve anti-oxidant properties.

The neuroprotective actions of minocycline were further investigated following TFD. AO/EB viability assays indicated that minocycline decreased apoptosis at comparable concentrations (0.02-200 μM) to those which increased cell viability in the

excitotoxicity experiments. Furthermore, minocycline provided retinal neuroprotection at concentrations that were similar to those previously shown to produce neuroprotection in other neuronal culture models (Tikka & Koistinaho, 2001; Zhu et al., 2002; Wang et al., 2003).

Glutamate excitotoxicity (Brecht et al., 2001) and TFD (Li et al., 1998) are known to activate caspase-3 in neuronal cultures. We showed that caspase-3 is also upregulated in the E1A-NR.3 retinal cell line following glutamate treatment and TFD. Although it is not known exactly how caspase-3 expression is enhanced in E1A-NR.3 following excitotoxic events, these cells have ionotropic GluRs and it is reasonable to assume that NMDAR-mediated $Ca^{2+}$-dependent processes may contribute to the activation of caspase-mediated apoptotic pathways. Research in spinal cord injury has demonstrated caspase-3 activation may occur via the activation of the $Ca^{2+}$-dependent phosphatase, calcineurin (Springer et al., 2000). Under non-apoptotic conditions the proapoptotic Bcl-2 member, Bad, exists in an inactive hyper-phosphorylated state which has been associated with 14-3-3 proteins within the cytosol. Following stimulation of NMDARs and elevation in $[Ca^{2+}]_i$, calcineurin frees Bad from 14-3-3 protein inhibition through dephosphorylation. Unrestricted Bad can then translocate to the mitochondrial membrane where it can promote apoptosis through the inhibition of anti-apoptotic members Bcl-2 and Bcl-$x_L$ and cyt c release from the mitochondria (Springer et al., 2000).

Trophic insufficiency may also increase neuronal mitochondrial release of cyt c through a $Ca^{2+}$-dependent mechanism. Rat dorsal root ganglion neurons deprived of NGF had increased $[Ca^{2+}]_i$ levels (Eichler et al., 1994). In addition, TFD promotes cyt c

release in superior cervical ganglia and cerebellar granular neurons through a JNK pathway which results in the enhanced transcription of the proapoptotic BH3-only Bcl-2 family members, Bcl-2 interacting mediator of cell death (Bim) and harakiri (Hrk) (Putcha et al., 2003). Once expressed Bim and Hrk promote Bax-mediated cyt c release through the inhibition of Bcl-2 and Bcl-$x_L$ (Putcha et al., 2003).

In studying the effects of minocycline on both caspase-3 mRNA and protein expression in E1A-NR.3 retinal cells, we noted that only the 0.2 μM concentration was able to decrease the levels of caspase-3. Therefore, although caspase-dependent mechanisms contribute to the death of E1A-NR.3 cells, we cannot rule out the contribution of caspase-independent apoptotic pathways in our excitotoxicity and TFD experiments. Apoptosis may occur through a caspase-independent route upon the release of the mitochondrial apoptosis-inducing factor (AIF) or endonuclease G (Cao et al., 2003). Furthermore, minocycline has been shown to block caspase-independent death triggered by etoposide in striatal neurons (Wang et al., 2003).

To determine whether the protective effects exerted by minocycline were mediated in part via direct actions on neurons we utilized pure cultures of the irreversibly NGF-differentiated PC12 cell line. Once differentiated, trophic starved PC12 cells cannot dedifferentiate by re-entering their cell cycle, instead the cells are committed to degenerate their neurites and consequently die through apoptosis (Lambeng et al., 1999). Furthermore, both caspase-3 (Vaghefi et al., 2004) and p38 mitogen-activated protein kinase (MAPK) (Lambeng et al., 2003) apoptotic pathways are activated in NGF-deprived PC12 cells. In our TFD experiments with differentiated PC12 cells, minocycline maintained the integrity of PC12 neuronal-like processes and prevented

morphological nuclear condensation. Minocycline-mediated PC12 protection may occur through inhibition of p38 MAPK as minocycline has been shown to inhibit this signalling pathway in MG (Tikka & Koitinaho, 2001). Alternatively, minocycline may exert its effects on the intrinsic apoptotic pathway thereby contributing to the inhibition of caspase-3 activation through the blockade of cyt c release (Zhu et al., 2002). In either situation, the above findings suggest that the neuroprotective effects of minocycline do not require vasculature or non-neuronal cells, both of which could potentially alter the excitotoxic environment through the uptake of extracellular glutamate and/or the release of glial-derived trophic factors, to promote neuroprotection.

The *in vitro* findings in this report are consistent with those previously published using other neurodegenerative models. Minocycline, but not tetracycline, proved to be neuroprotective in our models of retinal cell death. The retinal neuroprotective properties of minocycline may hinge on its ability to function as an antioxidant, and/or to inhibit caspase-dependent and caspase-independent cellular apoptotic pathways.

In conclusion, these findings support and extend previous observations in two ways. First, we demonstrated that minocycline could function as a neuroprotective agent in cell culture models of retinal pathophysiology. Second, we demonstrated that minocycline could protect retinal neurons independent of actions on non-neuronal cells. Taken together, these results provide the rationale for further investigation of minocycline as a possible therapeutic agent for degenerative diseases of the retina and ON.

# CHAPTER 5

# A COMPARISON OF THE NEUROPROTECTIVE EFFECTS OF TETRACYCLINE DERIVATIVES IN AN AXOTOMY MODEL OF RETINAL GANGLION CELL DEATH

## 5.1. Introduction

The CNS can no longer be considered an exclusive 'immune-privileged' system. Evidence that neurodegenerative disorders are associated with MG activation and the upregulation of pro-inflammatory cytokines suggests that the immune system is involved in certain diseases of the CNS (Giovannoni & Baker, 2003). Currently, AD, PD (Ringheim & Conant, 2004), MS (Benveniste et al., 2004), AIDS dementia (Bright et al., 2004) and GON (Yuan & Neufeld, 2001) are all believed to have some involvement of MG-mediated inflammatory processes within their respective etiologies. Although the exact origin of activated MG within the CNS remains unknown, it is thought that MG are derived from hematopoietic stem cells as the two cell types share both phenotypic and functional qualities (Flügel & Bradl, 2001).

MG are the resident macrophage and immune-sentry cells of the CNS (Benveniste et al., 2004). In response to neuronal injury, MG metamorphose from a quiescent cell with ramified processes into a reactive cell with amoeboid cell shape ready to proliferate, phagocytose debris from dying cells and initiate a T-cell response via the presentation of antigens with major histocompatibility complex (MHC) class II, CD40 and B7 (Benveniste et al., 2004). Activated MG release glutamate, TNF-α, NO, hydrogen peroxide, super oxide anion (Streit, 1993), interleukin (IL)-1β, IL-6, matrix

metalloproteinases (MMPs) (Chauvet et al., 2001) and COX-2, all of which likely work in concert to further enhance degenerative processes in CNS pathology (Gebicke-Haerter, 2001; Liu & Hong, 2003).

Although the majority of the actions by activated MG are pro-inflammatory, opposing protective capabilities are also apparent. As professional phagocytes, activated MG facilitate tissue homeostasis and remove injurious debris (Kreutzberg, 1996). Alternately, in response to neuron degeneration, activated MG release NGF (Heese et al., 1997) and glial-derived neurotrophic factor (GDNF) (Liu & Hong, 2003) and this may promote increased neuronal survival, either directly or indirectly through enhanced secretion of Müller cell-derived trophic factors. In addition, activated MG are known to secrete TGF-β1 and plasminogen, which promote reduced astrocytic scar formation and neurite outgrowth *in vitro*, respectively (Kreutzberg, 1996). Thus, collectively the actions of activated MG are truly a 'double-edged' response (Kempermann & Neumann, 2003). Despite the apparent opposing functions of reactive MG, drugs capable of inhibiting MG activation preserve neuronal integrity and increase neuronal survival in cell and animal models of neurodegeneration (Thanos et al., 1993; Liu et al., 2003).

Minocycline is used clinically as an antimicrobial agent for the treatment of conditions such as acne (Wells et al., 2003) and is currently being evaluated for its effectiveness in treating rheumatoid arthritis (Stone, 2003). In addition to its antimicrobial properties, minocycline readily crosses the BBB and in recent years has been shown to provide neuroprotection in a variety of neurodegenerative models via inhibition of MG activation (Yrjänheikki et al., 1998; Yrjänheikki et al., 1999; Tikka & Koistinaho, 2001, Tikka et al., 2001; Kriz et al., 2002; Tikka et al., 2002; Wu et al., 2002;

Dommergues et al., 2003). Thanos and colleagues (1993) previously demonstrated the potential benefit of inhibiting MG activation on RGC survival in a rat model of ON axotomy. However, the actions of the tetracycline derivatives and their ability to promote survival via inhibition of MG in the retina have not yet been assessed.

ON axotomy is a reproducible and well-accepted model for investigating RGC death while studying the effects of putative neuroprotectants in an animal model of axonal trauma (Kermer et al., 2001). Furthermore, retrograde labelling of RGCs from the SC with a stable fluorescent dye enables the simultaneous visualization and quantification of RGCs and MG in retinal whole-mounts, because activated MG phagocytose fluorescent RGC debris (Naskar et al., 2002).

In the present research we investigated the ability of systemically administered tetracycline derivatives, tetracycline and minocycline, to protect RGCs from intraorbital ON transection. In addition, we also examined the effects of these drugs on MG activation.

## 5.2. Materials & Methods

### *5.2.1. Retrograde Labelling of Retinal Ganglion Cells*

Forty-two adult Long Evans male rats weighing 225-275 g were retrogradely labelled via the SC (see General Methods, section 2.4.3). Rats used for labelling were maintained in a 12 hr light:12 hr dark cycle (7 am:7pm) and were anesthetized by intraperitoneal injection with 1 mg/kg body weight of anesthetic cocktail consisting of 1 mg/kg ketamine hydrochloride (Vetalar; Vetrepharm, Belleville, ON), 1 mg/kg xylazine (Rompun; Bayer Inc., Toronto, ON) and 1 mg/kg acepromazine (Atravet; Ayerst Veterinary Laboratories, Guelph, ON). Using a binocular microscope, two oval shaped

holes were drilled into the skull on each side of the midpoint between Bregma and Lambda to expose both lobes of the SC. A single small piece of gelfoam soaked in 2% FG was placed over the top of each SC. The incision was sealed and the animals were given 0.6 ml of 0.9% NaCl by intraperitoneal injection to account for blood loss. Upon completion of the labelling procedure, animals were returned to fresh cages and allowed to recover under a heat lamp.

### *5.2.2. Optic Nerve Transection*

ON transection was carried out 5-7 days following retrograde labelling using the protocol outlined in the General Methods, section 2.4.4. Briefly, FG-labelled rats were anesthetized and secured within a stereotaxic apparatus. Using binocular microscopy, the right superior conjunctiva was sutured and retracted to place the ON into a more accessible position for transection. The conjunctiva was incised close to the orbital rim and lateral to the cornea. The orbit was opened, lacrimal glands were moved out of view to the side and extra-ocular muscles were separated to expose the ON. After removing the overlying dura, complete transection of the ON was completed at a distance of 1-2 mm from the back of the globe using micro-scissors, while taking care not to interrupt the blood supply via the central retinal artery. Following axotomy, the characteristic arbor of blood vessels for the operated right eye was fundoscopically checked with an ophthalmoscope. The contralateral unoperated left eye served as control. Animals were returned to their cages and allowed to recover under a heat lamp.

### *5.2.3. Drug Administration & Treatment Regimen*

A total of 24 animals that had previously undergone procedures for retrograde labelling were utilized for the study of systemically administered tetracycline drugs.

Three consecutive days proceeding ON transection animals received daily single intraperitoneal injections of either 45 mg/kg tetracycline, 45 mg/kg minocycline or an equal volume of 0.9% NaCl vehicle. Concurrent with ON transection, the drug concentration was halved to 22.5 mg/kg. Drug dosing at 22.5 mg/kg was continued 1X daily at roughly the same time of day for another 6 days. On the $7^{th}$ day animals were sacrificed by $CO_2$ inhalation and retinas were processed for histology.

### *5.2.4. Retinal Whole-mounts*

Processing of retinal whole-mounts was carried out as outlined in the General Methods, section 2.4.5. In short, 5-14 days following ON transection, rats were sacrificed by $CO_2$ overdose and the eyes were enucleated and transferred to a dissecting dish where the lens was removed under binocular microscopy. The remaining ocular tissues were then fixed in 4% paraformaldehyde for 3 hr on a mechanical shaker. Following fixation, the retinas were carefully dissected, cut into quadrants and whole-mounted in mounting media on glass slides. The slides were covered with a 22x22 $mm^2$ cover-slip and sealed with nail polish. All slides were labelled with water-soluble marker and given to an independent investigator for recoding to mask the identification of retinal tissue from the initial investigator. The slides were examined using a Nikon C1 microscope equipped for epifluorescence with filters for UV-2A (excitation 330-380 nm; barrier 420 nm; emission 400 nm). Black and white images of retinal whole-mounts were captured with a COHU High Performance CCD camera using a 20X objective (standard area of 0.23 $mm^2$). Experimental and control retinas had FG-positive cells quantified at eccentric distances of 1, 2 and 3 mm from the ONH for each quadrant. RGCs were distinguished by their large circular cell bodies, while retinal MG were

identified as small rod shaped cells, which were often, aligned parallel to the retinal vasculature (Thanos et al., 1994; Naskar et al., 2002).

### *5.2.5. Statistical Analysis*

*In vivo* data were analyzed by the non-parametric two-tailed Mann-Whitney Rank Sum test. On normalization to contralateral controls, *in vivo* data were tested for normality with the Kolmogorov-Smirnov test followed by a parametric one-way ANOVA with a Dunnett Multiple Comparison post-test. All statistics were computed using GraphPad Instat version 3.00 Software for Windows 95 (San Diego, CA). The criterion for noting a significant difference was $p<0.05$.

## 5.3. Results

### *5.3.1. Retinal Ganglion Cell & Microglial Cell Profiles Following Optic Nerve Transection*

Figure 5.1 shows the profile of RGC viability and MG activation over the course of 5, 7, 10 and 14 days after intraorbital transection of the ON 1-2 mm from the eye globe. At 5 days following ON transection, the mean RGC density from axotomized retinas was 1799 ± 143 cells/mm$^2$ (n=4). By 7, 10 and 14 days after axotomy the mean RGC densities were decreased to 1014 ± 86 (n=4), 651 ± 234 (n=4) and 386 ± 102 cells/mm$^2$ (n=6), respectively. Furthermore, the decreases in FG-labelled RGCs quantified at 7, 10 and 14 days following ON transection were all significant ($p<0.05$, $p<0.05$ and $p<0.01$, respectively). MG were not observed in axotomized retinas until 7 days following ON transection. At 7, 10 and 14 days following ON transection the mean MG densities were 167 ± 72, 348 ± 99 and 415 ± 59 cells/mm$^2$, respectively. This data

**Figure 5.1 RGC and MG densities following optic nerve transection.** RGC (  ) and MG (  ) counts made within a 0.23 $mm^2$ area at distances of 1, 2 and 3 mm from the optic disc for each quadrant of the retina 5-14 days following ON transection. Data points represent mean ± SD for groups of 2-6 experimental animals. *$p$<0.05 and **$p$<0.01 RGC densities compared to RGC densities at 5 days post-axotomy.

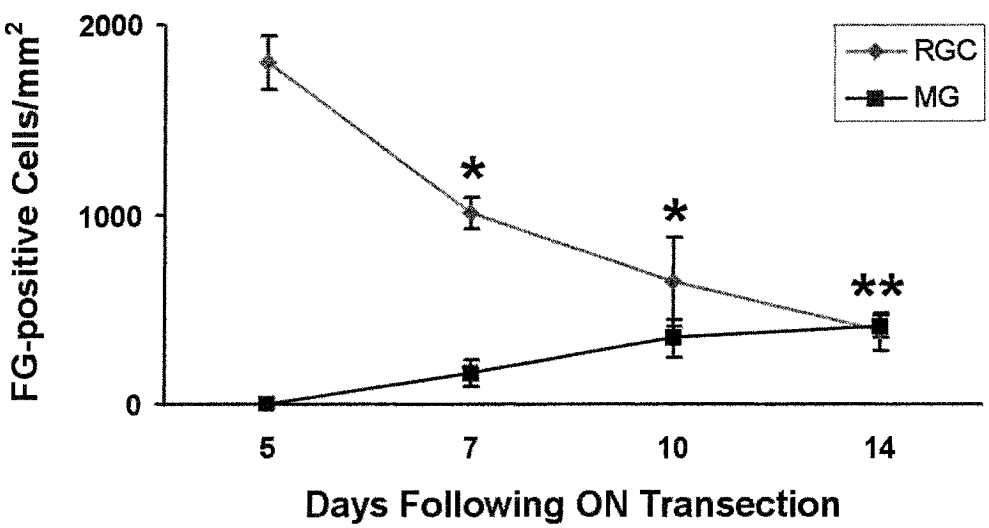
2000
1000
0
FG-positive Cells/mm2
RGC
MG
*
*
**
5
7
10
14
Days Following ON Transection

**Figure 5.1**

suggests that a delayed pattern of RGC death and MG activation results following intraorbital transection the ON. Subsequent experiments investigating the potential of tetracycline drugs to protect RGCs and reduce MG activation were carried out at 7 days post-axotomy. In the rat, RGC death occurs through a predictable course following a complete intraorbital transection of the ON (Chaudhary et al., 1999; Kermer et al., 2001). Virtually all RGCs survive the first 5 days after sustaining axonal injury and then die abruptly in large numbers, reducing the RGC population to approximately 50% by day 7 and to less than 10% by day 14 (Berkelaar et al., 1994). Therefore, we felt that the greatest opportunity to observe tetracycline derivative-mediated neuroprotection in axotomized eyes would occur at 7 days post injury.

### *5.3.2. Effect of Tetracycline Derivatives on Retinal Ganglion Cell & Microglial Cell Densities Following Optic Nerve Transection*

The effects of systemically administered tetracycline derivatives on RGC death induced by ON transection were compared to saline vehicle controls. Histological analysis of retinal whole-mounts from animals treated with 0.9% NaCl showed a noticeable decrease in RGC density at each of the eccentric distances (Figure 5.2). In addition, the pattern of phagocytosis-dependent labelling of MG in axotomized retinas displayed a dependence on eccentric distance from the ONH, with less MG at more distal regions of the retina. Similar observations were made when analyzing the tetracycline-treated retinas. In contrast, minocycline treatment decreased RGC loss and MG activation in comparison to vehicle and tetracycline-treated retinas. Quantification of the FG-labelled RGCs in the contralateral controls of tetracycline derivative-treated animals

**Figure 5.2 Retinal histology for saline control, tetracycline and minocycline treated animals.** Representative photomicrographs of whole-mounted retinas derived from animals receiving either 0.9% NaCl, tetracycline or minocycline intraperitoneal injections. FG-labelled cells were analyzed at eccentric distances of 1, 2 and 3 mm from the optic disc of contralateral control or axotomized retinas 7 days following ON transection. RGCs exhibited typical round somas (arrows), while MG presented as small elongated cells (arrowheads). FG-labelled MG were not present in contralateral control retinas. Scale bar = 20 μm.

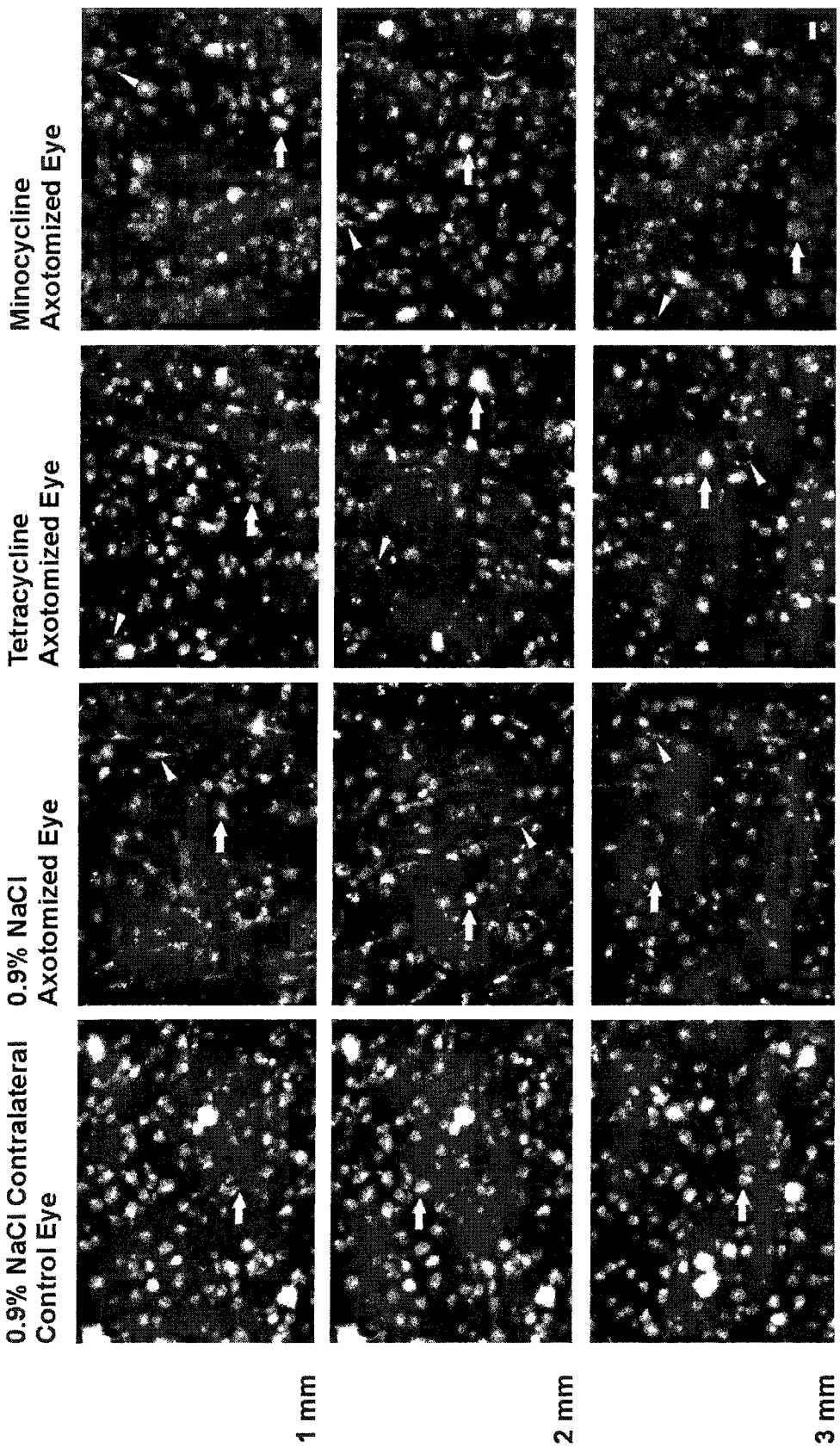
0.9% NaCl Contralateral Control Eye
0.9% NaCl Axotomized Eye
Tetracycline Axotomized Eye
Minocycline Axotomized Eye
1 mm
2 mm
3 mm

Figure 5.2

Densities of FG-Labelled Cells Following Transection of the Optic Nerve 1-2 mm From the Eye Globe

| Survival Interval | Vehicle 0.9% NaCl Contralateral Control Left Eye | Vehicle 0.9% NaCl Axotomized Right Eye | Tetracycline Contralateral Control Left Eye | Tetracycline Axotomized Right Eye | Minocycline Contralateral Control Left Eye | Minocycline Axotomized Right Eye |
|---|---|---|---|---|---|---|
| *7-Days* | | | | | | |
| *n*= | 8 | 8 | 8 | 8 | 8 | 8 |
| RGC Density/mm$^2$ | 1895 +/- 147 | 1030 +/- 186 | 1926 +/- 247 | 1158 +/- 190 | 2174 +/- 280 [a] | 1456 +/- 336 [b] |
| % RGC Survival | 100 | 54 +/- 7 | 100 | 60 +/- 8 | 100 | 67 +/- 11 [c] |
| Phagocyte Density/mm$^2$ | 0 | 345 +/- 74 | 0 | 295 +/- 126 | 0 | 257 +/- 107 |
| % Phagocyte Activation | - | 25 +/- 6 | - | 20 +/- 8 | - | 16 +/- 7 [d] |

***Density data are expressed as MEAN +/- SD. Drugs and vehicle were administered intraperitoneally.***

[a] Significantly greater RGC density than in vehicle-treated left eye contralateral control retinas ($p$=0.00487, Dunnett Multiple Comparison Test).

[b] Significantly greater RGC density than in vehicle-treated axotomized retinas (P=0.0074, Dunnett Multiple Comparison Test).

[c] Significantly greater % RGC survival than in vehicle-treated axotomized retinas (P=0.0321, Dunnett Multiple Comparison Test).

[d] Significantly less % phagocyte activation than in vehicle-treated retinas (P=0.0340, Dunnett Multiple Comparison Test).

**Table 5.1**

**Figure 5.3 Mean densities of FG-labelled RGCs 7 days following ON transection.** Retrogradely FG-labelled RGCs were quantified in rats receiving intraperitoneal injections of 0.9% NaCl, tetracycline or minocycline 7 days following ON transection in 0.23 $mm^2$ retinal areas. Data are from 8 separate experiments and are expressed as the mean ± SD (%) of the contralateral unoperated eye. *$p<0.05$ compared to 0.9% NaCl controls.

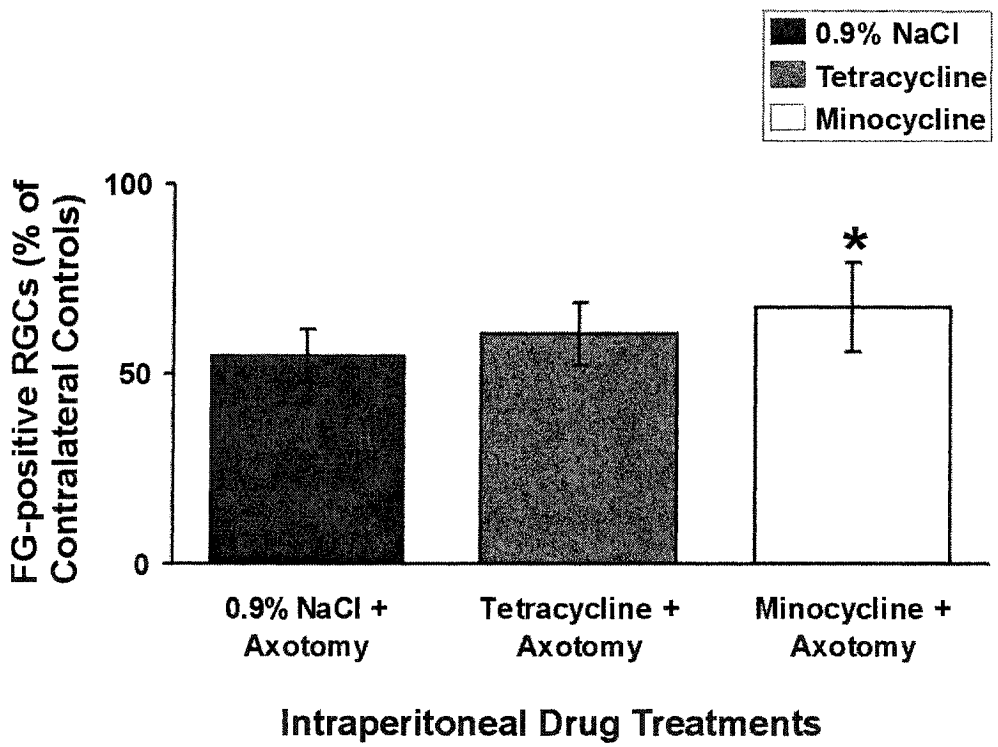
0.9% NaCl
Tetracycline
Minocycline
FG-positive RGCs (% of Contralateral Controls)
100
50
0
*
0.9% NaCl + Axotomy
Tetracycline + Axotomy
Minocycline + Axotomy
Intraperitoneal Drug Treatments

**Figure 5.3**

**Figure 5.4 Mean densities of FG-labelled MG 7 days following ON transection.** FG-labelled MG were quantified in rats receiving intraperitoneal injections of 0.9% NaCl, tetracycline or minocycline 7 days following ON transection in 0.23 $mm^2$ retinal areas. Data are from 8 separate experiments and are expressed as the mean ± SD (%) of the total FG-positive cell density in axotomized retinas. *$p<0.05$ compared to 0.9% NaCl controls.

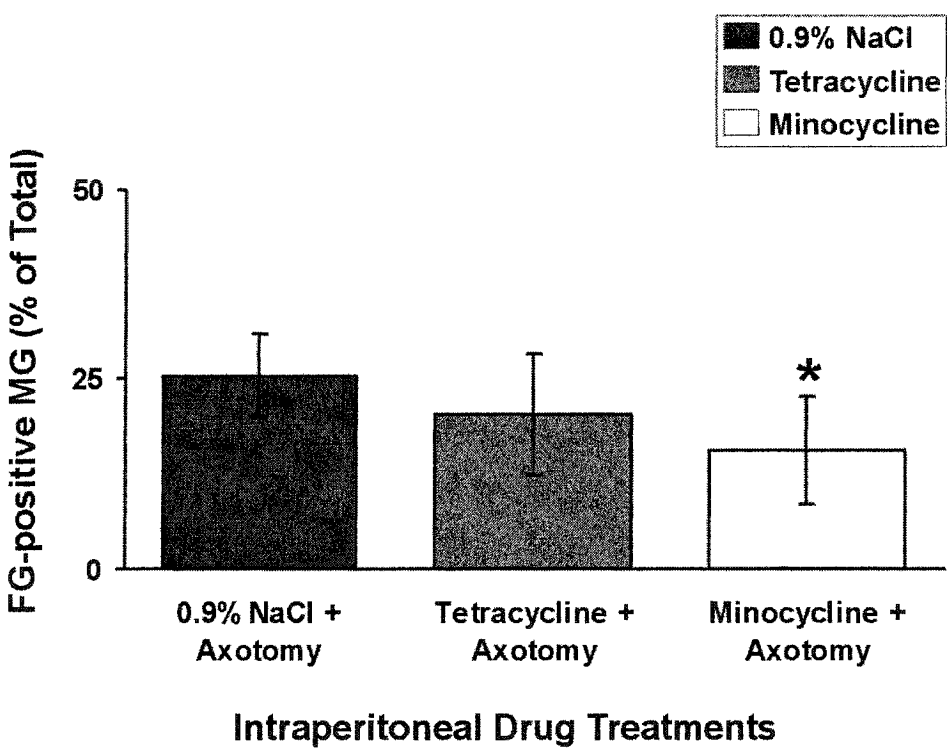
0.9% NaCl
Tetracycline
Minocycline
FG-positive MG (% of Total)
50
25
0
*
0.9% NaCl + Axotomy
Tetracycline + Axotomy
Minocycline + Axotomy
Intraperitoneal Drug Treatments

**Figure 5.4**

indicated increased densities relative to contralateral controls in 0.9% NaCl treated animals (Table 5.1). Therefore, the results from axotomized eyes were normalized to RGC densities from their respective contralateral controls (Figure 5.3). In axotomized retinas of vehicle-treated animals, RGC densities were decreased to 54% ± 7% of those found in corresponding contralateral control retinas. Intraperitoneal injections of tetracycline and minocycline elevated the mean RGC densities to 60% ± 8% and 67% ± 11%, respectively, however, only the increase in FG-labelled RGCs measured in the minocycline treatment group was significant ($p<0.05$). Quantification of FG-positive MG indicated that the tetracycline derivatives had inhibited the activation of MG (Figure 5.4). Vehicle-treated animals had a MG density corresponding to 25% ± 6% of the total FG-positive cells within axotomized retinas. Systemic tetracycline or minocycline treatment reduced MG densities in axotomized eyes to 20% ± 8% and 16% ± 7%, respectively. Furthermore, the decrease in MG density seen with minocycline treatment was significant ($p<0.05$). Collectively, these results suggest that the minocycline-mediated increase in FG-labelled RGCs occurs in conjunction with the inhibition of MG activation.

### *5.3.3. Effect of Tetracycline Derivatives on Retinal Ganglion Cell & Microglial Cell Densities Following Optic Nerve Transection At Differing Eccentricities*

A comparison of systemic tetracycline derivative treatment on RGC densities at the different retinal eccentricities of 1, 2 and 3 mm from the ONH revealed that both of the tetracycline derivatives increased RGC survival in comparison to saline vehicle-treated animals (Figure 5.5). At the 1 mm eccentricity, the mean RGC density percentage for saline vehicle, tetracycline and minocycline-treated animals was 52% ± 11%, 57% ±

**Figure 5.5 Mean eccentric densities of FG-labelled RGCs 7 days following ON transection**. Retrogradely FG-labelled RGCs were quantified in 0.23 $mm^2$ retinal areas at distances of 1, 2 and 3 mm from the optic disc in rats receiving intraperitoneal injections of 0.9% NaCl, tetracycline or minocycline at 7 days following ON transection. Data are from 8 separate experiments and are expressed as the mean ± SD (%) of unoperated contralateral eyes. *$p<0.05$ compared to 0.9% NaCl controls.

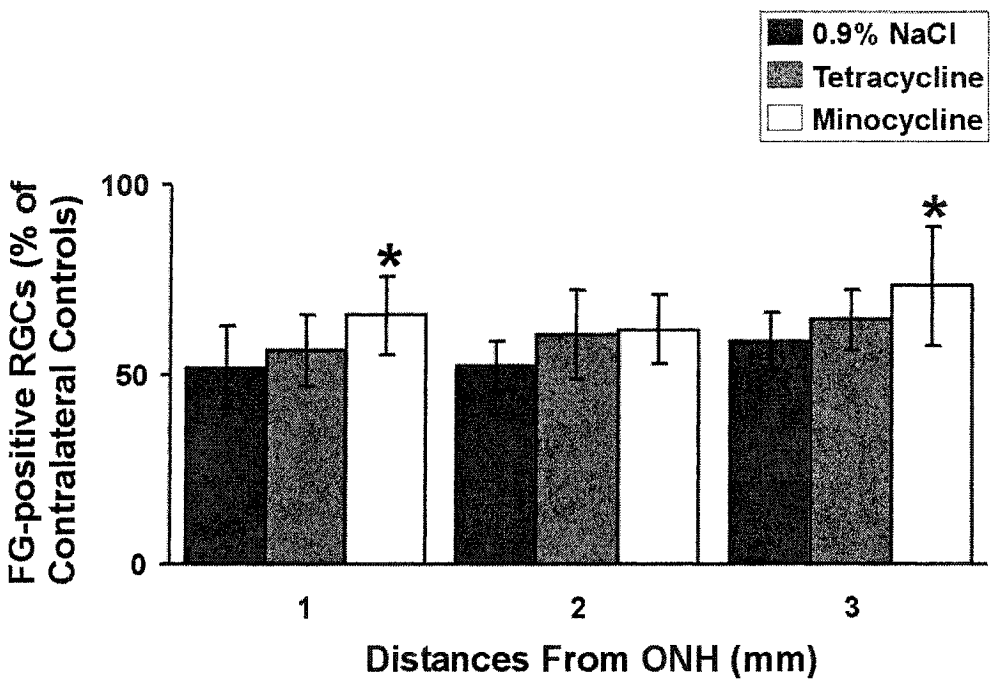
0.9% NaCl
Tetracycline
Minocycline
FG-positive RGCs (% of Contralateral Controls)
100
50
0
*
*
1
2
3
Distances From ONH (mm)

**Figure 5.5**

9% and 66% ± 10%, respectively. However, in comparison to saline control axotomized eyes, the increase in RGC density at this distance was significant ($p<0.05$) only for minocycline-treated animals. At the 2 mm eccentricity the percentages for RGC survival for saline vehicle, tetracycline and minocycline-treated animals corresponded to 52% ± 6%, 61% ± 12% and 62% ± 9%, however, in comparison to saline controls, both of the tetracycline derivatives failed to significantly increase the FG-positive RGC densities. At the 3 mm eccentricity, the percentages for FG-positive RGC density for vehicle, tetracycline and minocycline-treated animals were 59% ± 8%, 65% ± 8% and 73% ± 16%, respectively and the increased RGC density quantified in minocycline-treated animals was significantly ($p<0.05$) greater than that in the saline control group.

The ability of the tetracycline derivatives to reduce the density of phagocytosis-dependent FG-positive MG were also assessed at 1, 2 and 3 mm retinal eccentricities 7-days post-transection (Figure 5.6). At the 1 mm eccentricity the mean percentage of FG-positive MG were 29% ± 6%, 23% ± 9% and 18% ± 8% for the saline vehicle, tetracycline and minocycline-treated animals, respectively. The reduction in the density of FG-positive MG was significant ($p<0.05$) only for animals treated with minocycline at this distance. Similar effects on MG activation were observed with the tetracycline derivatives at the 2 and 3 mm retinal eccentric distances. At the 2 mm eccentricity the mean FG-positive MG density percentages for saline controls, tetracycline and minocycline-treated animals corresponded to 27% ± 5%, 21% ± 8% and 16% ± 8%, with a significant ($p<0.05$) reduction occurring only with minocycline treatment. While, at the 3 mm eccentricity, the mean FG-positive MG density percentages for saline controls,

**Figure 5.6 Mean eccentric densities of FG-positive MG 7 days following ON transection.** FG-labelled MG were quantified in 0.23 $mm^2$ retinal areas at distances of 1, 2 and 3 mm from the optic disc in rats receiving intraperitoneal injections of 0.9% NaCl, tetracycline or minocycline at 7 days following ON transection. Data are from 8 separate experiments and are expressed as the mean ± SD (%) of the total FG-positive cell density within axotomized eyes. *$p<0.05$ and compared to 0.9% NaCl controls.

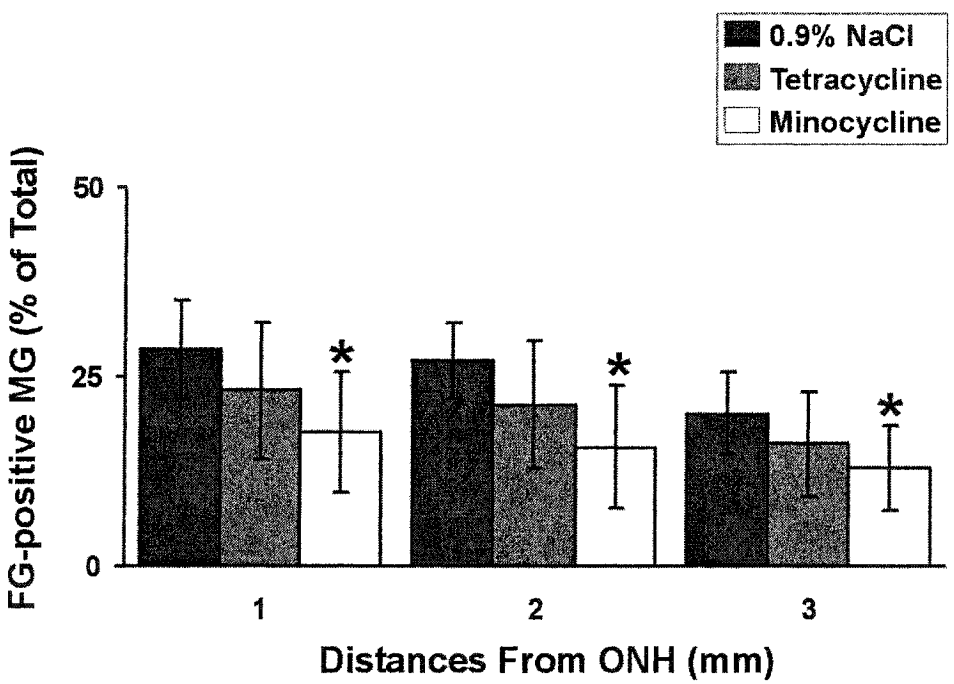
0.9% NaCl
Tetracycline
Minocycline
FG-positive MG (% of Total)
50
25
0
*
*
*
1
2
3
Distances From ONH (mm)

**Figure 5.6**

tetracycline and minocycline-treated animals corresponded to 20% ± 5%, 16% ± 7% and 13% ± 5%. In comparison to the saline vehicle control group, the reduction of FG-positive MG density in minocycline-treated animals was significant ($p<0.05$). Collectively, the results from the retinal eccentricity analyses suggest that MG activation contributes to axotomy-induced RGC death and that the tetracycline derivatives can promote increased RGC survival through inhibition of MG activation. However, it is also likely that in addition to MG activation other pro-apoptotic processes are initiated that affect RGC viability and these may be negatively affected by derivatives of tetracycline. Our previous findings indicated that minocycline might also act independently of MG targets to enhance RGC viability via inhibition of neuronal caspase-dependent and caspase-independent cell death pathways (Chapter 4).

## 5.4. Discussion

RGC death after transection of the ON provides a useful model system in which one can study RGC death and retinal neuroprotection. Following ON transection, RGCs undergo apoptotic death (Berkelaar et al., 1994; Chaudary et al., 1999) as a consequence of a loss of trophic support and/or changes in trophic responsiveness (Näpänkangas et al., 2003). Elevated intraocular levels of the excitatory amino acids glutamate and aspartate (Yoles & Schwartz, 1998) and deleterious inflammatory effects by activated MG (Yaun & Neufeld, 2001) may also contribute to RGC death following axotomy. Successful neuroprotective strategies previously demonstrated in models of axotomy-induced RGC death include the administration of caspase inhibitors (Chaudhary et al., 1999), GluR antagonist (Yoles & Schwartz, 1998), trophic factors (Klöcker et al., 2000) and inhibitors of MG activation (Thanos et al., 1993).

In the present study, we compared the neuroprotective actions of tetracycline and minocycline in an axotomy model of RGC death. This study demonstrated that minocycline, but not tetracycline, was able to significantly prevent RGC death following ON transection and activation of MG. These findings are supported by our previous *in vitro* studies, in which we have verified that minocycline is neuroprotective in retinal cell cultures following glutamate excitotoxicity and TFD while tetracycline did not have any neuroprotective effects (Chapter 4). In other experimental studies, using mouse models of ALS (Kriz et al., 2002) and PD (Wu et al., 2002) minocycline was found to effectively inhibit activated MG with minimal effects on astrocytes. However, the neuroprotective effects of minocycline seen in the 1-methyl-4-phenyl-1,2,3,6-tetrahydropyridine Parkinson's mouse model appeared to exceed the beneficial effects that would be expected by MG-derived iNOS inhibition, implying an additional direct protective effect of minocycline on neurons and/or inhibition of other MG associated cytotoxins (Wu et al., 2002).

Previous experimental studies of brain ischemia have demonstrated that minocycline is significantly more lipid soluble than tetracycline and is able to effectively cross the BBB to distribute throughout the CNS, including the retina, producing a reduction in ischemic neuronal damage (Yrjänheikki et al., 1998; Yrjänheikki et al., 1999; Chen et al., 2000). The lack of a significant neuroprotective effect by tetracycline in this and other studies has been attributed to the poor tissue distribution of this drug into the CNS. However, the present research is in support that systemically administered tetracycline can cross the blood-retinal-barrier (BRB) to impact neuronal viability and MG responses. Moreover, others have observed that tetracycline can cross the BBB

following systemic intraperitoneal injections (Yang et al., 2003). Furthermore, in an experimental rat model of PD following 1-methyl-4-phenyl-1,2,3,6-tetrahydropyridine challenge, brain tetracycline levels were shown to be significantly increased, suggesting that CNS injury may weaken the BBB increasing tetracycline entry. Bruch's membrane, the margin of the ON that is unmyelinated, represents a weakened area of the BRB (Neufeld, 1999). Bruch's membrane may represent an entry point for which systemically administered tetracycline derivatives can accumulate within the retina. Furthermore, a complete transection of the ON may also permit the accumulation of tetracycline in the retina. Thus, it would be of interest to test the efficacy of tetracycline derivatives in other animal models of RGC death that maintain an intact ON. Despite ability for tetracycline to enter the retina, tetracycline still did not produce a significant neuroprotective effect. The ineffectiveness by tetracycline to significantly increase RGC survival is supported by our *in vitro* results with E1A.NR3 retinal cell line cultures, where despite adequate drug concentrations at cellular targets, tetracycline was markedly less efficacious than minocycline and produced no significant neuroprotection (Chapter 4).

In the present research we used the contralateral unoperated eyes as internal controls to assess RGC protection following unilateral ON lesion. We expected that the effects of unilateral lesion and systemic drug treatments would not significantly affect the contralateral eye. However, parallel with increased RGC densities in injured retinas of animals receiving systemic minocycline treatments, we noted significantly increased RGC densities in corresponding contralateral controls relative to saline vehicle-treated controls. Tetracycline treatment also produced a small increase in contralateral control RGC densities relative to vehicle-treated contralateral retinas. Thus, systemic treatment

with the tetracycline derivatives following unilateral ON transection generated a bilateral effect that was apparent as an increase in FG-labelled cells in both contralateral controls and axotomized eyes. Although it is possible that a common proportion of retino-retinal projections were damaged following unilateral ON transection, the percentage number axons that project to both eyes in the adult rat is small (Müller & Holländer, 1998).

An alternative explanation for increased RGC densities in the unoperated eyes of tetracycline derivative-treated animals may stem from the technique used to visualize MG in this study. We investigated the effects of tetracycline derivatives on MG activities by pre-labelling RGCs with the vital fluorescent dye, FG. FG-labelling of MG occurred via phagocytosis of apoptotic FG-labelled RGCs. The major advantage of this imaging technique is that it allows the selective detection of MG that have become activated and internalized dying RGCs. However, this technique does not account for the subpopulation of activated MG, which have not yet engulfed the debris of injured FG-labelled RGCs (Thanos et al., 1994). Potentially, unlabelled activated MG that have escaped detection in contralateral eyes may release pro-inflammatory cytokines that initiate RGC death and thus, reduce the numbers of FG-positive RGCs. Therefore, the inhibition of inflammatory processes by the systemic administration of tetracycline derivatives may account for the increased numbers of FG-labelled RGCs in the contralateral control eyes. In support of this hypothesis Bodeutsch et al. (1999) noted increased MG in both the crushed ON and the ON situated contralateral to injury. Moreover, the same study demonstrated that the immediate early gene transcription factor, c-jun, was uniformly expressed within the GCL of the unlesioned eye (Bodeutsch et al., 1999). It is therefore clear that caution must be exercised when using the

contralateral side as an internal control for a unilateral lesion of the CNS. Analyses of naïve controls treated with minocycline and tetracycline, as well as the use of additional immunohistochemical labelling techniques for assessing the effects of the tetracycline derivatives on MG activities following ON transection will allow clarification of these observations.

Although ON transection is not a GON model, there are characteristics that are common to both. For example, degeneration in both the animal model of axotomy and GON result in the selective apoptotic loss of RGCs and MG activation (Yoles & Schwartz, 1998). Moreover, both may include excitotoxic and TFD-induced stresses (Yoles & Schwartz, 1998; Dreyer et al., 1996; Quigley, 1999; Kikuchi et al., 2000). Thus, ON transection is a valuable model for screening neuroprotective drugs that may be efficacious for adjunctive treatment along side of conventional therapies for optic neuropathies related to GON. The results from this research corroborate and extend previous findings that minocycline promotes neuroprotection in degenerative models of the CNS. Following intraorbital transection of the ON, RGC survival can be enhanced with minocycline, in part via inhibition of retinal MG activation. Minocycline is a multi-faceted neuroprotectant that has already been demonstrated to have a good safety record during prolonged use in humans to treat infections associated with acne (Wells et al., 2003). In light of the findings reported here, further research with minocycline in animal models that are more representative of GON appears to be justified.

# CHAPTER 6

# GENERAL DISCUSSION & FUTURE DIRECTION

Neuroprotective research is relevant to the treatment of optic neuropathies (Marcic et al., 2003), where the underlying etiology results in the death of RGC populations (Levin, 2003). Therapeutic interventions for neurodegenerative disorders of the CNS are hindered, largely because the complete pathogenic process remains unknown (Doble, 1999). However, the development of novel neuroprotective strategies are at a major advantage in comparison to traditional treatment modalities because neuroprotection prevents neuronal death without necessarily targeting every risk factor involved in the etiology of the neurologic disease (Weinreb & Levin, 1999). Moreover, when neuroprotection is combined with standard therapies, an additive or synergistic response is expected (Levin et al., 1999).

The major goal of this thesis was to use both *in vitro* cell cultures and *in vivo* animal models to compare the abilities of AR-drugs and tetracycline derivatives to prevent apoptotic death of retinal neurons and to resolve the pharmacologic mechanism(s) accounting for the neuroprotective actions of these drugs. The neural retina and ON are often used to model the CNS and coupled with their relative easy accessibility, the retina and ON represent ideal model systems for testing putative neuroprotectants (He et al., 2003).

Chapter 3 of this thesis investigated the β-AR antagonists: betaxolol, timolol and metoprolol; and the α2-AR agonist, brimonidine (UK14, 304), in an *in vitro* model of retinal neuron excitotoxicity. Of the drugs tested only betaxolol (10-100 μM) and

brimonidine (10 μM) effectively increased retinal neuron survival. Considering the β-AR drugs together, this result suggested that the neuroprotection provided by betaxolol occurred independent of interactions with β-ARs since neither the non-selective β-AR blocker, timolol nor the selective β1-AR blocker, metoprolol increased retinal neuron survival. In contrast, the neuroprotective effects of brimonidine were dependent on interactions with α2-ARs as treatment of retinal neurons with brimonidine (10 μM) and yohimbine (1-10 μM) completely abolished any neuroprotective effects. Furthermore, ratiometric fura-2 $Ca^{2+}$ imaging experiments on isolated rat retinal neurons revealed that both betaxolol and brimonidine could prevent glutamate (100 μM)-induced increases in $[Ca^{2+}]_i$ (Baptiste et al., 2002).

Chapter 4 of this thesis compared the neuroprotective capabilities of the tetracycline derivatives, tetracycline and minocycline in cell culture models of retinal neuron excitotoxicity and TFD-induced death. Effective retinal neuroprotection was only observed following minocycline treatment (0.02-200 μM). We also demonstrated that the neuroprotection elicited by minocycline in retinal cell cultures likely occurs downstream of interactions with NMDARs. Enhanced survival of neurons exposed to excitotoxic conditions was observed in retinal cell cultures receiving a combination of sub-maximal concentrations of the selective NMDAR antagonist, MK-801 (1μM) and minocycline (0.002 μM). Moreover, in ratiometric fura-2 $Ca^{2+}$ imaging experiments, minocycline (1 μM) treatment of isolated rat retinal neurons did not prevent glutamate induced increases in $[Ca^{2+}]_i$ (data not shown). The inhibitory effects of minocycline on apoptosis were investigated both morphologically with AO/EB nuclear imaging and biochemically with RT-PCR and Western blot analysis of caspase-3. We observed that

minocycline inhibited TFD-induced apoptosis in both the E1A-NR.3 rat retinal cell line and in pure cultures of the NGF-differentiated rat PC12 cell line. We also reported that both the gene transcript and proteolytic processing of caspase-3 following TFD were reduced upon treatment with minocycline (0.2 μM).

Chapter 5 of this thesis compared the efficacy for the tetracycline derivatives to increase RGC survival and decrease MG activation following intraorbital transection of the rat ON. Using a histological technique to simultaneously visualize RGCs and activated MG we were able to determine that of the tetracycline drugs studied only minocycline provides significant neuroprotection of axotomized RGCs and reduced MG activation. These results further corroborated findings in other systems that demonstrated minocycline could significantly enhance neuronal survival and inhibit MG activation (Yrjänheikki et al., 1998; Yrjänheikki et al., 1999; He et al., 2001; Dommergues et al., 2003; Kremlev et al., 2004).

Although a variety of studies have investigated the neuroprotective properties of the β-AR antagonists, α2-AR agonists and tetracycline derivatives using animal models of CNS degeneration, few experiments have been carried out using *in vitro* cell preparations of the retina. Furthermore, with regard to the tetracycline-derivatives, our findings are the first to report neuroprotective effects of minocycline in cell and animal models of retinal neuron death. Given that apoptosis has now been described in several optic neuropathies (Levin & Gordon, 2002) and is also believed to be the final common pathway for selective neuron loss in a variety of other neurodegenerative diseases (Larner, 2000; Friedlander, 2003; Levin, 2003), the use of *in vitro* models of retinal

neuron excitotoxicity and TFD, as well as animal models of ON injury leading to RGC apoptosis are relevant for the study of neuroprotective drugs in the retina.

The work reported in this thesis utilized the rat as a representative mammalian model for retinal neuron death. Similarities in anatomical structure and physiology to the human primate retina, lower associated costs and the availability of molecular tools were all reasons in support of this choice (Quigley & Hothman, 1983). Furthermore, a great deal of previous retinal neuroprotection research has utilized rat models, providing insightful information to aid our understanding of the patterns of retinal neuron death.

Since both betaxolol (Suzuki et al., 2003) and α-AR agonists (Jarajapu et al., 2001) have previously been demonstrated to have effects on vasculature, it was necessary to determine whether their retinal neuroprotective properties resulted from actions on retinal neurons directly or if the protective effects were secondary to changes in vasculature. The findings from our cell culture studies allowed us to rule out any contributing effects of drug-induced changes in retinal vasculature for each drug's pharmacological effect. Another advantage in using cell culture models to investigate retinal neuroprotection is the ability to 'control' the extracellular environment (i.e. media). However, as with any experimental model, disadvantages were also associated with the use of these cell culture preparations. First, the use of a mixed preparation of retinal cells makes it difficult to determine the specific cell type(s) that were lost or survived following exposure to the death stimulus (excitotoxicity or TFD) or to the neuroprotectant, respectively. Where RGCs are the predominant neuronal type that is lost in optic neuropathies (Levin & Gordon, 2002), the results from this research would have been more applicable to the neuroprotection in optic neuropathies related to GON

had it demonstrated that the drug-induced neuroprotection was specific to RGCs. This could have been accomplished by identifying RGCs within mixed retinal cultures via retrograde labelling with a vital dye such as FG or via the immunocytochemical identification of RGCs with Thy-1 antibody (Takahashi et al., 1991). Alternatively, the establishment of pure RGC cultures would permit the observation of direct neuroprotective effects. However, in the case of pure RGC cultures the numbers of cells produced are small and growing neurons in the absence of supporting glia may change their properties. Krishnamoorthy et al. (2001) have recently developed a transformed rat retinal cell line (RGC-5) that has been shown to positively express markers specific for RGCs including Thy-1, Brn-3C, neuritin, NMDAR and GABA receptor. In addition, the RGC-5 line did not express markers for GFAP, syntaxin and HPC-1, or 8A1, which eliminated the possibility of this cell line containing Müller glial, amacrine or horizontal cells, respectively (Krishnamoorthy et al., 2001). Like native RGCs, the RGC-5 cell line undergoes apoptotic cell death following excitotoxicity and TFD (Krishnamoorthy et al., 2001). Thus, use of the RGC-5 line could potentially further our understanding of the retinal neuroprotective actions of β-AR antagonists, α2-AR agonists and tetracycline derivatives by providing a representative cell culture model for RGCs.

The second disadvantage associated with the culture models used in this research is that these cultures were derived from early postnatal animals. It is both more costly and challenging to produce neuronal cultures from adult retinas (López et al., 1999). Therefore, the *in vitro* results reported in this thesis research may inadvertently reflect processes of retinal neuron death and drug-induced protection during a period of time that coincides with developmental retinal cell death (López et al., 1999). Moreover, the

sensitivity of retinal neurons to excitotoxicity and loss of target derived trophic factors is known to change with maturation (Luo et al., 2001; Isenmann et al., 2003). For example, injection of NMDA into the corpus striatum of 7 day old rats generates greater toxic effects in comparison to adult rats receiving even larger NMDA doses (McDonald et al., 1988). Furthermore, following ON axotomy, the time course for massive RGC death occurs within 48 hr in the neonatal rat (Rabacchi et al., 1994), whereas, 2 weeks are required for similar RGC death to occur in the adult rat (Berkelaar et al., 1994). Thus, direct extrapolations of our *in vitro* results to disorders affecting the adult CNS may be difficult to make.

The *in vivo* model used in this thesis research also had its advantages and disadvantages. The primary benefit for using ON transection as a model for studying neuroprotectants in the retina is that this injury provides a relatively straightforward and consistent pattern of selective RGC death and MG activation, which in turn can be analyzed after retrograde labelling with FG in retinal whole-mounts. Thus, in this research the rat ON axotomy model was useful as an initial screening of the neuroprotection provided by the tetracycline derivatives. However, the major disadvantages with this model are: (1) it does not likely reflect the pathogenesis of optic neuropathies in humans; (2) the damage inflicted on the ON is irreversible. The only conceivable scenario where such an acute event may occur is in direct traumatic optic neuropathy (e.g. from a bullet or knife) and iatrogenic transection during surgical resection of an adjacent or intrinsic tumor (Levin & Gordon, 2002). In contrast to complete transection of the ON, optic neuropathies involving a compression of the ON, such as that resulting from neoplasms or aneurysms, occur more commonly and in

degenerative models that maintain an intact ON the neuroprotective properties of minocycline may be more pronounced. Similarly, in GON where damage is slow and progressive, minocycline may be efficacious in delaying or preventing vision loss occurring via loss of RGCs. Furthermore, complete transection of the ON represents an irreversible injury to the RGC. For this reason, apart from regenerative strategies, no intervention is likely to preserve the function or integrity of the axotomized RGC in an indefinite manner.

A number of the neuroprotective agents that have reached clinical trials target a specific event within the ischemic cascade, such as blockade of NMDAR-mediated toxicity (De Keyser et al., 1999). However, despite proven success in cell and animal models of neuronal death, neuroprotective strategies targeting specific events within the ischemic cascade have failed to improve the outcome of patients with neurodegenerative disease in clinical trials (De Keyser et al., 1999). Accordingly, a more suitable neuroprotective strategy would be one that involves a multi-faceted approach for neuroprotection. The drugs shown to be neuroprotective in this thesis research, namely betaxolol, brimonidine and minocycline, all appear to provide neuroprotection in the retina via actions at several different targets. For example, both betaxolol and brimonidine, in addition to their ability to reduce IOP (Hoyng & van Beek, 2000) also reduce glutamate-induced $Ca^{2+}$ influx in isolated rat retinal neurons (Baptiste et al., 2002). Our research with the tetracycline-derivatives showed that minocycline also increases retinal neuron survival following glutamate-induced excitotoxicity, TFD (Chapter 4) and intraorbital ON transection (Chapter 5). Furthermore, we provide novel information that minocycline was able to inhibit apoptosis by acting directly at retinal

neuronal targets (Chapter 4), as well as inhibiting MG activation (Chapter 5). Another advantage that supports the use of these drugs as retinal neuroprotectants is that following topical or systemic administration, these drugs all enter the CNS at concentrations comparable to those required for *in vitro* neuroprotection (Wood et al., 2001; Lai et al., 2002; Kent et al., 2001; Yrjänheikki et al., 1999).

The findings from this research provide a strong rationale for further investigation into the neuroprotective properties of AR-drugs and tetracycline derivatives in experimental models that are more representative of clinical optic neuropathies. These models may include: (1) the retinal ischemia/reperfusion model, in which saline is forced into the anterior chamber through a cannulated syringe to elevate the IOP above the systolic blood pressure for various periods of time, thereby causing retinal damage that closely resembles central retinal artery occlusion (Büchi, 1992); (2) the ON crush model in which an acute, calibrated and reproducible partial compression of the ON in adult rodents results in degeneration of RGCs and activation of MG (Schwartz et al., 1996); (3) the intraocular hypertension rat model, in which IOP is chronically elevated by scarring the episcleral veins with hypertonic saline injections (Morrison et al., 1997), cauterization of episcleral veins (Laquis et al., 1998) or via translimbal laser photocoagulation of the trabecular meshwork (Levkovitch-Verbin et al., 2002b). All three of the chronic intraocular hypertension models resemble GON in that they increase IOP to a level that generates RGC death and ON injury, while causing minimal ancillary damage to the retina and ocular structures (Levkovitch-Verbin et al., 2002b).

The research in this thesis has focused on the use of pharmacological agents to interfere with neuronal apoptotic pathways in the retina. However, another approach for

retinal neuroprotection may involve gene therapy. There is a strong association of race and family history with GON, suggesting that there may be a significant genetic cause for the disease. Mapping techniques based on large families with well-defined glaucoma have led to the localization and identification of several genes related to GON (Wirtz & Samples, 2003). The first major breakthroughs in POAG genetic research occurred in 1996 and 1997 with the discoveries of the gene loci *GLC1A* and *GLC1B*, respectively (Stoilova et al., 1996; Stone et al., 1997). At present there are six different loci for POAG, denoted *GLC1A-F* (Budde, 2000).

The *GLC1A* gene comprises three exons and encodes a 504 amino acid glycoprotein called trabecular meshwork-induced glucocorticoid response protein (TIGR), also known as myocilin (MYOC) (Stoilova et al., 1996). TIGR/MYOC has been mapped to chromosome 1q23-q25 (Sarfarazi, 1997). TIGR/MYOC mRNA has been isolated from trabecular meshwork, ciliary body, retina, iris, sclera, choroid and cornea ocular tissues, as well as several locations outside of the eye (Tamm, & Polansky, 2001). Currently there are more than 30 different mutations identified for TIGR/MYOC associated with POAG in populations of different ethnic backgrounds around the world and transmission of the disease within *GLC1A* families is believed to follow an autosomal dominant inheritance with varying penetrance (Buddle, 2000). Kim et al. (2001) generated mice heterozygous and homozygous for null TIGR/MYOC mutations. No changes in IOP, ocular histopathology, vitality or fertility were found in either of the genetically altered mice, leading to the conclusion that mutated TIGR/MYOC did not contribute to the pathogenesis of POAG through a loss of function, but rather resulted in a gain of function (Kim et al., 2001). Joe et al. (2003) proposed that the commonly

occurring mutant TIGR/MYOC peptides exert cytotoxic effects within trabecular meshwork cells through uncontrolled accumulation within the endoplasmic reticulum. The proposed mechanism may lead to dysfunction of trabecular meshwork cells resulting in reduced AH outflow in POAG.

The *GLC1E* gene has been mapped to a 21 cM region on chromosome 10p14-15 within a large British family with typical NTG (Sarfarazi et al., 1998). More recently the gene product for *GLC1E,* optineurin (OPTN), has been identified (Rezaie et al., 2002). OPTN contains three non-coding exons in the 5'-untranslated region (UTR) and 13 exons that encode a 577 amino acid protein and is expressed in trabecular meshwork, non-pigmented ciliary epithelium, retina, as well as non-ocular tissues including the brain (Rezaie et al., 2002). Detectable levels of OPTN have been found in AH samples from humans and a variety of other species suggesting that it is a secreted protein (Rezaie et al., 2002). OPTN has previously been identified as NF-κB essential modulator related protein (NRP) (Schwamborn et al., 2000). NRP has been shown to assist TNF-α signalling (Li et al., 1998). A pathogenic role for TNF-α in the course of glaucomatous progression may exist through elevated IOP- or ischemia-induced activation of ONH astrocytes (Tezel & Wax, 2000). However, protective mechanisms mediated through the TNFR-NF-κB signalling pathway have also been demonstrated (Chen & Goeddle, 2002). OPTN gene mutations have been reported in 16.7% of families with hereditary POAG (Rezaie et al., 2002). Wildtype OPTN may have a neuroprotective function, whereas mutated OPTN results in optic neuropathy due to an inability of defective OPTN to assist TNF-α signalling in increasing NF-κB activation and translocation to the nucleus (Rezaie et al., 2002; Chen & Goeddle, 2002).

While an exact etiology for GON remains unknown, understanding the functions of these newly identified genes may provide researchers with a mechanism for GON. Furthermore, it is likely that due to the heterogeneous nature of GON that more genes will be discovered in the near future expanding the need for additional functional studies. Increased genetic knowledge about GON together with effective neuroprotective strategies may lead to the identification of therapies that can bypass the genetic defect and lead to treatment of GON patients at the earliest stages of the disease, thus resulting in more effective treatment and improved vision.

# APPENDIX

## Terms

**1. Payment**
Client is advised to adhere to the following payment schedule. 100% payment due upon delivery of final artwork. Payments must be received within 30 days of receipt of invoice. A 1.5 % monthly service charge will be billed for late payment.

**2. Grant of Rights**
Usage rights outlined on page one are conditioned on receipt of full payment.

**3. Estimates**
The fees and expenses shown will change only when some change is requested by the client. Final fees shall be shown when invoice in rendered. The Client's approval shall be obtained for any increase in fees.

**4. Sales Tax**
The client is responsible for the payment of sales tax if any such tax is due.

**5. Cancellation**
In the event of cancellation or breach by the client, the illustrator shall retain ownership of all rights of copyright and the original artwork, including sketches and any other preliminary materials. The Client shall pay the illustrator according to the following schedule. 25% of original fee if cancellation occurs before preliminary sketches, 50% of original fee if canceled after preliminary sketches are completed, 100% if canceled after completion of finished art.

**6. Alterations**
Alteration to artwork shall not be made without consulting the initial illustrator, and the illustrator shall be allowed the first option to make alterations when possible.

**7. Revisions**
The Client and/or medical advisor has the right to request revisions to the artwork as needed at the sketch stage and also minor revisions after reviewing the final artwork. After approval of artwork by the Client, and/or medical experts in the field, medical/scientific accuracy of the final artwork is the responsibility of the Client. Revisions not due to the fault of the illustrator shall be billed separately.

**8. Credit Lines**
On any contribution for magazine, book, print or digital use, the illustrator shall receive name credit.

**9. Warranty of Originality**
The illustrator warrants and represents that, to the best of her knowledge, the work assigned hereunder is original and has not been previously published, or that consent to use has been obtained on an unlimited basis; that all work or portions thereof obtained through the undersigned from third parties is original or, if previously published, that consent to use has been obtained on an unlimited basis; that the illustrator has full authority to make this agreement; and that the work prepared by the illustrator does not contain any scandalous, libelous, or unlawful matter. This warranty does not extend to any uses that the Client or others may make of the Artist's product that may infringe on the rights of others. Client expressly agree that it will hold the illustrator harmless for all liability caused by the Client's use of the illustrator's product to the extent such use infringes on the rights of others.

**10. Acceptance of Terms**
The signature of both parties shall evidence acceptance of these terms.

**Consented and Agreed to:** Marjorie Calderon

Nobuko Kelly

27 Judy Anne Ct • Sackville, NS • B4C 3X8 • 902-452-3576 • www.users.eastlink.ca/~medicaldesign

# REFERENCES


Aarts, M.M. & Tymianski, M. (2003) Novel treatment of excitotoxicity: targeted disruption of intracellular signalling from glutamate receptors. *Biochem Pharmacol*, **66**, 877-886.

Agarwal, N., Martin, E., Krishnamoorthy, R.R., Landers, R., Wen, R., Krueger, S., Kapin, M.A. & Collier, R.J. (2002) Levobetaxolol-induced Up-regulation of retinal bFGF and CNTF mRNAs and preservation of retinal function against a photic-induced retinopathy. *Exp Eye Res*, **74**, 445-453.

Ahmed, F.A., Hegazy, K., Chaudhary, P. & Sharma, S.C. (2001) Neuroprotective effect of α2 agonist (brimonidine) on adult rat retinal ganglion cells after increased intraocular pressure. *Brain Res*, **913**, 133-139.

Alward, W.L. (1998) Medical management of glaucoma. *N Engl J Med*, **339**, 1298-1307.

Ansah, T.A., Ramamoorthy, S., Montanez, S., Daws, L.C. & Blakely, R.D. (2003) Calcium-dependent inhibition of synaptosomal serotonin transport by the α 2-adrenoceptor agonist 5-bromo-N-[4, 5-dihydro-1H-imidazol-2-yl]-6-quinoxalinamine (UK14304). *J Pharmacol Exp Ther*, **305**, 956-965.

Ballif, B.A. & Blenis, J. (2001) Molecular mechanisms mediating mammalian mitogen-activated protein kinase (MAPK) kinase (MEK)-MAPK cell survival signals. *Cell Growth Differ*, **12**, 397-408.

Baptiste, D.C., Hartwick, A.T., Jollimore, C.A., Baldridge, W.H., Chauhan, B.C., Tremblay, F. & Kelly, M.E.M. (2002) Comparison of the neuroprotective effects of adrenoceptor drugs in retinal cell culture and intact retina. *Invest Ophthalmol Vis Sci*, **43**, 2666-2676.

Benveniste, E.N., Nguyen, V.T. & Wesemann, D.R. (2004) Molecular regulation of CD40 gene expression in macrophages and microglia. *Brain Behav Immun*, **18**, 7-12.

Berkelaar, M., Clarke, D.B., Wang, Y.C., Bray, G.M. & Aguayo, A.J. (1994) Axotomy results in delayed death and apoptosis of retinal ganglion cells in adult rats. *J Neurosci*, **14**, 4368-4374.

Berlie, J.R., Iversen, L.J., Blaxall, H.S., Cooley, M.E., Chacko, D.M. & Bylund, D.B. (1995) Alpha-2 adrenergic receptors in the bovine retina. Presence of only the alpha-2D subtype. *Invest Ophthalmol Vis Sci*, **36**, 1885-1892.

Bertolesi, G.E., Shi, C., Elbaum, L., Jollimore, C., Rozenberg, G., Barnes, S. & Kelly, M.E.M. (2002) The $Ca^{2+}$ channel antagonists mibefradil and pimozide inhibit cell growth via different cytotoxic mechanisms. *Mol Pharmacol*, **62**, 210-219.

Blomgren, K. & Karlsson, J.O. (1990) Calpain and calpastatin activity in the optic pathway. *Neurosci Lett*, **112**, 179-183.

Bloomfield, S.A. & Dowling, J.E. (1985a) Roles of aspartate and glutamate in synaptic transmission in rabbit retina. I. Outer plexiform layer. *J Neurophysiol*, **53**, 699-713.

Bloomfield, S.A. & Dowling, J.E. (1985b) Roles of aspartate and glutamate in synaptic transmission in rabbit retina. II. Inner plexiform layer. *J Neurophysiol*, **53**, 714-725.

Bodeutsch, N., Siebert, H., Dermon, C. & Thanos, S. (1999) Unilateral injury to the adult rat optic nerve causes multiple cellular responses in the contralateral site. *J Neurobiol*, **38**, 116-128.

Bonelli, R.M., Heuberger, C. & Reisecker, F. (2003) Minocycline for Huntington's disease: an open label study. *Neurology*, **60**, 883-884.

Bonne, C., Muller, A. & Villain, M. (1998) Free radicals in retinal ischemia. *Gen Pharmacol*, **30**, 275-280.

Brandoli, C., Sanna, A., De Bernardi, M.A., Follesa, P., Brooker, G. & Mocchetti, I. (1998) Brain-derived neurotrophic factor and basic fibroblast growth factor downregulate NMDA receptor function in cerebellar granule cells. *J Neurosci*, **18**, 7953-7961.

Brecht, S., Gelderblom, M., Srinivasan, A., Mielke, K., Dityateva, G. & Herdegen, T. (2001) Caspase-3 activation and DNA fragmentation in primary hippocampal neurons following glutamate excitotoxicity. *Mol Brain Res*, **94**, 25-34.

Bright, J.J., Natarajan, C., Sriram, S. & Muthian, G. (2004) Signaling through JAK2-STAT5 pathway is essential for IL-3-induced activation of microglia. *Glia*, **45**, 188-196.

Brubaker, R.F. (1996) Delayed functional loss in glaucoma. LII Edward Jackson Memorial Lecture. *Am J Ophthalmol*, **121**, 473-483.

Brubaker, R.F. (2003) Targeting outflow facility in glaucoma management. *Surv Ophthalmol*, **48 Suppl 1**, S17-S20.

Buchi, E.R. (1992) Cell death in the rat retina after a pressure-induced ischaemia-reperfusion insult: an electron microscopic study. I. Ganglion cell layer and inner nuclear layer. *Exp Eye Res*, **55**, 605-613.

Budde, W.M. (2000) Heredity in primary open-angle glaucoma. *Curr Opin Ophthalmol*, **11**, 101-106.

Bustin, S.A. (2000) Absolute quantification of mRNA using real-time reverse transcription polymerase chain reaction assays. *J Mol Endocrinol*, **25**, 169-193.

Bylund, D.B. & Chacko, D.M. (1999) Characterization of α2 adrenergic receptor subtypes in human ocular tissue homogenates. *Invest Ophthalmol Vis Sci*, **40**, 2299-2306.

Calzada, J.I., Jones, B.E., Netland, P.A. & Johnson, D.A. (2002) Glutamate-induced excitotoxicity in retina: neuroprotection with receptor antagonist, dextromethorphan, but not with calcium channel blockers. *Neurochem Res*, **27**, 79-88.

Cantor, L. (2003) Achieving low target pressures with today's glaucoma medications. *Surv Ophthalmol*, **48 Suppl 1**, S8-16.

Cao, G., Pei, W., Ge, H., Liang, Q., Luo, Y., Sharp, F.R., Lu, A., Ran, R., Graham, S.H. & Chen, J. (2002) *In vivo* delivery of a Bcl-xL fusion protein containing the TAT protein transduction domain protects against ischemic brain injury and neuronal apoptosis. *J Neurosci*, **22**, 5423-5431.

Cao, G., Clark, R.S., Pei, W., Yin, W., Zhang, F., Sun, F.Y., Graham, S.H. & Chen, J. (2003) Translocation of apoptosis-inducing factor in vulnerable neurons after transient cerebral ischemia and in neuronal cultures after oxygen-glucose deprivation. *J Cereb Blood Flow Metab*, **23**, 1137-1150.

Carter-Dawson, L., Crawford, M.L., Harwerth, R.S., Smith, E.L., 3rd, Feldman, R., Shen, F.F., Mitchell, C.K. & Whitetree, A. (2002) Vitreal glutamate concentration in monkeys with experimental glaucoma. *Invest Ophthalmol Vis Sci*, **43**, 2633-2637.

Chao, H.M., Chidlow, G., Melena, J., Wood, J.P. & Osborne, N.N. (2000) An investigation into the potential mechanisms underlying the neuroprotective effect of clonidine in the retina. *Brain Res*, **877**, 47-57.

Chaudhary, P., Ahmed, F., Quebada, P. & Sharma, S.C. (1999) Caspase inhibitors block the retinal ganglion cell death following optic nerve transection. *Mol Brain Res*, **67**, 36-45.

Chauhan, B.C., LeVatte, T.L., Jollimore, C.A., Yu, P.K., Reitsamer, H.A., Kelly, M.E.M., Yu, D.Y., Tremblay, F. & Archibald, M.L. (2004) Model of endothelin-1-induced chronic optic neuropathy in rat. *Invest Ophthalmol Vis Sci*, **45**, 144-152.

Chauvet, N., Palin, K., Verrier, D., Poole, S., Dantzer, R. & Lestage, J. (2001) Rat microglial cells secrete predominantly the precursor of interleukin-1beta in response to lipopolysaccharide. *Eur J Neurosci*, **14**, 609-617.

Chen, G. & Goeddel, D.V. (2002) TNF-R1 signaling: a beautiful pathway. *Science*, **296**, 1634-1635.

Chen, M., Ona, V.O., Li, M., Ferrante, R.J., Fink, K.B., Zhu, S., Bian, J., Guo, L., Farrell, L.A., Hersch, S.M., Hobbs, W., Vonsattel, J.P., Cha, J.H. & Friedlander, R.M. (2000) Minocycline inhibits caspase-1 and caspase-3 expression and delays mortality in a transgenic mouse model of Huntington disease. *Nat Med*, **6**, 797-801.

Cheon, E.W., Park, C.H., Kang, S.S., Cho, G.J., Yoo, J.M., Song, J.K. & Choi, W.S. (2003) Betaxolol attenuates retinal ischemia/reperfusion damage in the rat. *Neuroreport*, **14**, 1913-1917.

Choi, D.W. (1987) Ionic dependence of glutamate neurotoxicity. *J Neurosci*, **7**, 369-379.

CNTGSG (1998a) Comparison of glaucomatous progression between untreated patients with normal-tension glaucoma and patients with therapeutically reduced intraocular pressures. Collaborative Normal-Tension Glaucoma Study Group. *Am J Ophthalmol*, **126**, 487-497.

CNTGSG (1998b) The effectiveness of intraocular pressure reduction in the treatment of normal-tension glaucoma. Collaborative Normal-Tension Glaucoma Study Group. *Am J Ophthalmol*, **126**, 498-505.

Coakes, R.L. & Brubaker, R.F. (1978) The mechanism of timolol in lowering intraocular pressure in the normal eye. *Arch Ophthalmol*, **96**, 2045-2048.

Congdon, N.G. & Friedman, D.S. (2003) Angle-closure glaucoma: impact, etiology, diagnosis, and treatment. *Curr Opin Ophthalmol*, **14**, 70-73.

Coleman, A.L. (1999) Glaucoma. *Lancet*, **354**, 1803-1810.

Coleman, A.L. (2003) Epidemiology of glaucoma. **In:** *Glaucoma: Science and Practice.* J.C. Morrison, I.P. Pollack editors. pp. 2-11. Thieme Medical Publishers, Inc., New York.

Cusato, K., Bosco, A., Linden, R. & Reese, B.E. (2002) Cell death in the inner nuclear layer of the retina is modulated by BDNF. *Brain Res Dev Brain Res*, **139**, 325-330.

Dangond, F., Hwang, D., Camelo, S., Pasinelli, P., Frosch, M.P., Stephanopoulos, G., Brown, R.H., Jr. & Gullans, S.R. (2004) Molecular signature of late-stage human ALS revealed by expression profiling of postmortem spinal cord gray matter. *Physiol Genomics*, **16**, 229-239.

Dawbarn, D. & Allen, S.J. (2003) Neurotrophins and neurodegeneration. *Neuropathol Appl Neurobiol*, **29**, 211-230.

De Keyser, J., Sulter, G. & Luiten, P.G. (1999) Clinical trials with neuroprotective drugs in acute ischaemic stroke: are we doing the right thing? *Trends Neurosci*, **22**, 535-540.

del Peso, L., Gonzalez-Garcia, M., Page, C., Herrera, R. & Nunez, G. (1997) Interleukin-3-induced phosphorylation of BAD through the protein kinase Akt. *Science*, **278**, 687-689.

Denovan-Wright, E.M., Howlett, S.E. & Robertson, H.A. (1999) Direct cloning of differential display products eluted from northern blots. *Biotechniques*, **26**, 1046-1050.

Dickson, D.W., Lee, S.C., Mattiace, L.A., Yen, S.H. & Brosnan, C. (1993) Microglia and cytokines in neurological disease, with special reference to AIDS and Alzheimer's disease. *Glia*, **7**, 75-83.

Dirnagl, U., Iadecola, C. & Moskowitz, M.A. (1999) Pathobiology of ischaemic stroke: an integrated view. *Trends Neurosci*, **22**, 391-397.

DiStefano, P.S., Friedman, B., Radziejewski, C., Alexander, C., Boland, P., Schick, C.M., Lindsay, R.M. & Wiegand, S.J. (1992) The neurotrophins BDNF, NT-3, and NGF display distinct patterns of retrograde axonal transport in peripheral and central neurons. *Neuron*, **8**, 983-993.

Distelhorst, J.S. & Hughes, G.M. (2003) Open-angle glaucoma. *Am Fam Physician*, **67**, 1937-1944.

Diverse-Pierluissi, M., Inglese, J., Stoffel, R.H., Lefkowitz, R.J. & Dunlap, K. (1996) G protein-coupled receptor kinase mediates desensitization of norepinephrine-induced $Ca^{2+}$ channel inhibition. *Neuron*, **16**, 579-585.

Doble, A. (1999) The role of excitotoxicity in neurodegenerative disease: implications for therapy. *Pharmacol Ther*, **81**, 163-221.

Dommergues, M.A., Plaisant, F., Verney, C. & Gressens, P. (2003) Early microglial activation following neonatal excitotoxic brain damage in mice: a potential target for neuroprotection. *Neuroscience*, **121**, 619-628.

Donello, J.E., Padillo, E.U., Webster, M.L., Wheeler, L.A. & Gil, D.W. (2001) α2-adrenoceptor agonists inhibit vitreal glutamate and aspartate accumulation and preserve retinal function after transient ischemia. *J Pharmacol Exp Ther*, **296**, 216-223.

Dowling, J.E. (1987) Retinal Cells and Information Processing. **In:** *The Retina: An Approchable Part of the Brain*. G. Frankfeldt editor. pp. 12-41. The Belknap Press of Harvard University Press., Cambridge.

Downen, M., Amaral, T.D., Hua, L.L., Zhao, M.L. & Lee, S.C. (1999) Neuronal death in cytokine-activated primary human brain cell culture: role of tumor necrosis factor-alpha. *Glia*, **28**, 114-127.

Dreyer, E.B., Zurakowski, D., Schumer, R.A., Podos, S.M. & Lipton, S.A. (1996) Elevated glutamate levels in the vitreous body of humans and monkeys with glaucoma. *Arch Ophthalmol*, **114**, 299-305.

Eichler, M.E., Dubinsky, J.M., Tong, J. & Rich, K.M. (1994) The ability of diphenylpiperazines to prevent neuronal death in dorsal root ganglion neurons *in vitro* after nerve growth factor deprivation and in vivo after axotomy. *J Neurochem*, **62**, 2148-2157.

Elena, P.P., Kosina-Boix, M., Denis, P., Moulin, G. & Lapalus, P. (1989) α2-adrenergic receptors in rat and rabbit eye: a tritium-sensitive film autoradiography. *Ophthalmic Res*, **21**, 309-314.

Elkington, A.R., Inman, C.B., Steart, P.V. & Weller, R.O. (1990) The structure of the lamina cribrosa of the human eye: an immunocytochemical and electron microscopical study. *Eye*, **4**, 42-57.

El-Remessy, A.B., Khalil, I.E., Matragoon, S., Abou-Mohamed, G., Tsai, N.J., Roon, P., Caldwell, R.B., Caldwell, R.W., Green, K. & Liou, G.I. (2003) Neuroprotective effect of (-) $^{9}$-tetrahydrocannabinol and cannabidiol in N-methyl-D-aspartate-induced retinal neurotoxicity: involvement of peroxynitrite. *Am J Pathol*, **163**, 1997-2008.

Farkas, R.H. & Grosskreutz, C.L. (2001) Apoptosis, neuroprotection, and retinal ganglion cell death: an overview. *Int Ophthalmol Clin*, **41**, 111-130.

Fern, R., Ransom, B.R. & Waxman, S.G. (1995) Voltage-gated calcium channels in CNS white matter: role in anoxic injury. *J Neurophysiol*, **74**, 369-377.

Finkbeiner, S. & Greenberg, M.E. (1996) $Ca^{2+}$-dependent routes to Ras: mechanisms for neuronal survival, differentiation, and plasticity? *Neuron*, **16**, 233-236.

Fiskum, G., Starkov, A., Polster, B.M. & Chinopoulos, C. (2003) Mitochondrial mechanisms of neural cell death and neuroprotective interventions in Parkinson's disease. *Ann N Y Acad Sci*, **991**, 111-119.

Flammer, J., Pache, M. & Resink, T. (2001) Vasospasm, its role in the pathogenesis of diseases with particular reference to the eye. *Prog Retin Eye Res*, **20**, 319-349.

Flammer, J., Orgul, S., Costa, V.P., Orzalesi, N., Krieglstein, G.K., Serra, L.M., Renard, J.P. & Stefansson, E. (2002) The impact of ocular blood flow in glaucoma. *Prog Retin Eye Res*, **21**, 359-393.

Flügel, A. & Bradl, M. (2001) New tools to trace populations of inflammatory cells in the CNS. *Glia*, **36**, 125-136.

Fournier, A.E., Beer, J., Arregui, C.O., Essagian, C., Aguayo, A.J. & McKerracher, L. (1997) Brain-derived neurotrophic factor modulates GAP-43 but not T alpha1 expression in injured retinal ganglion cells of adult rats. *J Neurosci Res*, **47**, 561-572.

Freeman, W.M., Walker, S.J. & Vrana, K.E. (1999) Quantitative RT-PCR: pitfalls and potential. *Biotechniques*, **26**, 112-124.

Friedlander, R.M. (2003) Apoptosis and caspases in neurodegenerative diseases. *N Engl J Med*, **348**, 1365-1375.

Gao, H., Qiao, X., Cantor, L.B. & WuDunn, D. (2002) Up-regulation of brain-derived neurotrophic factor expression by brimonidine in rat retinal ganglion cells. *Arch Ophthalmol*, **120**, 797-803.

Garcia-Valenzuela, E., Shareef, S., Walsh, J. & Sharma, S.C. (1995) Programmed cell death of retinal ganglion cells during experimental glaucoma. *Exp Eye Res*, **61**, 33-44.

Gebicke-Haerter, P.J. (2001) Microglia in neurodegeneration: molecular aspects. *Microsc Res Tech*, **54**, 47-58.

Geyer, O., Almog, J., Lupu-Meiri, M., Lazar, M. & Oron, Y. (1995) Nitric oxide synthase inhibitors protect rat retina against ischemic injury. *FEBS Lett*, **374**, 399-402.

Giovannoni, G. & Baker, D. (2003) Inflammatory disorders of the central nervous system. *Curr Opin Neurol*, **16**, 347-350.

Gotz, R., Koster, R., Winkler, C., Raulf, F., Lottspeich, F., Schartl, M. & Thoenen, H. (1994) Neurotrophin-6 is a new member of the nerve growth factor family. *Nature*, **372**, 266-269.

Green, K. & Pederson, J.E. (1973) Aqueous humor formation. *Exp Eye Res*, **16**, 273-286.

Greene, L.A. (1978) Nerve growth factor prevents the death and stimulates the neuronal differentiation of clonal PC12 pheochromocytoma cells in serum-free medium. *J Cell Biol*, **78**, 747-755.

Gupta, S.K., Jollimore, C.A., McLaren, M.J., Inana, G. & Kelly, M.E.M. (1997) Mammalian retinal pigment epithelial cells in vitro respond to the neurokines ciliary neurotrophic factor and leukemia inhibitory factor. *Biochem Cell Biol*, **75**, 119-125.

Hahn, J.S., Aizenman, E. & Lipton, S.A. (1988) Central mammalian neurons normally resistant to glutamate toxicity are made sensitive by elevated extracellular $Ca^{2+}$: toxicity is blocked by the N-methyl-D-aspartate antagonist MK-801. *Proc Natl Acad Sci U S A*, **85**, 6556-6560.

Halpern, D.L. & Grosskreutz, C.L. (2002) Glaucomatous optic neuropathy: mechanisms of disease. *Ophthalmol Clin North Am*, **15**, 61-68.

Hangai, M., Miyamoto, K., Hiroi, K., Tujikawa, A., Ogura, Y., Honda, Y. & Yoshimura, N. (1999) Roles of constitutive nitric oxide synthase in postischemic rat retina. *Invest Ophthalmol Vis Sci*, **40**, 450-458.

Hardingham, G.E., Fukunaga, Y. & Bading, H. (2002) Extrasynaptic NMDARs oppose synaptic NMDARs by triggering CREB shut-off and cell death pathways. *Nat Neurosci*, **5**, 405-414.

Harrison, D.C., Davis, R.P., Bond, B.C., Campbell, C.A., James, M.F., Parsons, A.A. & Philpott, K.L. (2001) Caspase mRNA expression in a rat model of focal cerebral ischemia. *Mol Brain Res*, **89**, 133-146.

Hartwick, A.T. (2001) Beyond intraocular pressure: neuroprotective strategies for future glaucoma therapy. *Optom Vis Sci*, **78**, 85-94.

Hayreh, S.S. (1999) The role of age and cardiovascular disease in glaucomatous optic neuropathy. *Surv Ophthalmol*, **43 Suppl 1**, S27-42.

He, S., Dong, W., Deng, Q., Weng, S. & Sun, W. (2003) Seeing more clearly: recent advances in understanding retinal circuitry. *Science*, **302**, 408-411.

Heese, K., Fiebich, B.L., Bauer, J. & Otten, U. (1997) Nerve growth factor (NGF) expression in rat microglia is induced by adenosine A2a-receptors. *Neurosci Lett*, **231**, 83-86.

Heidenreich, K.A. (2003) Molecular mechanisms of neuronal cell death. *Ann N Y Acad Sci*, **991**, 237-250.

Heijl, A., Leske, M.C., Bengtsson, B., Hyman, L. & Hussein, M. (2002) Reduction of intraocular pressure and glaucoma progression: results from the Early Manifest Glaucoma Trial. *Arch Ophthalmol*, **120**, 1268-1279.

Hernandez, M.R., Ye, H. & Roy, S. (1994) Collagen type IV gene expression in human optic nerve heads with primary open angle glaucoma. *Exp Eye Res*, **59**, 41-51.

Hetman, M., Kanning, K., Cavanaugh, J.E. & Xia, Z. (1999) Neuroprotection by brain-derived neurotrophic factor is mediated by extracellular signal-regulated kinase and phosphatidylinositol 3-kinase. *J Biol Chem*, **274**, 22569-22580.

Hirakawa, T., Rokutan, K., Nikawa, T. & Kishi, K. (1996) Geranylgeranylacetone induces heat shock proteins in cultured guinea pig gastric mucosal cells and rat gastric mucosa. *Gastroenterology*, **111**, 345-357.

Hirooka, K., Kelly, M.E.M., Baldridge, W.H. & Barnes, S. (2000) Suppressive actions of betaxolol on ionic currents in retinal ganglion cells may explain its neuroprotective effects. *Exp Eye Res*, **70**, 611-621.

Hirooka, K., Bertolesi, G.E., Kelly, M.E.M., Denovan-Wright, E.M., Sun, X., Hamid, J., Zamponi, G.W., Juhasz, A.E., Haynes, L.W. & Barnes, S. (2002) T-Type calcium channel α1G and α1H subunits in human retinoblastoma cells and their loss after differentiation. *J Neurophysiol*, **88**, 196-205.

Hong, S.J., Wu, K.Y., Wang, H.Z. & Fong, J.C. (2003) Effects of commercial antiglaucoma drugs to glutamate-induced $[Ca^{2+}]i$ increase in cultured neuroblastoma cells. *J Ocul Pharmacol Ther*, **19**, 205-215.

Honkanen, R.A., Baruah, S., Zimmerman, M.B., Khanna, C.L., Weaver, Y.K., Narkiewicz, J., Waziri, R., Gehrs, K.M., Weingeist, T.A., Boldt, H.C., Folk, J.C., Russell, S.R. & Kwon, Y.H. (2003) Vitreous amino acid concentrations in patients with glaucoma undergoing vitrectomy. *Arch Ophthalmol*, **121**, 183-188.

Hoste, A.M. & Sys, S.U. (1998) Ca2+ channel-blocking activity of propranolol and betaxolol in isolated bovine retinal microartery. *J Cardiovasc Pharmacol*, **32**, 390-396.

Hoyng, P.F. & van Beek, L.M. (2000) Pharmacological therapy for glaucoma: a review. *Drugs*, **59**, 411-434.

Hylton, C. & Robin, A.L. (2003) Update on prostaglandin analogs. *Curr Opin Ophthalmol*, **14**, 65-69.

Ikonomidou, C. & Turski, L. (2002) Why did NMDA receptor antagonists fail clinical trials for stroke and traumatic brain injury? *Lancet Neurol*, **1**, 383-386.

Isenmann, S., Kretz, A. & Cellerino, A. (2003) Molecular determinants of retinal ganglion cell development, survival, and regeneration. *Prog Retin Eye Res*, **22**, 483-543.

Ishii, Y., Kwong, J.M. & Caprioli, J. (2003) Retinal ganglion cell protection with geranylgeranylacetone, a heat shock protein inducer, in a rat glaucoma model. *Invest Ophthalmol Vis Sci*, **44**, 1982-1992.

Iskedjian, M., Walker, J., Vicente, C., Trope, G.E., Buys, Y., Einarson, T.R. & Covert, D. (2003) Cost of glaucoma in Canada: analyses based on visual field and physician's assessment. *J Glaucoma*, **12**, 456-462.

Jarajapu, Y.P., Coats, P., McGrath, J.C., MacDonald, A. & Hillier, C. (2001) Increased α1- and α2-adrenoceptor-mediated contractile responses of human skeletal muscle resistance arteries in chronic limb ischemia. *Cardiovasc Res*, **49**, 218-225.

Jiang, Q. & Stys, P.K. (2000) Calpain inhibitors confer biochemical, but not electrophysiological, protection against anoxia in rat optic nerves. *J Neurochem*, **74**, 2101-2107.

Joe, M.K., Sohn, S., Hur, W., Moon, Y., Choi, Y.R. & Kee, C. (2003) Accumulation of mutant myocilins in ER leads to ER stress and potential cytotoxicity in human trabecular meshwork cells. *Biochem Biophys Res Commun*, **312**, 592-600.

Johnson, E.C. & Morrison, J.C. (2003) Neuroprotection. **In:** *Glaucoma: Science and Practice*. J.C. Morrison, I.P. Pollack editors. pp. 412-424. Thieme Medical Publishers, Inc., New York.

Johnstone, M.A. (1997) Hypertrichosis and increased pigmentation of eyelashes and adjacent hair in the region of the ipsilateral eyelids of patients treated with unilateral topical latanoprost. *Am J Ophthalmol*, **124**, 544-547.

Johnstone, M.A. & Grant, W.G. (1973) Pressure-dependent changes in structures of the aqueous outflow system of human and monkey eyes. *Am J Ophthalmol*, **75**, 365-383.

Jonas, J.B., Schmidt, A.M., Muller-Bergh, J.A., Schlotzer-Schrehardt, U.M. & Naumann, G.O. (1992) Human optic nerve fiber count and optic disc size. *Invest Ophthalmol Vis Sci*, **33**, 2012-2018.

Källberg, M.E., Brooks, D.E., Garcia-Sanchez, G.A., Komáromy, A.M., Szabo, N.J. & Tian, L. (2002) Endothelin 1 levels in the aqueous humor of dogs with glaucoma. *J Glaucoma*, **11**, 105-109.

Kelekar, A. & Thompson, C.B. (1998) Bcl-2-family proteins: the role of the BH3 domain in apoptosis. *Trends Cell Biol*, **8**, 324-330.

Kempermann, G. & Neumann, H. (2003) Neuroscience. Microglia: the enemy within? *Science*, **302**, 1689-1690.

Kent, A.R., Nussdorf, J.D., David, R., Tyson, F., Small, D. & Fellows, D. (2001) Vitreous concentration of topically applied brimonidine tartrate 0.2%. *Ophthalmology*, **108**, 784-787.

Kermer, P., Klöcker, N., Weishaupt, J.H. & Bahr, M. (2001) Transection of the optic nerve in rats: studying neuronal death and survival in vivo. *Brain Res Protoc*, **7**, 255-260.

Kerr, J.F., Wyllie, A.H. & Currie, A.R. (1972) Apoptosis: a basic biological phenomenon with wide-ranging implications in tissue kinetics. *Br J Cancer*, **26**, 239-257.

Kerrigan, L.A., Zack, D.J., Quigley, H.A., Smith, S.D. & Pease, M.E. (1997) TUNEL-positive ganglion cells in human primary open-angle glaucoma. *Arch Ophthalmol*, **115**, 1031-1035.

Kikuchi, M., Tenneti, L. & Lipton, S.A. (2000) Role of p38 mitogen-activated protein kinase in axotomy-induced apoptosis of rat retinal ganglion cells. *J Neurosci*, **20**, 5037-5044.

Kilpatrick, G.J. & Tilbrook, G.S. (2002) Memantine. Merz. *Curr Opin Investig Drugs*, **3**, 798-806.

Kim, B.S., Savinova, O.V., Reedy, M.V., Martin, J., Lun, Y., Gan, L., Smith, R.S., Tomarev, S.I., John, S.W. & Johnson, R.L. (2001) Targeted disruption of the myocilin gene (MYOC) suggests that human glaucoma-causing mutations are gain of function. *Mol Cell Biol*, **21**, 7707-7713.

Klöcker, N., Kermer, P., Gleichmann, M., Weller, M. & Bahr, M. (1999) Both the neuronal and inducible isoforms contribute to upregulation of retinal nitric oxide synthase activity by brain-derived neurotrophic factor. *J Neurosci*, **19**, 8517-8527.

Klöcker, N., Kermer, P., Weishaupt, J.H., Labes, M., Ankerhold, R. & Bahr, M. (2000) Brain-derived neurotrophic factor-mediated neuroprotection of adult rat retinal ganglion cells in vivo does not exclusively depend on phosphatidyl-inositol-3'-kinase/protein kinase B signaling. *J Neurosci*, **20**, 6962-6967.

Kobayashi, T. & Mori, Y. (1998) $Ca^{2+}$ channel antagonists and neuroprotection from cerebral ischemia. *Eur J Pharmacol*, **363**, 1-15.

Koufali, M.M., Moutsatsou, P., Sekeris, C.E. & Breen, K.C. (2003) The dynamic localization of the glucocorticoid receptor in rat C6 glioma cell mitochondria. *Mol Cell Endocrinol*, **209**, 51-60.

Kremlev, S.G., Roberts, R.L. & Palmer, C. (2004) Differential expression of chemokines and chemokine receptors during microglial activation and inhibition. *J Neuroimmunol*, **149**, 1-9.

Kreutzberg, G.W. (1996) Microglia: a sensor for pathological events in the CNS. *Trends Neurosci*, **19**, 312-318.

Krishnamoorthy, R.R., Agarwal, P., Prasanna, G., Vopat, K., Lambert, W., Sheedlo, H.J., Pang, I.H., Shade, D., Wordinger, R.J., Yorio, T., Clark, A.F. & Agarwal, N. (2001) Characterization of a transformed rat retinal ganglion cell line. *Mol Brain Res*, **86**, 1-12.

Kriz, J., Nguyen, M.D. & Julien, J.P. (2002) Minocycline slows disease progression in a mouse model of amyotrophic lateral sclerosis. *Neurobiol Dis*, **10**, 268-278.

Kronfeld, P.C. (1974) Glaucoma and the optic nerve: a historical review. *Surv Ophthalmol*, **19**, 154-165.

Lafuente López-Herrera, M.P., Mayor-Torroglosa, S., Miralles de Imperial, J., Villegas-Pérez, M.P. & Vidal-Sanz, M. (2002) Transient ischemia of the retina results in altered retrograde axoplasmic transport: neuroprotection with brimonidine. *Exp Neurol*, **178**, 243-258.

Lai, R.K., Chun, T., Hasson, D., Lee, S., Mehrbod, F. & Wheeler, L. (2002) Alpha-2 adrenoceptor agonist protects retinal function after acute retinal ischemic injury in the rat. *Vis Neurosci*, **19**, 175-185.

Lambeng, N., Michel, P.P., Brugg, B., Agid, Y. & Ruberg, M. (1999) Mechanisms of apoptosis in PC12 cells irreversibly differentiated with nerve growth factor and cyclic AMP. *Brain Res*, **821**, 60-68.

Lambeng, N., Willaime-Morawek, S., Mariani, J., Ruberg, M. & Brugg, B. (2003) Activation of mitogen-activated protein kinase pathways during the death of PC12 cells is dependent on the state of differentiation. *Mol Brain Res*, **111**, 52-60.

Laquis, S., Chaudhary, P. & Sharma, S.C. (1998) The patterns of retinal ganglion cell death in hypertensive eyes. *Brain Res*, **784**, 100-104.

Larner, A.J. (2000) Neuronal apoptosis as a therapeutic target in neurodegenerative disease. *Exp Opin Ther Patents*, **10**, 1493-1518.

Leist, M., Volbracht, C., Kuhnle, S., Fava, E., Ferrando-May, E. & Nicotera, P. (1997) Caspase-mediated apoptosis in neuronal excitotoxicity triggered by nitric oxide. *Mol Med*, **3**, 750-764.

Lesar, T.S. (2002) Glaucoma. **In:** *Pharmacology: A Pathological Approach.* J.T. Dipiro, R.L. Talbert, G.C. Yee, G.R. Matzke, B.G. Wells, L.M. Posey, editors. pp. 1665-1678. McGraw-Hill Companies, Inc., New York.

Levin, L. & Gordon, L. (2002) Retinal ganglion cell disorders: types and treatments. *Prog Retin Eye Res*, **21**, 465-484.

Levin, L.A. (1999) An introduction to neuroprotection in glaucoma: mechanisms and implications. *Eur J Ophthalmol*, **9 Suppl 1**, S7-8.

Levin, L.A. (2003) Retinal ganglion cells and neuroprotection for glaucoma. *Surv Ophthalmol*, **48 Suppl 1**, S21-24.

Levkovitch-Verbin, H., Harris-Cerruti, C., Groner, Y., Wheeler, L.A., Schwartz, M. & Yoles, E. (2000) RGC death in mice after optic nerve crush injury: oxidative stress and neuroprotection. *Invest Ophthalmol Vis Sci*, **41**, 4169-4174.

Levkovitch-Verbin, H., Martin, K.R., Quigley, H.A., Baumrind, L.A., Pease, M.E. & Valenta, D. (2002a) Measurement of amino acid levels in the vitreous humor of rats after chronic intraocular pressure elevation or optic nerve transection. *J Glaucoma*, **11**, 396-405.

Levkovitch-Verbin, H., Quigley, H.A., Martin, K.R., Valenta, D., Baumrind, L.A. & Pease, M.E. (2002b) Translimbal laser photocoagulation to the trabecular meshwork as a model of glaucoma in rats. *Invest Ophthalmol Vis Sci*, **43**, 402-410.

Lewden, O., Garcher, C., Assem, M., Morales, C., Rochette, L. & Bron, A.M. (1998) Changes of the inducible heat shock protein 70 mRNA level in rat retina after ischemia and reperfusion. *Ophthalmic Res*, **30**, 291-294.

Lewis, P.R., Phillips, T.G. & Sassani, J.W. (1999) Topical therapies for glaucoma: what family physicians need to know. *Am Fam Physician*, **59**, 1871-1879, 1882.

Li, L., Prevette, D., Oppenheim, R.W. & Milligan, C.E. (1998) Involvement of specific caspases in motoneuron cell death in vivo and in vitro following trophic factor deprivation. *Mol Cell Neurosci*, **12**, 157-167.

Li, Y., Kang, J. & Horwitz, M.S. (1998) Interaction of an adenovirus E3 14.7-kilodalton protein with a novel tumor necrosis factor alpha-inducible cellular protein containing leucine zipper domains. *Mol Cell Biol*, **18**, 1601-1610.

Li, Y., Schlamp, C.L. & Nickells, R.W. (1999) Experimental induction of retinal ganglion cell death in adult mice. *Invest Ophthalmol Vis Sci*, **40**, 1004-1008.

Lilienbaum, A. & Israel, A. (2003) From calcium to NF-κB signaling pathways in neurons. *Mol Cell Biol*, **23**, 2680-2698.

Lin, H.J., Chen, W.C., Tsai, F.J. & Tsai, S.W. (2002) Distributions of p53 codon 72 polymorphism in primary open angle glaucoma. *Br J Ophthalmol*, **86**, 767-770.

Lin, S., Wei, X., Xu, Y., Yan, C., Dodel, R., Zhang, Y., Liu, J., Klaunig, J.E., Farlow, M. & Du, Y. (2003) Minocycline blocks 6-hydroxydopamine-induced neurotoxicity and free radical production in rat cerebellar granule neurons. *Life Sci*, **72**, 1635-1641.

Lipton, S.A. (2003) Possible role for memantine in protecting retinal ganglion cells from glaucomatous damage. *Surv Ophthalmol*, **48 Suppl 1**, S38-46.

Lipton, S.A. & Rosenberg, P.A. (1994) Excitatory amino acids as a final common pathway for neurologic disorders. *N Engl J Med*, **330**, 613-622.

Liu, B. & Hong, J.S. (2003) Role of microglia in inflammation-mediated neurodegenerative diseases: mechanisms and strategies for therapeutic intervention. *J Pharmacol Exp Ther*, **304**, 1-7.

Liu, Q.Y., Schaffner, A.E., Chang, Y.H., Vaszil, K. & Barker, J.L. (1997) Astrocytes regulate amino acid receptor current densities in embryonic rat hippocampal neurons. *J Neurobiol*, **33**, 848-864.

Liu, S., Bishop, W.R. & Liu, M. (2003) Differential effects of cell cycle regulatory protein $p21^{WAF1/Cip1}$ on apoptosis and sensitivity to cancer chemotherapy. *Drug Resist Updat*, **6**, 183-195.

López, A.A., Cioffi, G., Hare, W.A., Johnson, C.A., Levin, L.A., Pilunat, L., Schwartz, M., Tatton, W.G., Weinreb, R.N., Wheeler, L.A. & Krieglstein, G.K. (1999) Mechanisms of neuroprotection and applications in ocular disease: a round table discussion. *Eur J Ophthalmol*, **9**, S52-S81.

Lucas, D.R. & Newhouse, J.P. (1957) The toxic effect of sodium L-glutamate on the inner layers of the retina. *Ama Arch Opthalmol*, **58**, 193-201.

Luo, X., Heidinger, V., Picaud, S., Lambrou, G., Dreyfus, H., Sahel, J. & Hicks, D. (2001) Selective excitotoxic degeneration of adult pig retinal ganglion cells in vitro. *Invest Ophthalmol Vis Sci*, **42**, 1096-1106.

Ma, Y.T., Hsieh, T., Forbes, M.E., Johnson, J.E. & Frost, D.O. (1998) BDNF injected into the superior colliculus reduces developmental retinal ganglion cell death. *J Neurosci*, **18**, 2097-2107.

Maguire, G., Simko, H., Weinreb, R.N. & Ayoub, G. (1998) Transport-mediated release of endogenous glutamate in the vertebrate retina. *Pflugers Arch*, **436**, 481-484.

Marcic, T.S., Belyea, D.A. & Katz, B. (2003) Neuroprotection in glaucoma: a model for neuroprotection in optic neuropathies. *Curr Opin Ophthalmol*, **14**, 353-356.

Martin, K.R., Levkovitch-Verbin, H., Valenta, D., Baumrind, L., Pease, M.E. & Quigley, H.A. (2002) Retinal glutamate transporter changes in experimental glaucoma and after optic nerve transection in the rat. *Invest Ophthalmol Vis Sci*, **43**, 2236-2243.

Marzo, I., Brenner, C., Zamzami, N., Susin, S.A., Beutner, G., Brdiczka, D., Remy, R., Xie, Z.H., Reed, J.C. & Kroemer, G. (1998) The permeability transition pore complex: a target for apoptosis regulation by caspases and bcl-2-related proteins. *J Exp Med*, **187**, 1261-1271.

Massey, S.C. & Miller, R.F. (1990) N-methyl-D-aspartate receptors of ganglion cells in rabbit retina. *J Neurophysiol*, **63**, 16-30.

Massieu, L. & Garcia, O. (1998) The role of excitotoxicity and metabolic failure in the pathogenesis of neurological disorders. *Neurobiology (Bp)*, **6**, 99-108.

Mattson, M.P. (1994) Calcium and neuronal injury in Alzheimer's disease. Contributions of beta-amyloid precursor protein mismetabolism, free radicals, and metabolic compromise. *Ann N Y Acad Sci*, **747**, 50-76.

McDonald, J.W., Silverstein, F.S. & Johnston, M.V. (1988) Neurotoxicity of N-methyl-D-aspartate is markedly enhanced in developing rat central nervous system. *Brain Res*, **459**, 200-203.

McDonnell, M.A., Wang, D., Khan, S.M., Vander Heiden, M.G. & Kelekar, A. (2003) Caspase-9 is activated in a cytochrome c-independent manner early during TNFα-induced apoptosis in murine cells. *Cell Death Differ*, **10**, 1005-1015.

McKinnon, S.J. (1997) Glaucoma, apoptosis, and neuroprotection. *Curr Opin Ophthalmol*, **8**, 28-37.

McKinnon, S.J., Lehman, D.M., Kerrigan-Baumrind, L.A., Merges, C.A., Pease, M.E., Kerrigan, D.F., Ransom, N.L., Tahzib, N.G., Reitsamer, H.A., Levkovitch-Verbin, H., Quigley, H.A. & Zack, D.J. (2002) Caspase activation and amyloid precursor protein cleavage in rat ocular hypertension. *Invest Ophthalmol Vis Sci*, **43**, 1077-1087.

McMahon, C.D., Shaffer, R.N., Hoskins, H.D., Jr. & Hetherington, J., Jr. (1979) Adverse effects experienced by patients taking timolol. *Am J Ophthalmol*, **88**, 736-738.

Messmer, C., Flammer, J. & Stumpfig, D. (1991) Influence of betaxolol and timolol on the visual fields of patients with glaucoma. *Am J Ophthalmol*, **112**, 678-681.

Mey, J. & Thanos, S. (1993) Intravitreal injections of neurotrophic factors support the survival of axotomized retinal ganglion cells in adult rats in vivo. *Brain Res*, **602**, 304-317.

Milton, I.D., Banner, S.J., Ince, P.G., Piggott, N.H., Fray, A.E., Thatcher, N., Horne, C.H. & Shaw, P.J. (1997) Expression of the glial glutamate transporter EAAT2 in the human CNS: an immunohistochemical study. *Brain Res Mol Brain Res*, **52**, 17-31.

Mishima, H.K., Kiuchi, Y., Takamatsu, M., Racz, P. & Bito, L.Z. (1997) Circadian intraocular pressure management with latanoprost: diurnal and nocturnal intraocular pressure reduction and increased uveoscleral outflow. *Surv Ophthalmol*, **41 Suppl 2**, S139-144.

Morgan, J.E. & Morrison, J.C. (2003) Anatomy and Physiology of the Optic Nerve. **In:** *Glaucoma: Science and Practice*. J.C. Morrison, I.P. Pollack editors. pp. 80-89. Thieme Medical Publishers, Inc., New York.

Morimoto, R.I. & Santoro, M.G. (1998) Stress-inducible responses and heat shock proteins: new pharmacologic targets for cytoprotection. *Nat Biotechnol*, **16**, 833-838.

Morrison, J.C. & Acott, T.S. (2003) Anatomy and Physiology of Aqueous Humor Outflow. **In:** *Glaucoma: Science and Practice*. J.C. Morrison, I.P. Pollack editors. pp. 34-41. Thieme Medical Publishers, Inc., New York.

Morrison, J.C., Moore, C.G., Deppmeier, L.M., Gold, B.G., Meshul, C.K. & Johnson, E.C. (1997) A rat model of chronic pressure-induced optic nerve damage. *Exp Eye Res*, **64**, 85-96.

Mosinger, J.L., Price, M.T., Bai, H.Y., Xiao, H., Wozniak, D.F. & Olney, J.W. (1991) Blockade of both NMDA and non-NMDA receptors is required for optimal protection against ischemic neuronal degeneration in the in vivo adult mammalian retina. *Exp Neurol*, **113**, 10-17.

Müller, M. & Holländer, H. (1988) A small population of retinal ganglion cells projecting to the retina of the other eye. An experimental study in the rat and the rabbit. *Exp Brain Res*, **71**, 611-617.

Nakla, M., Caprioli, J. & Morgan, J.E. (2003) Glaucomatous Optic Neuropathy. **In:** *Glaucoma: Science and Practice*. J.C. Morrison, I.P. Pollack editors. pp. 94-105. Thieme Medical Publishers, Inc., New York.

Näpänkangas, U., Lindqvist, N., Lindholm, D. & Hallböök, F. (2003) Rat retinal ganglion cells upregulate the pro-apoptotic BH3-only protein Bim after optic nerve transection. *Mol Brain Res*, **120**, 30-37.

Naskar, R., Vorwerk, C.K. & Dreyer, E.B. (2000) Concurrent downregulation of a glutamate transporter and receptor in glaucoma. *Invest Ophthalmol Vis Sci*, **41**, 1940-1944.

Naskar, R., Wissing, M. & Thanos, S. (2002) Detection of early neuron degeneration and accompanying microglial responses in the retina of a rat model of glaucoma. *Invest Ophthalmol Vis Sci*, **43**, 2962-2968.

Neufeld, A.H. (1999) Microglia in the optic nerve head and the region of parapapillary chorioretinal atrophy in glaucoma. *Arch Ophthalmol*, **117**, 1050-1056.

Neves, G. & Lagnado, L. (1999) The retina. *Curr Biol*, **9**, R674-677.

Nickells, R.W. (1999) Apoptosis of retinal ganglion cells in glaucoma: an update of the molecular pathways involved in cell death. *Surv Ophthalmol*, **43 Suppl 1**, S151-161.

Noske, W., Hensen, J. & Wiederholt, M. (1997) Endothelin-like immunoreactivity in aqueous humor of patients with primary open-angle glaucoma and cataract. *Graefes Arch Clin Exp Ophthalmol*, **235**, 551-552.

Olney, J.W. (1969) Glutamate-induced retinal degeneration in neonatal mice. Electron microscopy of the acutely evolving lesion. *J Neuropathol Exp Neurol*, **28**, 455-474.

Olney, J.W., Zorumski, C.F., Stewart, G.R., Price, M.T., Wang, G.J. & Labruyere, J. (1990) Excitotoxicity of L-dopa and 6-OH-dopa: implications for Parkinson's and Huntington's diseases. *Exp Neurol*, **108**, 269-272.

Osborne, N.N., Wood, J.P., Chidlow, G., Bae, J.H., Melena, J. & Nash, M.S. (1999a) Ganglion cell death in glaucoma: what do we really know? *Br J Ophthalmol*, **83**, 980-986.

Osborne, N.N., Chidlow, G., Nash, M.S. & Wood, J.P. (1999b) The potential of neuroprotection in glaucoma treatment. *Curr Opin Ophthalmol*, **10**, 82-92.

Osborne, N.N., Melena, J., Chidlow, G. & Wood, J.P. (2001) A hypothesis to explain ganglion cell death caused by vascular insults at the optic nerve head: possible implication for the treatment of glaucoma. *Br J Ophthalmol*, **85**, 1252-1259.

Oshitari, T. & Adachi-Usami, E. (2003) The effect of caspase inhibitors and neurotrophic factors on damaged retinal ganglion cells. *Neuroreport*, **14**, 289-292.

Otori, Y., Kusaka, S., Kawasaki, A., Morimura, H., Miki, A. & Tano, Y. (2003) Protective effect of nilvadipine against glutamate neurotoxicity in purified retinal ganglion cells. *Brain Res*, **961**, 213-219.

Pan, Z. & Kupper, L.L. (1999) Sample size determination for multiple comparison studies treating confidence interval width as random. *Stat Med*, **18**, 1475-1488.

Pape, L.G. & Forbes, M. (1978) Retinal detachment and miotic therapy. *Am J Ophthalmol*, **85**, 558-566.

Park, E.M., Joh, T.H., Volpe, B.T., Chu, C.K., Song, G. & Cho, S. (2004) A neuroprotective role of extracellular signal-regulated kinase in n-acetyl-o-methyldopamine-treated hippocampal neurons after exposure to *in vitro* and *in vivo* ischemia. *Neuroscience*, **123**, 147-154.

Pellegrini, J.W. & Lipton, S.A. (1993) Delayed administration of memantine prevents N-methyl-D-aspartate receptor-mediated neurotoxicity. *Ann Neurol*, **33**, 403-407.

Pena, J.D., Agapova, O., Gabelt, B.T., Levin, L.A., Lucarelli, M.J., Kaufman, P.L. & Hernandez, M.R. (2001) Increased elastin expression in astrocytes of the lamina cribrosa in response to elevated intraocular pressure. *Invest Ophthalmol Vis Sci*, **42**, 2303-2314.

Pluchino, S., Zanotti, L. & Martino, G. (2003) Antibodies and myelination: facts and misacts. *Neurol Sci*, **24 Suppl 4**, S231-233.

Prasanna, G., Krishnamoorthy, R., Clark, A.F., Wordinger, R.J. & Yorio, T. (2002) Human optic nerve head astrocytes as a target for endothelin-1. *Invest Ophthalmol Vis Sci*, **43**, 2704-2713.

Pringle, A.K., Iannotti, F., Wilde, G.J., Chad, J.E., Seeley, P.J. & Sundstrom, L.E. (1997) Neuroprotection by both NMDA and non-NMDA receptor antagonists in *in vitro* ischemia. *Brain Res*, **755**, 36-46.

Putcha, G.V., Harris, C.A., Moulder, K.L., Easton, R.M., Thompson, C.B. & Johnson, E.M., Jr. (2002) Intrinsic and extrinsic pathway signaling during neuronal apoptosis: lessons from the analysis of mutant mice. *J Cell Biol*, **157**, 441-453.

Putcha, G.V., Le, S., Frank, S., Besirli, C.G., Clark, K., Chu, B., Alix, S., Youle, R.J., LaMarche, A., Maroney, A.C. & Johnson, E.M., Jr. (2003) JNK-mediated BIM phosphorylation potentiates BAX-dependent apoptosis. *Neuron*, **38**, 899-914.

Quigley, H.A. (1977) Gap junctions between optic nerve head astrocytes. *Invest Ophthalmol Vis Sci*, **16**, 582-585.

Quigley, H.A. & Addicks, E.M. (1980) Chronic experimental glaucoma in primates. II. Effect of extended intraocular pressure elevation on optic nerve head and axonal transport. *Invest Ophthalmol Vis Sci*, **19**, 137-152.

Quigley, H.A., Addicks, E.M., Green, W.R. & Maumenee, A.E. (1981) Optic nerve damage in human glaucoma. II. The site of injury and susceptibility to damage. *Arch Ophthalmol*, **99**, 635-649.

Quigley, H.A. & Hohman, R.M. (1983) Laser energy levels for trabecular meshwork damage in the primate eye. *Invest Ophthalmol Vis Sci*, **24**, 1305-1307.

Quigley, H.A., Brown, A. & Dorman-Pease, M.E. (1991) Alterations in elastin of the optic nerve head in human and experimental glaucoma. *Br J Ophthalmol*, **75**, 552-557.

Quigley, H.A. (1993) Open-angle glaucoma. *N Engl J Med*, **328**, 1097-1106.

Quigley, H.A. (1999) Neuronal death in glaucoma. *Prog Retin Eye Res*, **18**, 39-57.

Quigley, H.A., McKinnon, S.J., Zack, D.J., Pease, M.E., Kerrigan-Baumrind, L.A., Kerrigan, D.F. & Mitchell, R.S. (2000) Retrograde axonal transport of BDNF in retinal ganglion cells is blocked by acute IOP elevation in rats. *Invest Ophthalmol Vis Sci*, **41**, 3460-3466.

Rabacchi, S.A., Bonfanti, L., Liu, X.H. & Maffei, L. (1994) Apoptotic cell death induced by optic nerve lesion in the neonatal rat. *J Neurosci*, **14**, 5292-5301.

Racette, L., Wilson, M.R., Zangwill, L.M., Weinreb, R.N. & Sample, P.A. (2003) Primary open-angle glaucoma in blacks: a review. *Surv Ophthalmol*, **48**, 295-313.

Rafuse, P. (2003) Adrenergic Antagonists. **In:** *Glaucoma: Science and Practice.* J.C. Morrison, I.P. Pollack editors. pp. 374-382. Thieme Medical Publishers, Inc., New York.

Rainer, G., Kiss, B., Dallinger, S., Findl, O., Georgopoulos, M., Vass, C., Menapace, R., Polak, K., Eichler, H.G., Wolzt, M. & Schmetterer, L. (2001) A double masked placebo controlled study on the effect of nifedipine on optic nerve blood flow and visual field function in patients with open angle glaucoma. *Br J Clin Pharmacol*, **52**, 210-212.

Ray, K., Mukhopadhyay, A. & Acharya, M. (2003) Recent advances in molecular genetics of glaucoma. *Mol Cell Biochem*, **253**, 223-231.

Ray, S.K., Shields, D.C., Saido, T.C., Matzelle, D.C., Wilford, G.G., Hogan, E.L. & Banik, N.L. (1999) Calpain activity and translational expression increased in spinal cord injury. *Brain Res*, **816**, 375-380.

Raymond, V. (1997) Molecular genetics of the glaucomas: mapping of the first five "GLC" loci. *Am J Hum Genet*, **60**, 272-277.

Rego, A.C. & Oliveira, C.R. (2003) Mitochondrial dysfunction and reactive oxygen species in excitotoxicity and apoptosis: implications for the pathogenesis of neurodegenerative diseases. *Neurochem Res*, **28**, 1563-1574.

Reichert, R.W., Shields, M.B. & Stewart, W.C. (1988) Intraocular pressure response to replacing pilocarpine with carbachol. *Am J Ophthalmol*, **106**, 747-748.

Reisberg, B., Doody, R., Stöffler, A., Schmitt, F., Ferris, S. & Möbius, H.J. (2003) Memantine in moderate-to-severe Alzheimer's disease. *N Engl J Med*, **348**, 1333-1341.

Reiss, G.R. & Brubaker, R.F. (1983) The mechanism of betaxolol, a new ocular hypotensive agent. *Ophthalmology*, **90**, 1369-1372.

Rezaie, T., Child, A., Hitchings, R., Brice, G., Miller, L., Coca-Prados, M., Heon, E., Krupin, T., Ritch, R., Kreutzer, D., Crick, R.P. & Sarfarazi, M. (2002) Adult-onset primary open-angle glaucoma caused by mutations in optineurin. *Science*, **295**, 1077-1079.

Ringheim, G.E. & Conant, K. (2004) Neurodegenerative disease and the neuroimmune axis (Alzheimer's and Parkinson's disease, and viral infections). *J Neuroimmunol*, **147**, 43-49.

Riordan-Eva, P. (1999) Anatomy & Embryology of the Eye. **In:** *General Ophthalmology*. D. Vaughan, T. Asbury, P. Riordan-Eva editors. pp. 1-26. Appleton & Lange. Stamford, Connecticut.

Ritch, R. (2000) Neuroprotection: is it already applicable to glaucoma therapy? *Curr Opin Ophthalmol*, **11**, 78-84.

Rothstein, J.D., Martin, L.J. & Kuncl, R.W. (1992) Decreased glutamate transport by the brain and spinal cord in amyotrophic lateral sclerosis. *N Engl J Med*, **326**, 1464-1468.

Rothstein, J.D., Van Kammen, M., Levey, A.I., Martin, L.J. & Kuncl, R.W. (1995) Selective loss of glial glutamate transporter GLT-1 in amyotrophic lateral sclerosis. *Ann Neurol*, **38**, 73-84.

Sambrook, J., Fritsch, E.F. & Maniatis, T. (1989) SDS-polyacrylamide Gel Electrophoresis of Proteins. **In**: *Molecular Cloning: A Laboratory Manual 2nd edition*. pp. 18.47-18.50. Cold Spring Harbor Laboratory Press, Cold Spring Harbor, New York.

Sarfarazi, M. (1997) Recent advances in molecular genetics of glaucomas. *Hum Mol Genet*, **6**, 1667-1677.

Sarfarazi, M., Child, A., Stoilova, D., Brice, G., Desai, T., Trifan, O.C., Poinoosawmy, D. & Crick, R.P. (1998) Localization of the fourth locus (GLC1E) for adult-onset primary open-angle glaucoma to the 10p15-p14 region. *Am J Hum Genet*, **62**, 641-652.

Schuettauf, F., Naskar, R., Vorwerk, C.K., Zurakowski, D. & Dreyer, E.B. (2000) Ganglion cell loss after optic nerve crush mediated through AMPA-kainate and NMDA receptors. *Invest Ophthalmol Vis Sci*, **41**, 4313-4316.

Schulz, J.B., Weller, M. & Moskowitz, M.A. (1999) Caspases as treatment targets in stroke and neurodegenerative diseases. *Ann Neurol*, **45**, 421-429.

Schuman, J.S. (1996) Clinical experience with brimonidine 0.2% and timolol 0.5% in glaucoma and ocular hypertension. *Surv Ophthalmol*, **41 Suppl 1**, S27-S37.

Schwamborn, K., Weil, R., Courtois, G., Whiteside, S.T. & Israel, A. (2000) Phorbol esters and cytokines regulate the expression of the NEMO-related protein, a molecule involved in a NF-κB-independent pathway. *J Biol Chem*, **275**, 22780-22789.

Schwartz, M., Belkin, M., Yoles, E. & Solomon, A. (1996) Potential treatment modalities for glaucomatous neuropathy: neuroprotection and neuroregeneration. *J Glaucoma*, **5**, 427-432.

Schwartz, M. & Yoles, E. (1999) Optic nerve degeneration and potential neuroprotection: implications for glaucoma. *Eur J Ophthalmol*, **9 Suppl 1**, S9-11.

Schwartz, M. (2003) Neurodegeneration and neuroprotection in glaucoma: development of a therapeutic neuroprotective vaccine: the Friedenwald lecture. *Invest Ophthalmol Vis Sci*, **44**, 1407-1411.

Seigel, G.M. (1996) Establishment of an E1A-immortalized retinal cell culture. *In Vitro Cell Dev Biol Anim*, **32**, 66-68.

Seigel, G.M., Takahashi, M., Adamus, G. & McDaniel, T. (1998) Intraocular transplantation of E1A-immortalized retinal precursor cells. *Cell Transplant*, **7**, 559-566.

Selmaj, K.W. & Raine, C.S. (1988) Tumor necrosis factor mediates myelin and oligodendrocyte damage in vitro. *Ann Neurol*, **23**, 339-346.

Serle, J.B. & Castelbuono, A.C. (2003) Adrenergic Agonists. **In:** *Glaucoma: Science and Practice*. J.C. Morrison, I.P. Pollack editors. pp. 363-373. Thieme Medical Publishers, Inc., New York.

Sheffield, V.C., Stone, E.M., Alward, W.L., Drack, A.V., Johnson, A.T., Streb, L.M. & Nichols, B.E. (1993) Genetic linkage of familial open angle glaucoma to chromosome 1q21-q31. *Nat Genet*, **4**, 47-50.

Spaeth, G.L. & Baez, K.A. (1992) Argon laser trabeculoplasty controls one third of cases of progressive, uncontrolled, open angle glaucoma for 5 years. *Arch Ophthalmol*, **110**, 491-494.

Springer, J.E., Azbill, R.D., Nottingham, S.A. & Kennedy, S.E. (2000) Calcineurin-mediated BAD dephosphorylation activates the caspase-3 apoptotic cascade in traumatic spinal cord injury. *J Neurosci*, **20**, 7246-7251.

Steelman, L.S., Pohnert, S.C., Shelton, J.G., Franklin, R.A., Bertrand, F.E. & McCubrey, J.A. (2004) JAK/STAT, Raf/MEK/ERK, PI3K/Akt and BCR-ABL in cell cycle progression and leukemogenesis. *Leukemia*, **18**, 189-218.

Stoilova, D., Child, A., Trifan, O.C., Crick, R.P., Coakes, R.L. & Sarfarazi, M. (1996) Localization of a locus (GLC1B) for adult-onset primary open angle glaucoma to the 2cen-q13 region. *Genomics*, **36**, 142-150.

Stone, E.M., Fingert, J.H., Alward, W.L., Nguyen, T.D., Polansky, J.R., Sunden, S.L., Nishimura, D., Clark, A.F., Nystuen, A., Nichols, B.E., Mackey, D.A., Ritch, R., Kalenak, J.W., Craven, E.R. & Sheffield, V.C. (1997) Identification of a gene that causes primary open angle glaucoma. *Science*, **275**, 668-670.

Stone, M., Fortin, P.R., Pacheco-Tena, C. & Inman, R.D. (2003) Should tetracycline treatment be used more extensively for rheumatoid arthritis? Metaanalysis demonstrates clinical benefit with reduction in disease activity. *J Rheumatol*, **30**, 2112-2122.

Streit, W.J. (1993) Microglial-neuronal interactions. *J Chem Neuroanat*, **6**, 261-266.

Stuiver, B.T., Douma, B.R., Bakker, R., Nyakas, C. & Luiten, P.G. (1996) *In vivo* protection against NMDA-induced neurodegeneration by MK-801 and nimodipine: combined therapy and temporal course of protection. *Neurodegeneration*, **5**, 153-159.

Sun, B.B. & Chiu, S.Y. (1999) N-type calcium channels and their regulation by $GABA_B$ receptors in axons of neonatal rat optic nerve. *J Neurosci*, **19**, 5185-5194.

Suzuki, J., Watanabe, K., Tsuruoka, T., Sueda, S., Funada, J., Kitakaze, M. & Sekiya, M. (2003) Beneficial effects of betaxolol, a selective antagonist of beta-1 adrenoceptors, on exercise-induced myocardial ischemia in patients with coronary vasospasm. *Int J Cardiol*, **91**, 227-232.

Takahashi, N., Cummins, D. & Caprioli, J. (1991) Rat retinal ganglion cells in culture. *Exp Eye Res*, **53**, 565-572.

Tamm, E.R. & Polansky, J.R. (2001) The TIGR/MYOC gene and glaucoma: opportunities for new understandings. *J Glaucoma*, **10**, S9-S12.

Tanihara, H., Hangai, M., Sawaguchi, S., Abe, H., Kageyama, M., Nakazawa, F., Shirasawa, E. & Honda, Y. (1997) Up-regulation of glial fibrillary acidic protein in the retina of primate eyes with experimental glaucoma. *Arch Ophthalmol*, **115**, 752-756.

Tatton, W.G., Chalmers-Redman, R.M., Sud, A., Podos, S.M. & Mittag, T.W. (2001) Maintaining mitochondrial membrane impermeability. An opportunity for new therapy in glaucoma? *Surv Ophthalmol*, **45 Suppl 3**, S277-S283.

Tatton, W.G., Chalmers-Redman, R., Brown, D. & Tatton, N. (2003) Apoptosis in Parkinson's disease: signals for neuronal degradation. *Ann Neurol*, **53 Suppl 3**, S61-S70.

Tenneti, L. & Lipton, S.A. (2000) Involvement of activated caspase-3-like proteases in N-methyl-D-aspartate-induced apoptosis in cerebrocortical neurons. *J Neurochem*, **74**, 134-142.

Tezel, G. & Wax, M.B. (1999) Inhibition of caspase activity in retinal cell apoptosis induced by various stimuli *in vitro*. *Invest Ophthalmol Vis Sci*, **40**, 2660-2667.

Tezel, G. & Wax, M.B. (2000) Increased production of tumor necrosis factor-α by glial cells exposed to simulated ischemia or elevated hydrostatic pressure induces apoptosis in cocultured retinal ganglion cells. *J Neurosci*, **20**, 8693-8700.

Tezel, G., Kass, M.A., Kolker, A.E., Becker, B. & Wax, M.B. (1997) Plasma and aqueous humor endothelin levels in primary open-angle glaucoma. *J Glaucoma*, **6**, 83-89.

Tezel, G.M., Seigel, G.M. & Wax, M.B. (1999) Density-dependent resistance to apoptosis in retinal cells. *Curr Eye Res*, **19**, 377-388.

Thanos, S., Mey, J. & Wild, M. (1993) Treatment of the adult retina with microglia-suppressing factors retards axotomy-induced neuronal degradation and enhances axonal regeneration in vivo and in vitro. *J Neurosci*, **13**, 455-466.

Thanos, S., Kacza, J., Seeger, J. & Mey, J. (1994) Old dyes for new scopes: the phagocytosis-dependent long-term fluorescence labelling of microglial cells in vivo. *Trends Neurosci*, **17**, 177-182.

Thompson, D.A. & Gal, A. (2003) Vitamin A metabolism in the retinal pigment epithelium: genes, mutations, and diseases. *Prog Retin Eye Res*, **22**, 683-703.

Thoreson, W.B. & Witkovsky, P. (1999) Glutamate receptors and circuits in the vertebrate retina. *Prog Retin Eye Res*, **18**, 765-810.

Thylefors, B. & Negrel, A.D. (1994) The global impact of glaucoma. *Bull World Health Organ*, **72**, 323-326.

Tielsch, J.M., Sommer, A., Katz, J., Royall, R.M., Quigley, H.A. & Javitt, J. (1991) Racial variations in the prevalence of primary open-angle glaucoma. The Baltimore Eye Survey. *Jama*, **266**, 369-374.

Tikka, T., Fiebich, B.L., Goldsteins, G., Keinänen, R. & Koistinaho, J. (2001) Minocycline, a tetracycline derivative, is neuroprotective against excitotoxicity by inhibiting activation and proliferation of microglia. *J Neurosci*, **21**, 2580-2588.

Tikka, T.M. & Koistinaho, J.E. (2001) Minocycline provides neuroprotection against N-methyl-D-aspartate neurotoxicity by inhibiting microglia. *J Immunol*, **166**, 7527-7533.

Tikka, T.M., Vartiainen, N.E., Goldsteins, G., Oja, S.S., Andersen, P.M., Marklund, S.L. & Koistinaho, J. (2002) Minocycline prevents neurotoxicity induced by cerebrospinal fluid from patients with motor neuron disease. *Brain*, **125**, 722-731.

Toris, C.B., Gleason, M.L., Camras, C.B. & Yablonski, M.E. (1995) Effects of brimonidine on aqueous humor dynamics in human eyes. *Arch Ophthalmol*, **113**, 1514-1517.

Toriu, N., Sasaoka, M., Shimazawa, M., Sugiyama, T. & Hara, H. (2001) Effects of lomerizine, a novel $Ca^{2+}$ channel blocker, on the normal and endothelin-1-disturbed circulation in the optic nerve head of rabbits. *J Ocul Pharmacol Ther*, **17**, 131-149.

Townsend, D.J. & Brubaker, R.F. (1980) Immediate effect of epinephrine on aqueous formation in the normal human eye as measured by fluorophotometry. *Invest Ophthalmol Vis Sci*, **19**, 256-266.

Trivino, A., Ramirez, J.M., Salazar, J.J., Ramirez, A.I. & Garcia-Sanchez, J. (1996) Immunohistochemical study of human optic nerve head astroglia. *Vision Res*, **36**, 2015-2028.

Vaghefi, H., Hughes, A.L. & Neet, K.E. (2004) Nerve growth factor withdrawal-mediated apoptosis in naive and differentiated PC12 cells through p53/caspase-3 dependent and independent pathways. *J Biol Chem.*

Vainio-Jylha, E. & Vuori, M.L. (1999) The favorable effect of topical betaxolol and timolol on glaucomatous visual fields: a 2-year follow-up study. *Graefes Arch Clin Exp Ophthalmol*, **237**, 100-104.

van Adel, B.A., Kostic, C., Deglon, N., Ball, A.K. & Arsenijevic, Y. (2003) Delivery of ciliary neurotrophic factor via lentiviral-mediated transfer protects axotomized retinal ganglion cells for an extended period of time. *Hum Gene Ther*, **14**, 103-115.

Vaughan, D. & Riordan-Eva, P. (1999) Glaucoma. **In:** *General Ophthalmology*. D. Vaughan, T. Asbury, P. Riordan-Eva, editors. pp. 200-215. Appelton & Lange, Stamford, Connecticut.

Vorwerk, C.K., Naskar, R., Schuettauf, F., Quinto, K., Zurakowski, D., Gochenauer, G., Robinson, M.B., Mackler, S.A. & Dreyer, E.B. (2000) Depression of retinal glutamate transporter function leads to elevated intravitreal glutamate levels and ganglion cell death. *Invest Ophthalmol Vis Sci*, **41**, 3615-3621.

Wang, X., Zhu, S., Drozda, M., Zhang, W., Stavrovskaya, I.G., Cattaneo, E., Ferrante, R.J., Kristal, B.S. & Friedlander, R.M. (2003) Minocycline inhibits caspase-independent and -dependent mitochondrial cell death pathways in models of Huntington's disease. *Proc Natl Acad Sci U S A*, **100**, 10483-10487.

Wang, Y.L., Hayashi, M., Yablonski, M.E. & Toris, C.B. (2002) Effects of multiple dosing of epinephrine on aqueous humor dynamics in human eyes. *J Ocul Pharmacol Ther*, **18**, 53-63.

Wax, M.B. (2000) Is there a role for the immune system in glaucomatous optic neuropathy? *Curr Opin Ophthalmol*, **11**, 145-150.

Wax, M.B., Tezel, G. & Edward, P.D. (1998) Clinical and ocular histopathological findings in a patient with normal-pressure glaucoma. *Arch Ophthalmol*, **116**, 993-1001.

Wein, F.B. & Levin, L.A. (2002) Current understanding of neuroprotection in glaucoma. *Curr Opin Ophthalmol*, **13**, 61-67.

Weinreb, R.N. & Levin, L.A. (1999) Is neuroprotection a viable therapy for glaucoma? *Arch Ophthalmol*, **117**, 1540-1544.

Weishaupt, J.H., Diem, R., Kermer, P., Krajewski, S., Reed, J.C. & Bahr, M. (2003) Contribution of caspase-8 to apoptosis of axotomized rat retinal ganglion cells in vivo. *Neurobiol Dis*, **13**, 124-135.

Wells, J.E., Hurlbert, R.J., Fehlings, M.G. & Yong, V.W. (2003) Neuroprotection by minocycline facilitates significant recovery from spinal cord injury in mice. *Brain*, **126**, 1628-1637.

Wen, R., Cheng, T., Li, Y., Cao, W. & Steinberg, R.H. (1996) α2-adrenergic agonists induce basic fibroblast growth factor expression in photoreceptors in vivo and ameliorate light damage. *J Neurosci*, **16**, 5986-5992.

Wheeler, L., WoldeMussie, E. & Lai, R. (2003) Role of alpha-2 agonists in neuroprotection. *Surv Ophthalmol*, **48 Suppl 1**, S47-51.

Wikberg-Matsson, A., Wikberg, J.E. & Uhlen, S. (1996) Characterization of α2-adrenoceptor subtypes in the porcine eye: identification of α2A-adrenoceptors in the choroid, ciliary body and iris, and α2A- and α2C-adrenoceptors in the retina. *Exp Eye Res*, **63**, 57-66.

Wirtz, M.K. & Samples, J.R. (2003) Glaucoma Genetics. In Morrison, J.C., Pollack, I.P. (eds.) *Glaucoma: Science and Practice*. Thieme Medical Publishers, Inc., New York, pp. 12-21.

Wistrand, P.J., Schenholm, M. & Lonnerholm, G. (1986) Carbonic anhydrase isoenzymes CA I and CA II in the human eye. *Invest Ophthalmol Vis Sci*, **27**, 419-428.

WoldeMussie, E., Ruiz, G., Wijono, M. & Wheeler, L.A. (2001) Neuroprotection of retinal ganglion cells by brimonidine in rats with laser-induced chronic ocular hypertension. *Invest Ophthalmol Vis Sci*, **42**, 2849-2855.

Woo Cheon, E., Hee Kim, Y., Yun Cho, Y., Joon Kim, H., Soo Kang, S., Jae Cho, G., Myong Yoo, J., Kyung Song, J. & Sung Choi, W. (2002) Betaxolol, a β1-adrenoceptor antagonist, protects a transient ischemic injury of the retina. *Exp Eye Res*, **75**, 591-601.

Wood, J.P., DeSantis, L., Chao, H.M. & Osborne, N.N. (2001) Topically applied betaxolol attenuates ischaemia-induced effects to the rat retina and stimulates BDNF mRNA. *Exp Eye Res*, **72**, 79-86.

Wood, J.P., Schmidt, K.G., Melena, J., Chidlow, G., Allmeier, H. & Osborne, N.N. (2003) The β-adrenoceptor antagonists metipranolol and timolol are retinal neuroprotectants: comparison with betaxolol. *Exp Eye Res*, **76**, 505-516.

World Health Organization (1997) Blindness and visual disability part II of VII: major causes world wide. *WHO Information Fact Sheet.*

Wu, D.C., Jackson-Lewis, V., Vila, M., Tieu, K., Teismann, P., Vadseth, C., Choi, D.K., Ischiropoulos, H. & Przedborski, S. (2002) Blockade of microglial activation is neuroprotective in the 1-methyl-4-phenyl-1,2,3,6-tetrahydropyridine mouse model of Parkinson disease. *J Neurosci*, **22**, 1763-1771.

Wyllie, A.H., Kerr, J.F. & Currie, A.R. (1980) Cell death: the significance of apoptosis. *Int Rev Cytol*, **68**, 251-306.

Xu, L., Ma, J., Seigel, G.M. & Ma, J.X. (1999) L-deprenyl, blocking apoptosis and regulating gene expression in cultured retinal neurons. *Biochem Pharmacol*, **58**, 1183-1190.

Yang, L., Sugama, S., Chirichigno, J.W., Gregorio, J., Lorenzl, S., Shin, D.H., Browne, S.E., Shimizu, Y., Joh, T.H., Beal, M.F. & Albers, D.S. (2003) Minocycline enhances MPTP toxicity to dopaminergic neurons. *J Neurosci Res*, **74**, 278-285.

Yoles, E. & Schwartz, M. (1998) Elevation of intraocular glutamate levels in rats with partial lesion of the optic nerve. *Arch Ophthalmol*, **116**, 906-910.

Yoles, E., Wheeler, L.A. & Schwartz, M. (1999) Alpha2-adrenoreceptor agonists are neuroprotective in a rat model of optic nerve degeneration. *Invest Ophthalmol Vis Sci*, **40**, 65-73.

Yrjänheikki, J., Keinänen, R., Pellikka, M., Hökfelt, T. & Koistinaho, J. (1998) Tetracyclines inhibit microglial activation and are neuroprotective in global brain ischemia. *Proc Natl Acad Sci U S A*, **95**, 15769-15774.

Yrjänheikki, J., Tikka, T., Keinänen, R., Goldsteins, G., Chan, P.H. & Koistinaho, J. (1999) A tetracycline derivative, minocycline, reduces inflammation and protects against focal cerebral ischemia with a wide therapeutic window. *Proc Natl Acad Sci U S A*, **96**, 13496-13500.

Yuan, L. & Neufeld, A.H. (2001) Activated microglia in the human glaucomatous optic nerve head. *J Neurosci Res*, **64**, 523-532.

Zar, J.H. (1999) Introduction to statistical hypothesis testing. **In**: *Biostatistical Analysis 4th edition.* T. Ryu, editor. pp. 79-85. Prentice-Hall, Inc., Upper Saddle River, New Jersey.

Zarbin, M.A., Wamsley, J.K., Palacios, J.M. & Kuhar, M.J. (1986) Autoradiographic localization of high affinity GABA, benzodiazepine, dopaminergic, adrenergic and muscarinic cholinergic receptors in the rat, monkey and human retina. *Brain Res*, **374**, 75-92.

Zeevalk, G.D. & Nicklas, W.J. (1992) Evidence that the loss of the voltage-dependent $Mg^{2+}$ block at the N-methyl-D-aspartate receptor underlies receptor activation during inhibition of neuronal metabolism. *J Neurochem*, **59**, 1211-1220.

Zeimer, R.C. & Ogura, Y. (1989) The relation between glaucomatous damage and optic nerve head mechanical compliance. *Arch Ophthalmol*, **107**, 1232-1234.

Zhang, X., Clark, A.F. & Yorio, T. (2003) Interactions of endothelin-1 with dexamethasone in primary cultured human trabecular meshwork cells. *Invest Ophthalmol Vis Sci*, **44**, 5301-5308.

Zhu, S., Stavrovskaya, I.G., Drozda, M., Kim, B.Y., Ona, V., Li, M., Sarang, S., Liu, A.S., Hartley, D.M., Wu, D.C., Gullans, S., Ferrante, R.J., Przedborski, S., Kristal, B.S. & Friedlander, R.M. (2002) Minocycline inhibits cytochrome c release and delays progression of amyotrophic lateral sclerosis in mice. *Nature*, **417**, 74-78.